ANALYTICAL AND NUMERICAL MODELING OF MECHANICAL CLEANING DEVICE (MCD) FOR HIGH ANGLE WELLS

A Thesis

Presented to

the Faculty of the Department of Petroleum Engineering

University of Houston

In Partial Fulfillment

of the Requirements for the Degree

Master of Science

in Petroleum Engineering

by

FNU Gaurav

December 2016

ANALYTICAL AND NUMERICAL MODELING OF MECHANICAL CLEANING DEVICE (MCD) FOR HIGH ANGLE WELLS

_____

FNU Gaurav

Approved:

_____

Chair of the Committee
Dr. Konstantinos Kostarelos, Associate Professor,
Department of Petroleum Engineering

Committee Members:

_____

Dr. Robello Samuel, Adjunct Faculty – Lecturer,
Department of Petroleum Engineering

_____

Dr. Cumaraswamy Vipulanandan, Professor,
Department of Civil Engineering

_____

Dr. Suresh K. Khator, Associate Dean,
Cullen College of Engineering

_____

Dr. Mohamed Soliman, Professor and Chair,
Department of Petroleum Engineering

ACKNOWLEDGEMENT

I would like to express my sincere gratitude to my thesis supervisor Dr. Robello Samuel for his sustained guidance and interest in my work. This project was possible because of his support, encouragement, advice and above all, his trust. He is and always will be a great source of encouragement to me. Other than his immense technical skills, I truly adore his working style and his way of thinking. Some of his great thoughts such as "thankfulness shall never be morphed into entitlement" and "to think out of the box, you must first know what is inside the box" will always stay with me. I am extremely thankful to Prof. Konstantinos Kostarelos, and Prof. Cumaraswamy Vipulanandan for being my mentors and making this project possible through their support and guidance.

I would like to thank all the faculty and staff of the Department of Petroleum Engineering at University of Houston for their invaluable inputs on different subjects. Special thanks to my colleagues, friends, and family who directly or indirectly helped me do this project. Last but not the least, I am indebted to my wonderful parents who always stood by me during every phase of my life.

University of Houston has very knowledgeable, positive minded, and helpful staff as well as outstanding faculty, some of whom are well renowned in the world. It also has good research facility which is expanding day by day. I wish Petroleum Engineering Department, UH and all incoming research students all the best in future projects.

ANALYTICAL AND NUMERICAL MODELING OF MECHANICAL CLEANING DEVICE (MCD) FOR HIGH ANGLE WELLS

An Abstract

of a

Thesis

Presented to

the Faculty of the Department of Petroleum Engineering

University of Houston

In Partial Fulfillment

of the Requirements for the Degree

Master of Science

In Petroleum Engineering

by

FNU Gaurav

December 2016

ABSTRACT

Drilling subs, having helical grooves or blades on their surface, assist in cuttings bed removal by creating turbulence and bringing the cuttings into suspension for removal by the drilling mud. Several of these subs, primarily meant for highly deviated and horizontal wells, are employed in a typical drilling application to reduce the *in-situ* cuttings concentration and hence prevent the occurrence of commonly-known drilling problems. A thorough analysis of these tools is required to determine their hole cleaning efficiency.

This report presents a new cutting transport model which includes the effect of pipe rotation. Also, the report presents CFD simulations to determine dissipation of turbulent kinetic energy (TKE) with distance. This TKE is then coupled with the transport model to give tool placement in the drill string. The results obtained from the simulations were analyzed giving valuable insights into the use of these devices for improving cuttings transport while drilling.

TABLE OF CONTENTS

LIST OF FIGURES

LIST OF TABLES

NOMENCLATURE

A	Cross sectional area available for flow
A_b	Cross sectional area of bed
A_p	Cross sectional area of particle
C_1	Constant of integration
C_1	Constant of integration
C_c	Cutting concentration
C_D	Drag coefficient
C_L	Lift coefficient
D_{hyd}	Hydraulic diameter
d_p	Particle diameter
F_1	Hypergeometric series function
F_b	Buoyancy force
F_D	Drag force
F_g	Gravitational force
F_l	Lift Force
F_p	Plastic force
$F_{\Delta P}$	Pressure force
g	Gravitational constant
GPM	Gallons per minute
h_b	Bed height

K	Consistency index of Herschel Bulkley fluid
k	Turbulent kinetic energy
KE	Kinetic energy
L	Length of deviated/horizontal section of the wellbore
l	Moment arm length
n	Power law index of Herschel Bulkley fluid
N_T	Number of tools placed in drillstring
r	Radius from the center of the wellbore
r_1	Drill string radius
r_2	Wellbore radius
Re_m	Modified Reynolds number
Re_p	Particle Reynold number
ROP	Rate of penetration
TKE	Turbulent kinetic energy
U	Average fluid velocity inside annulus
u'	Reynolds stress in X direction
v'	Reynolds stress in Y direction
V_a	Volume of annular section of wellbore
V_c	Volume of cuttings inside annulus
V_{CL}	Critical velocity for lifting
V_{CR}	Critical velocity for rolling
V_f	Fluid velocity

V_p	Particle velocity
V_θ	Tangential fluid velocity
w'	Reynolds stress in Z direction
α	Wellbore inclination
ΔL	Spacing between two tools
ε	Dissipation rate of turbulent kinetic energy
ϑ	Kinematic viscosity
λ	Angle inscribed at the center by chord of a sector in a circle
μ	Dynamic viscosity
ρ_f	Fluid density
ρ_p	Particle density
$\tau_{r\theta}$	Tangential shear stress
τ_w	Wall shear stress
τ_y	Yield stress of Herschel Bulkley fluid
ϕ	Angle of repose
Ω	Revolutions per minute (RPM)

CHAPTER 1

INTRODUCTION

It has been clearly understood that effective hole cleaning of a borehole is essential to avoid problems like reduction of torque and drag, differential sticking, lost circulation, premature bit wear, reduced rate of penetration (ROP), fracturing of formation, and difficulties in logging, cementing, casing landing etc. Mostly used approaches to increase cutting transport efficiency include management of annular velocities, mud viscosity, drill string rotational speed measured in rotations per minute (RPM), and pipe eccentricity. Vertical and simple wells can be managed by these approaches however in cases of complex wells, extended reach drilling, horizontal wells, and highly deviated wells, cutting transport can be troublesome and inefficient. In such wells, cuttings have natural propensity to settle at the low side of the borehole and form a thick bed. This reduces the annular cross sectional area resulting in greater pressure losses and higher Equivalent Circulating Density (ECD). ECD manipulation may not always be feasible because of the narrow margin between the pore pressure and the fracture gradient. Apart from this, excessive torque and drag caused by cutting beds puts a limit on the distance that can be drilled in high-angle/extended-reach drilling. To overcome all these problems and to keep the well clean enough for a trouble-free operation, mechanical cleaning devices (MCD) have been developed by industry. These tools increase the turbulence, enhance cutting transport efficiency and push the cuttings to the surface.

A mechanical cleaning device has helical groves on its surface that induces turbulence and helps cuttings to remain suspended, which then can be carried away by circulating drilling fluid. It also scoops cuttings from the deposited bed and conveys them

backwards while the string rotates. This innovative tool allows drilling with safe ECD margin and reduces time spent on hole cleaning operations. MCD is an add-on to the drill string which can augment cutting removal when adequately spaced and properly used.

Despite worldwide use of hydro-mechanical cleaning tools, very few studies have been conducted so far to determine its placement in the drill string. Due to very complex fluid mechanics governing the interaction between MCD and mud, most of the studies have been experimental in nature. Though experimental studies provide a good understanding of tool performance, a mathematical model is required to design and optimize the tool. This project focuses on the development of a cuttings transport model and coupling it with Ansys Fluent simulations to determine tool placement. It also aims to investigate effects of various operating parameters in MCD performance.

CHAPTER 2

PROBLEM STATEMENT

In the absence of an MCD, deviated wellbore looks like the way it is shown in Fig. 2.1. This poses several problems that are discussed in the previous chapter. To overcome these problems, a down-hole cleaning device with helical grooves in it is under investigation in this report. The purpose of this tool is to assist in cuttings removal in highly deviated and horizontal wells. It is important to quantitatively determine its hole cleaning efficiency and perform an exhaustive qualitative analysis to gain insight into the use of this tool in drilling. At the same time, it is necessary to determine the effect of drilling parameters, such as wellbore inclination, mud flow rate, pipe rotation speed, ROP, etc, on hole-cleaning within an annulus with MCD installed in the drill pipe. It is also necessary to optimize the performance of the tool through careful control of these parameters. The project focuses on developing a mathematical model for cutting transport, determining turbulent kinetic energy using simulations for different operating parameters, plugging the data obtained from simulations into the mathematical model, and determining the placement of MCD tool based on preset value of cutting concentration in the wellbore.

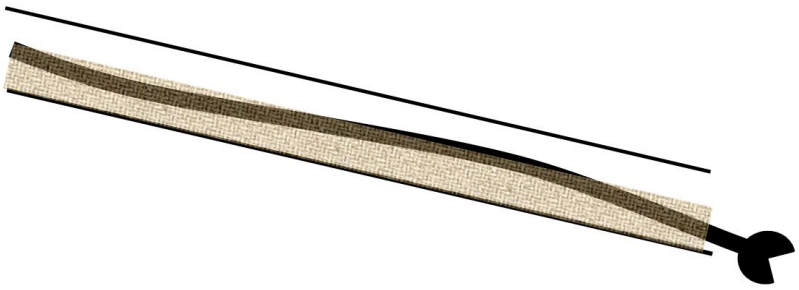

Figure 2.1 Depiction of cutting deposition in wellbore

Approach

A mathematical model was developed to determine whether cuttings will be transported or not for a given set of parameters including flowrate, inclination, mud rheology, pipe RPM, and ROP. This model basically gives critical velocity of fluid that will lift and transport cuttings of fixed size and shape. Next, for different ROPs, bed height was calculated using maximum cutting concentration of 10% in the wellbore annulus followed by calculation of actual flow velocity (V) in the annulus. Critical flow velocities (V_{cr}) were then obtained for different combinations of parameters using the cutting transport model. Difference between critical velocities and actual velocity (V_{cr} - V) is used to calculate additional flow velocity required for cleaning. Additional velocity required is then converted to turbulent kinetic energy. Once TKE requirements were calculated, simulations were run using the tool to see for how much distance TKE > Additionally-Required-TKE is maintained in the annulus. The distance thus obtained is considered as the best location for placement of another tool.

CHAPTER 3

LITERATURE REVIEW

Pigott (1941) conducted exhaustive research experiments on cutting transport using different fluid parameters and different particle shapes. He found that in the turbulent region of flow, non-Newtonian mud behaves as true liquids where all the variations in the viscosity disappears. Also, he concluded that pressure drop and sustaining effect of any mud can be determined if viscosity-velocity relations and mud density are known. Apart from this, he reported better cutting transport when mud weight and mud velocity were increased.

Hall et al. (1950) conducted extensive series of lab experiments to determine slip velocities of particles with various shapes and sizes in mud of different physical properties. From the experimental data, they derived empirical equations for calculating slip velocity. The equations showed that slip velocity depends on cutting size, cutting shape, mud flow rate, and type of mud.

P. Saffman (1964) made significant contribution in the theoretical development of lift force and lift coefficient for flow involving low Reynolds number hydrodynamics. He showed that sphere moving through viscous fluid experiences a lift force, perpendicular to the flow, due to unevenness of flow field around spherical particle.

E.A. Hopkin (1967) conducted lab experiments along with actual field experiment to determine factors that affect hole cleaning efficiency of drilling mud. From his experimental results, he developed correlations between fluid viscosity, slip velocity of cutting particles, and Bingham yield value of the mud. He calculated maximum slip velocity of normal size cutting particles to be about 100 to 110 ft/min in low viscosity and

low density muds. He found that slip velocity is a function of mud viscosity and it decreases with increasing mud density. He also proposed that annular velocity of about 200 ft/min in excess of the maximum slip velocity is required to keep the hole clean in case of fast upper-hole drilling and annular velocity of about 20 to 30 ft/min in excess of the maximum slip velocity is required to keep the hole clean in case of slow, hard rock drilling.

Launder and Spalding (1974) in their paper described turbulence models, numerical solution to which can give turbulence kinetic energy and the dissipation rate of TKE when Reynolds stresses were solved simultaneously with Navier Stokes equations. Wide applicability of model was demonstrated by considering 9 different types of turbulent flow computations.

R.P Thomas (1981) simulated wellbore conditions in a test apparatus and studied effects of drillpipe eccentricity and rotation of eccentric drillpipe on carrying capacity of mud. He also tested the validity and applicability of Zeilder Transport model using two velocity values, four eccentric positions and four RPMs, and concluded that cutting concentration in vertical wellbores may be incorrectly high at low fluid velocities. However, the equation gave correct cutting concentration when fluid velocity is at least twice the particle settling velocity. From his experimental results he found that effect of drillpipe eccentricity on cutting concentration is minimal. Also, effect of rotation was found to be significant at lower flow rates and negligible at higher flow rates.

Gavignet and Sobey (1989), developed two-layer model for cutting transport in deviated wells. Their model was based on momentum balance equations and assumption that all the cuttings fall down at the bottom section of inclined wellbore and that the whole bed slides up the well. From their research, they found that coefficient of friction between

cuttings and wellbore walls has a strong influence on bed formation. They validated the model by conducting experiments and studied effects of sliding friction, inclination, viscosity, pipe eccentricity, bit-drillpipe size, rate of penetration, and cutting size. They concluded that highly deviated wells should always be drilled using a large diameter drillpipe.

J.M. Peden et al. (1990) carried out experiments to determine effect of various parameters including hole angle, fluid rheology, cutting size, drillpipe eccentricity, mud flow rate, wellbore and drillpipe diameter, and pipe RPM on cutting transport efficiency. They developed a mechanistic model for cutting transport which can give minimum transport velocity (MTV) required to clean the wellbore. His results showed that drillpipe eccentricity, annular size, fluid rheology, and fluid flow regime have significant impact on MTV. Also, with low viscosity mud, particle rolling and suspension is attained at low MTV values due to prevalence of turbulent flow regime. He also found that high viscosity fluids improve cutting transport efficiency, especially at high inclination angles.

J.T. Ford et al. (1990) studied cutting transport in inclined wells experimentally and identified rolling and suspension mechanism for cutting transport. He concluded that hole angle plays an important role in determining the velocities required to clean the hole in both the transport mechanisms. Also, for both the transport mechanisms, velocity required to clean the wellbore has different relation with wellbore inclination angle. He also found that cuttings transport efficiency depends on both fluid type as well as fluid flow regime. From the experiments he observed that low viscosity fluids can transport cuttings well in turbulent regime and are not effected much by drillpipe rotation. However, drillpipe rotation had a significant impact when the drilling fluid was highly viscous. Also, he found

that cuttings transport efficiency increases with increasing mud viscosity as the viscosity decreases minimum transport velocity required for hole cleaning. MTV required to clean the hole and transport the cuttings increases with increasing size of cutting particles.

Martins and Santana (1992) presented a mechanistic model to describe stratified flow of solids and non-Newtonian fluid mixtures in case of horizontal and eccentric wells. His model is based on mass and momentum conservation as well as includes interactions between phases and walls. He modified Lockhart-Martinelli dimensionless parameters for solid-liquid flows and applied it to evaluate cuttings transport phenomena. Also, a procedure for calculating frictional losses was presented. He concluded that use of large diameter drillpipe, increase of fluid density, and increase of fluid flow rate are effective in maintaining a clean hole in horizontal wells.

Sifferman and Becker (1992) conducted a series of experiments to study hole cleaning in inclined wellbores. They varied ten parameters viz. annular mud velocity, mud density, mud rheology, mud type, cutting size, rate of penetration, drillpipe rotational speed, drillpipe eccentricity, and hole inclination angle. From their experiments they concluded that annular mud velocity, mud density, hole inclination angle, and drillpipe rotation has significant impact on cleaning. Also, effect of drillpipe rotation was found to be maximum when the hole was horizontal. During experiments, they observed an interesting phenomena of large dune formation and its dispersion periodically in the hole.

Javadpour and Bhattacharya (1992) derived equations to determine shear stress, shear rate, viscosity, and velocity profile for Herschel Bulkley fluid in annulus of a rotational coaxial rheometer. They also described relationship between shear stress and shear rate and their dependence on axial flow in annular region.

Reed and Pilehvari (1993) came up with a concept of effective diameter, which accounted for both annular geometry and effect of non-Newtonian fluid, for flow of drilling mud through annuli. Their analysis gave a procedure to calculate frictional pressure gradient in laminar, turbulent, and transitional flow regimes. Also, they accounted for wall roughness, yield stress of fluid, drillpipe diameter, and wellbore size in their equations. They ran finite-difference computations of Herschel Bulkley fluid and found good agreement with their model predictions.

Clark and Bikham (1994) developed a mechanistic cutting transport model to determine critical velocities for lifting and rolling without including effect of pipe rotation in it. They proposed that cutting transport occurs through rolling mechanism in case of high angled wells where stationary bed can form. They also conducted experiments to validate their cutting transport models and found that transport model was in good agreement with experimental results. Apart from this, they quantified plastic force and pressure forces that act on a particle inside wellbore.

Luo et al. (1994) took a simple rig-site graphical approach to determine requirements for hole cleaning for various hole sizes. They obtained charts from a computer model based on both laboratory data and field data, and used those charts to determine variables on hole cleaning requirements. Major controllable variables in the charts included mud weight, mud rheology, mud flow rate, inclination angle, and fluid flow regime. They concluded that mud theology is the key variable and that effect of yield point adjustment on cleaning of wellbore is much more when compared to adjustment of plastic viscosity of the mud.

M. Rasi (1994) described a new hole cleaning tool which he developed using fluid mechanics based analytical model, field data and experimental data. His tool allowed drilling engineers to choose best pump flow rates, fluid rheological properties, drill string configurations, and well profile to optimize hole cleaning. He addressed the calculation of bed height in details and conducted several pull-out-of-hole experiments to determine maximum allowable bed height while tripping in and tripping out operations. Also, he came up with hole cleaning ratio (HCR) which can fully characterize hole cleaning performance.

To further extend his existing research on stratified flows, Martins et al. (1996) carried out experimental work on a large scale flow loop simulator and quantified parameters such as shear stresses at interface between fluid and bed, as well as maximum friction factor between cuttings and wellbore walls. He used different polymeric fluids to analyze erosion of sandstone bed and to quantify the conditions required for the beginning of movement of a stationary bed. Also, he developed set of correlations to predict static forces and friction factors, and concluded that his correlations were accurate.

T.I. Larsen (1997) developed a new cutting transport model that gave critical cutting transport velocity required for hole cleaning and enabled drillers to select best hydraulic/flow parameters to optimize cutting transport in case of highly deviated wells. He carried out experiments using full scale flow loop and developed empirical correlations for cuttings transport. Also, he defined and developed equations for several correction factors including angle of inclination correction factor, cutting size correction factor, mud weight correction factor, and slip velocity correction factor. Apart from this, he developed equations for finding cutting concentrations in inclined wellbores when fluid velocity is less that critical transport velocity.

Boulet et al. (2000) described successful application and effects of a completely new Hydro-mechanical cleaning tool, machined externally on drilling equipment, to enhance wellbore cleaning and reduce friction. They studied lifting effect, scooping effect, Archimedean screw effect, and particle boosting & recirculation effect of the tool followed by CFD analysis. Their CFD results showed that particles get trapped by vortexes in the flow and are conveyed upwards by screw effect. Also, field trials of the new tool were run showing improved hole cleaning.

Bilgesu et al. (2002) ran CFD simulations to determine the parameters that affect cutting transport in both vertical and horizontal wellbores. From their CFD simulations, they found that annular velocity plays an important role in hole cleaning. Also, they developed curves for cutting transport efficiency which showed that efficiency decreases with increasing annular velocity. They concluded that unrealistically high flow rates are needed to achieve totally clean wellbore.

Ali Qureshi (2004) conducted experimental studies on effective hole cleaning using a mechanical cleaning device at Tulsa University. He studied effects of flowrate and pipe rotation on volumetric cutting concentration in a simulated wellbore using different fluids. Using regression modeling technique (Buckingham Pi Theorem), the experimental results were translated into mathematical equations for estimating cuttings concentration. He also developed several correlations to estimate cuttings concentration in terms of various non dimensional parameters.

Danielson (2007) developed a model for determining critical solid-carrying velocity which gave good fit of bed height and critical transport velocities with his

experimental data in case of sand transport. He assumed critical slip velocity between sand and liquid to be constant in his model.

Duan et al. (2007) developed expressions to determine Critical Re-suspension velocity (CRV), which is the velocity required to keep a particle suspended, and Critical Deposition velocity (CDV), which is the minimum fluid velocity required to start cutting bed erosion. They also conducted experiments in flow loop to validate their mathematical cuttings transport model. Errors between mathematical model and experimental results were reported to be about 12%. They concluded that CDV is about 2 to 3 time CRV and that for particles smaller than 0.2 mm, inter-particle forces play an important role in preventing re-suspension. An interesting conclusion was that polymer solution is more effective in prevention of bed formation whereas water is more effective in eroding bed.

R. Samuel (2007) in his book Downhole Drilling Tools has described several hole cleaning tools and mechanical hole cleaning devices. An in-depth description of problems associated with improper hole cleaning, factors that affect hole cleaning, mechanical hole cleaning devices, and adjustable mechanical cleaning device has been given in the book. Correlations can also be found for predicting cuttings concentration in terms of various non dimensional parameters to determine efficiency of hole cleaning devices.

Pressure drop across various stand-off devices, including MCDs, was studied thoroughly by D. Yao and R. Samuel et al. (2008). They ran CFD simulations to study the effect of blade length, blade angle, and fluid rheology on pressure drop. Using the CFD data, they also built a mathematical model to calculate frictional losses and pressure drop across various devices in the drill string. Their research can be used to determine pressure drop and estimate pressure limitations while drilling.

Costa et al. (2008) presented a computer model to determine cuttings concentration in wellbore. Their model allowed users to calculate cutting bed formation, position, and height as well as to determine whether the bed will remain stationary or not. They developed a particle transport model based on mass conservation equations and proposed a finite difference solution for the same while considering a treatment for slip phenomena.

A. Singh and R. Samuel (2009) examined the effect of the various geometrical parameters of the commonly used standoff devices, eccentricity, rotation of the devices, flow rate, and rheological properties on the annular pressure loss using computational fluid dynamics (CFD). The results of the study of alteration and effects of various rheology models on the flow profile and annular pressure losses were presented. Their study explored the importance of eccentricity and device rotation and presented a simple set of comprehensive equations and guidelines to calculate the pressure losses for commonly used devices. The equations and guidelines are useful in the determination of the number of devices and their optimum placement in the string. Case studies in which the pressure losses were not negligible was also presented stressing the importance of considering the pressure losses encountered while using standoff devices.

Ahmed et al. (2010) carried out experiments to explore the effectiveness of a mechanical cleaning device. Their experimental results showed that the tool significantly reduces the amount of cuttings concentration in wellbore. Also, they evaluated results and found that flow rate and inclination angle have the most significant impact on hole cleaning efficiency of a mechanical cleaning device. In addition to that, they developed generalized correlations based on dimensional analysis. They concluded that drillpipe RPM has a

moderate effect on cleaning efficiency of MCD, bed area is sensitive to MCD spacing, and ROP effect in bed area is minimal.

Through experiments, Han et al. (2010) examined transport of solid particles in solid-liquid mixture for both vertical and inclined annuli with rotating inner cylinder at the center. They observed that lift forces act on fluidized particles and play an important role in their transport and removal. They varied annular fluid velocities from 0.4m/s to 1.2m/s as well as used two types of fluids viz. water and cellulose-bentonite solution. To develop a two-phase numerical model, they further compared their experimental data with numerical results. Also, they found that for higher rate of penetrations or higher particle feed rates, hydraulic pressure drop was more because of increased friction between wall and solids.

Wang et al. (2010) developed three-layer dynamic cutting transport model based on drillpipe rotation, flow mechanics, slip velocity, and interaction between layers. They ran numerical simulations for the same and found that high angle hold segment is most difficult to clean. In order to clean a wellbore, they recommended to use low viscosity drilling fluid with high fluid velocity and high drillpipe RPM. To support their model, they implemented their guidelines in the oil fields of South China Sea and validated their model predictions.

Sulaymon (2011) conducted several experiments to quantify hydrodynamic interactions between two spheres in Newtonian and non-Newtonian fluid. He found that drag coefficient depended strongly on separation distance between the spheres and particle Reynold number. They also correlated drag coefficient with Reynolds number and fluid index.

A. Kumar and R. Samuel (2012) developed a mathematical model to analyze the frictional heat generated from wellbore and to predict drilling fluid temperature profile during drilling operation at any depth in the well. They presented a steady state solution for heat transfer between drill string and the fluids in the drill pipe and annulus, as well as heat transfer between the annular fluid and the formation. Their exhaustive study gave a valuable insight of energy losses (other than pressure energy loss) in the wellbore.

Mme and Skalle (2012) used Discrete Phase model in Ansys Fluent to simulate cuttings transport process in wellbore annulus and to determine effects of annular flow behavior, cutting size, cutting shape, and fluid thixotropic properties on cuttings transport in inclined wells. From the simulations, they found that viscosity of plastic fluids is low near the walls and high at the center. Also, they observed that as the inclination of wellbore approached zero, cleaning was better. Effect of cutting size showed that transport is easy with smaller cuttings. Shape factor was also included in their research which allowed them to conclude that spherical particles are easier to clean.

To improve hole cleaning, L. V. Puymbroeck and H. Williams (2013) proposed a new design for drill pipe which included hydro-mechanical features in the tool joint (Hydroclean Tool). They carried out flow loop tests and studied the effect of wellbore inclination and flow rate on cleaning efficiency. Also, they defined a hole cleaning efficiency index which compared cleaning performances with and without Hydroclean tools. They concluded that as long as inclination is above 30 degrees, Hydroclean tool increases hole cleaning in high angle wells. Also, effect of rate of penetration was found to be minimal on annular cutting bed and tool performance was found to be strongly governed by spacing between two tools.

Mulchandani (2013) measured fluid velocities as well as velocity of bidispersed particles and their position distribution using particle image velocimetry technique. He used this experimental technique to determine flow fields of suspended 4mm particles when they were mixed with 5 and 6mm particles at different concentrations. Also, he obtained histograms of particle positions to inquire into the effect of velocity gradients on lateral distributions of suspensions. He observed that increase in concentration of 5mm particles had no effect on the distribution of 4mm particles. Also, he concluded that bigger particles tend to position themselves in the center with flat velocity profile whereas smaller particles tend to stay near the walls and form bed.

Cayeux et al. (2014) integrated closure laws for cuttings transport into a transient drilling model, to account for both drillpipe mechanics and fluid dynamics, and developed a new transient cuttings transport model. They used the model in drilling operations in North Sea and successfully confirmed cutting bed locations as predicted by the model.

Akhshik et al. (2015) coupled computational fluid dynamic and discrete element method (CFD-DEM) to simulate collision dynamics of cutting particles in wellbore with rotating eccentric drill string. They conducted a series of lab scale experiments which were used to generate data for validation of simulations. Also, they plotted velocity contours and cutting concentration contours. From their conclusions, their numerical model gave good results when compared with other CFD models that exist in literature.

Amanna and Movaghar (2016) ran CFD simulations to solve equations, that govern cutting transport, in Eulerian-Eulerian CFD framework. A comparison of their CFD result with their experimental data showed that the selected CFD model is able to make good predictions. Also, they investigated into the effect of wellbore inclination, flow rate,

drillpipe RPM, and cuttings size on cuttings transport. From the simulation and experimental results, they concluded that wellbores between 45º and 60º inclination are most difficult to clean, higher flow rates are able to clean more because of strengthened intensity of eddy turbulent flow, larger sized cuttings are more easy to remove than smaller cuttings, and at high drill pipe rotational speeds, drag on cuttings is more which improves transport efficiency.

Table 3.1 Summary table of important hole cleaning references

S. No	Paper number	Year	Contribution
1	SPE-172403-MS	2014	Applied MCD in real field and discussed about its applications.
2	SPE-134269	2010	Conducted flow loop experiments with MCD, did sensitivity analysis, and developed a mathematical model for cutting concentration calculation.
3	SPE-168690	2013	Explained a new design for drill pipe with hydro-mechanical features in each joint and conducted flow loop testing to study effects of inclination angle, flow rate, RPM, and mud rheology.
4	SPE-175165	2015	A new MCD was trial tested in a 30480 ft long well by placing the tool every 3 stands. Thorough description of bottom hole assembly was given and torque & drag charts were presented. Also, hole cleaning analysis was made graphically.

Table 3.1 continued

5	1697-PA SPE Journal Paper -	1967	Lab experiments and actual field experiments were conducted and several correlations between fluid viscosity, slip velocity and yield stress were developed.
6	15417-PA SPE Journal Paper	1989	Two-layer cutting transport model was developed using momentum balance equations.
7	20925-MS SPE	1990	Carried out experiments and developed a mechanistic model for cutting transport which can give minimum transport velocity.
8	23643-MS SPE	1992	Mechanistic model to describe stratified flow of solid-liquid was presented based on mass and momentum balance equations and interaction between phases and walls.
9	28306-MS SPE	1994	Mechanistic cutting transport model was developed to determine critical velocities for cleaning wellbore. Also, experiments were conducted to validate the models.
10	25872-PA SPE	1997	Experiments were conducted to develop several empirical correlations for cuttings transport. Also, equations to calculate cutting concentration were developed.

Table 3.1 continued

11	59143-MS SPE	2000	Described successful application and effects of a completely new Hydro-mechanical cleaning tool machined externally on drilling equipment to enhance wellbore cleaning and reduce friction.
12	Mohammad Ali Qureshi, MS Thesis, University of Tulsa, OK	2004	Experimental studies were conducted to study the effects of different parameters on effectiveness of an MCD. Correlations to find cutting concentration were also developed.
13	Downhole Drilling Tools book by Dr. Samuel	2007	Several hole cleaning tools have been described including in-depth description of problems associated with improper hole cleaning. Correlations to calculate cutting concentration are also given.
14	134306-MS SPE	2010	Three-layered dynamic cutting transport model was developed and numerical simulations were run to predict cuttings transport.
15	18691-MS OTC	2007	Developed a model for determining critical solid carrying velocities which gave good fit of bed height and velocities with experimental data.

Several other authors including Ansley et al. (1967), John B. Thuren (1979), Gu and Tanner (1985), Bourgoyne et al. (1991), White (1991), Munson et al. (1994), Chien (1997), Walker and Li (2000), Tabuteau et al. (2007), Ahmed and Miska (2009), and Salyzhyn and Myslyuk (2011), have studied the interaction of fluid on solid particles to understand various hydrodynamic forces and to apply it to the field of drilling engineering. Some of them conducted experiments to determine mud properties, drilling parameters, and other factors related to drilling industry. Through various theoretical and experimental attempts, they have tried to address the issue of inefficient hole cleaning during drilling.

CHAPTER 4

DEVELOPMENT OF MATHEMATICAL MODEL

The mathematical model that is developed here is an extension of the already existing model developed by Clark and Bickham (1994). They developed the model to predict critical transport velocities without formation of a cutting bed. However, they did not include the effect of rotating drill pipe in it.

This model considers the effect of drill pipe rotation along with other major forces. Physical assumptions made in order to develop the model are: eccentricity is zero, steady flow, isothermal flow, uniform bed thickness, and no effect of particle collision on critical velocity. Also, an assumption of negligible variation in the thickness of bed along the length of wellbore makes the geometry dunes free and simple. Another important assumption is that solids in the fluid phase remain in the fluid phase and do not interact with the bed at critical velocity of the fluid. Hence, there is no exchange of energy by virtue of collision of particles with the bed. All these assumptions were taken to simplify the model. In real cases, pipe eccentricity is never zero and affects the cutting transport efficiency. Also, bed thickness is not uniform and there is periodic dune formation and dispersion in the wellbore (Sifferman and Becker). Assumption of no energy exchange between fluid phase and solid phase ignores the energy loss in lifting and transporting the cuttings. Moreover, collisions between particles and energy exchange between them, which are ignored in this model, can also result in sudden lifting and rolling of a particle. Because of geothermal gradient, mud goes through various temperature change during drilling operations. Determination of these temperature changes can result in better

estimation of fluid physical properties which were limited by assumption of isothermal system.

4.1 Analysis of forces

Analysis of the phenomena of resuspension processes of solid particles and formation of bed requires a good understanding of the all the forces that acts on particles in wellbore. There are several forces that act on a particle when it is inside annulus at any given point of time. These forces are buoyancy, gravity, lift, drag, pressure, and plastic force acting in the directions shown in Fig. 4.1. Hydrodynamic forces, that includes drag and lift, are generated by virtue of flow of fluid across the geometry of solid particle that is present in the fluid. When these hydrodynamic forces are sufficiently large, they can help particles to either roll or get lifted by the fluid, leading to hole cleaning. Apart from this, the net torque that is generated by all the forces including hydrodynamic forces helps cutting to roll. This means that a particle can roll on the surface of the bed if the moment generated by all the forces at point P shown in the Fig. 4.1 is greater than the net torque. Similar to rolling, the phenomena of lifting occur when the net force generated by the effect of all the forces is in direction perpendicular to the flow, i.e., in upward direction.

4.1.1 Gravity and Buoyancy Forces

Because of the gravitational pull of the earth and mass of particles, gravity force acts on every particle and is directed towards the center of the earth. Also, based on Archimedes' principle, an upward buoyancy force acts on every particle that is immersed in drilling fluid and is equal to the weight of fluid that has been displaced by the volume

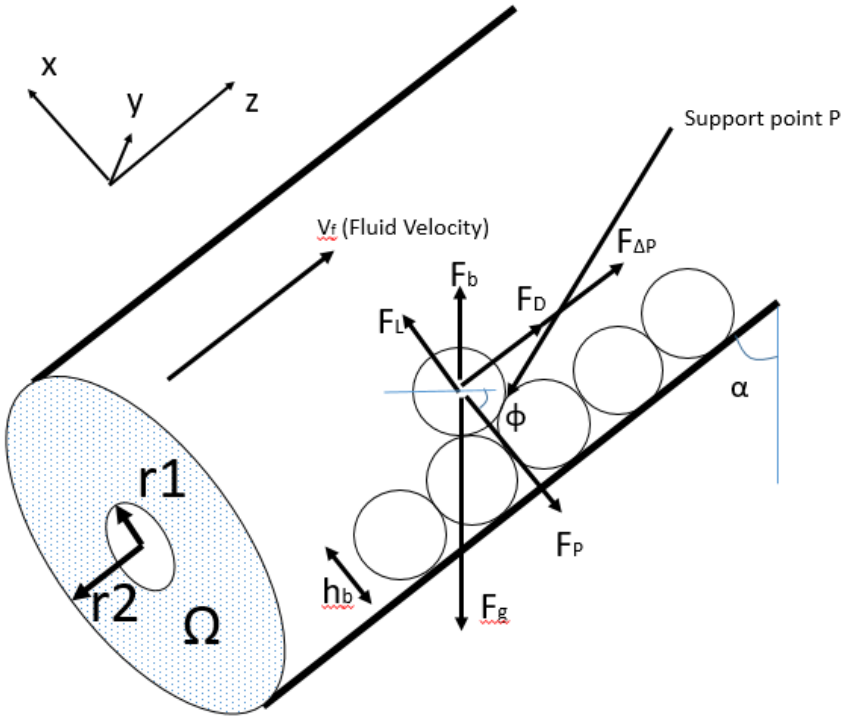

Figure 4.1 Forces acting on a particle on cutting bed

of particle. These two forces are the main forces that act on a cutting particle under any given circumstance, i.e., both dynamic and static condition. As can be seen in the Fig. 4.1, these two forces act in opposite direction and have opposing effect on cutting transport. When gravity dominates, cutting particles settle down at the bottom section of the wellbore and form a cutting bed. On the other hand, if buoyancy force, which is a function of fluid density, dominates, particles tend to rise and float without forming any bed. However, due to equivalent circulating density limitation on drilling fluid, mud density cannot be increased much to improve hole cleaning. Gravitational force is given by the formula

$$F_g = g\rho_p \frac{\pi {d_p}^3}{6} \quad , \tag{1}$$

where g is gravity, ρ_p is particle density, and $d_p$is particle diameter. Buoyancy force is similar to gravity force and acts opposite to it because of the Archimedes' principal. Expression for buoyancy force is similar to gravitational force expression and is given by

$$F_b = g\rho_f \frac{\pi {d_p}^3}{6} \quad , \tag{2}$$

where ρ_f is fluid density. These two are the major forces that act on a particle when it is in the annulus.

4.1.2 Hydrodynamic forces

Both the hydrodynamic forces viz. drag force and lift force are created when the drilling fluid is moving. As the name says, drag force acts on the particle in the direction of fluid flow and is a function of particle geometry, fluid density and fluid velocity. Lift force on the other hand acts in the direction of buoyancy force which is perpendicular to fluid flow. Both these forces are generated as a result of stress variations on the surface of the particle due to the action of the surrounding fluid. They both can be quantified by integrating the wall shear stress and pressure distributions on the surface of the particle. However, it is difficult to determine stress and pressure distributions mathematically. Therefore, most of the works in literature rely on experimental determination of these forces. The drag force is given as

$$F_D = 10^{-3} C_D A_P \rho_f {V_f}^2 \quad , \tag{3}$$

where C_D is the drag coefficient, A_P is the cross sectional area of the particle that is perpendicular to fluid flow, ρ_f is the density of fluid, and V_f is fluid velocity.

Similarly, lift force is given by the equation

$$F_L = 10^{-3} C_L A_P \rho_f {V_f}^2 \quad , \tag{4}$$

where C_L is the lift coefficient, A_P is the cross sectional area of the particle that is perpendicular to the fluid flow, ρ_f is the density of fluid, and V_f is fluid velocity.

4.1.3 Drag coefficient

Various research scholars have experimentally tried to find the values of drag coefficient for different geometries. One of the assumption on this work is that particles are spherical in shape with a fixed diameter for which drag coefficient determination is exhaustively studied by several people. Most commonly used correlation (White, 1991) for a wide range of particle Reynolds number can be used to determine the drag coefficient for both creeping and turbulent flow regimes. The same is given by the equation

$$C_D = \frac{24}{Re_p} + \frac{6}{1 + Re_p^{0.5}} + 0.4 \quad , \tag{5}$$

where Re_p is the Particle Reynolds number which in turn is given by the equation

$$Re_p = \frac{V_p d_p}{\vartheta} \quad , \tag{6}$$

where V_p is particle velocity, d_p is particle diameter and ϑ is kinematic viscosity of the fluid. These equations however work well with Newtonian fluids. For power law fluid, the equations are slightly modified and are given as (Sulaymon)

$$C_D = \frac{24}{Re_m}\left(1 + 0.16 Re_m^{\left(\frac{2.55n}{1.5n+2.35}\right)}\right) \tag{7}$$

and

$$R_{em} = \frac{(10^{-3} d_p)^n V_p^{(2-n)} (10^3 \rho_f)}{K} \quad , \tag{8}$$

where R_{em} is modified Reynolds number, n is power law index and K is consistency index for a power law fluid. For Herschel Bulkley fluid model, an expression for C_D was given by Harve Tabuteau (2006) as

$$C_D = \frac{24X(n)}{Q} \quad , \tag{9}$$

where,

$$Q = \frac{Re_m}{1 + k.Bi} \quad . \tag{10}$$

Re_m is the modified Reynolds number given by the equation 8 and Bi is Bingham number given by equation (Harve Tabuteau)

$$Bi = \frac{\tau_y}{K\left(V/d_p\right)^n} \quad . \tag{11}$$

The value of numerical constant k was determined to be equal to 1 by Ansley and Smith (1967) whereas Harve Tabuteau (2006) determined its value to be 0.823. X(n) in equation is the crag correction factor and it is a strong function of power-law-index n. Values of X(n) for different n was calculated by Gu and Tanner (1985).

4.1.4 Lift Coefficient

As discussed earlier, the unevenness of flow field around particle gives rise to lift force. This unevenness of the flow field is present due to no slip assumption at the bed surface. And as we move above the bed surface, flow velocity increases. Saffman (1964) predicted that a spherical particle moving in a viscous fluid flow experiences a lift force because of the velocity gradient. In his paper he made two important assumptions viz. one,

the particle remains unaffected by solid boundaries, and two, the velocity gradient in the fluid is constant and not parabolic. Lift force equation is given as

$$F_L = 1.615\ \frac{4d_p^2\mu}{\vartheta^2}\left(\frac{dV_f}{dx}\right)^{0.5} \quad , \tag{12}$$

where F_L is the lift force, μ is dynamic viscosity, ϑ is kinematic viscosity, V_f is fluid velocity, and x is the vertical distance from the mean bed level. Combining the previous equation for lift force with this one we can get an equation for lift coefficient and the same is given as

$$C_L = 4.11\left[\frac{d_p}{4Re_p}\ \frac{dV_f}{dx}\right]^{0.5} \quad . \tag{13}$$

Because dV_f/dy can only be determined experimentally, value for C_L has been taken from numerical simulation results in this report.

4.1.5 Plastic Force

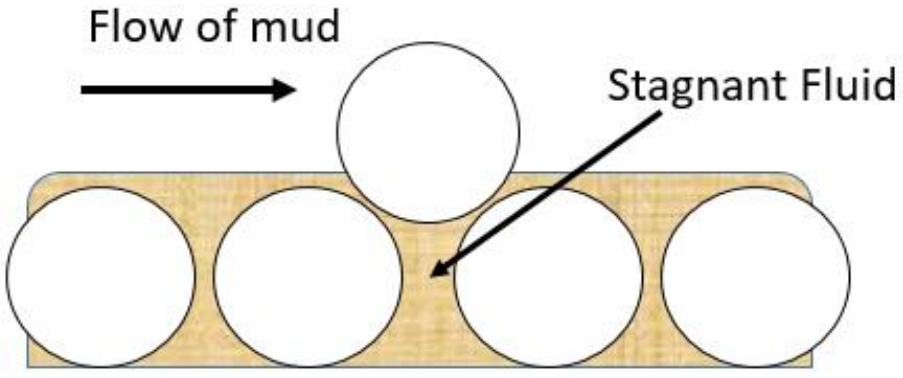

Figure 4.2 Stagnant fluid surrounding bed particles giving rise to plastic force.

As shown in the Figure 4.2, pore spaces in the cutting bed is filled with stagnant mud while the upper layer in the cutting bed is in contact with moving mud. It is a property of non-newtonian fluids to form gel when allowed to sit for a while. Because of this, the stagnant mud in the pore spaces behaves as a gel and gives rise to plastic force which opposes the particle lift in upward direction. Plastic force on a particle fully surrounded by stagnant fluid is given as

$$F_p = 0.5\pi d_p^2 \tau_y \quad . \tag{14}$$

In this report, a different correlation that was introduced by Clark and Bickham (1984) is used. Their equation is given as

$$F_p = \frac{\pi {d_p}^2 \tau_w}{2}\left[\phi + \left(\frac{\pi}{2} - \phi\right) sin^2\phi - sin\phi cos\phi\right] \quad , \tag{15}$$

where, τ_w is the wall shear stress on particle, and ϕ is the angle of repose of cutting bed. The wall shear stress for yield power law fluid can be obtained using the equation by Ahmed and Miska (2009)

$$\frac{24U}{r_2 - r_1} = \frac{\left(\tau_w - \tau_y\right)^{1+1/n}}{K^{1/n}\tau_w^2}\left(\frac{3n}{1+2n}\right)\left(\tau_w + \left(\frac{n}{1+2n}\right)\tau_y\right) \quad , \tag{16}$$

where, r_2 is wellbore radius, r_1 is drill pipe radius, τ_w is wall shear stress, τ_y is yield stress, n is fluid index, U is average fluid velocity in annulus, and K is consistency index.

4.1.6 Pressure Force

This force arises due to pressure difference in the flowing fluid. The force that acts in the Z direction (Fig. 4.1) due to gradient of pressure is given by Clark and Bickham (1994) as

$$F_{\Delta p} = \frac{2\tau_w \pi {d_p}^3}{3D_{hyd}} \quad , \tag{17}$$

where D_{hyd} is the hydraulic diameter and is given as $D_{hyd} = 2(r_2 - r_1)$.

4.2 Velocity profile due to pipe rotation

Apart from velocity of mud along the length of pipe, drilling fluid has a specific velocity distribution, as shown in Fig. 4.3, due to the rotation of drill pipe present at the center of the wellbore. Determination of this tangential velocity is important to predict actual amount of hydrodynamic forces that act on particles on a bed of given height. The mud is considered to be yield power law fluid (Herschel Bulkley Fluid) for which the mathematical model is given as

$$\tau = K\left(\frac{dV_f}{dy}\right)^n + \tau_y \quad , \tag{18}$$

where τ_y is yield stress, K is flow consistency index, n is flow behavior index, V_f is fluid velocity and y is distance. In polar coordinates, it can be written as

$$\tau_{r\theta} = -\mu r \frac{d}{dr}\left(\frac{V_\theta}{r}\right) + \tau_y \quad , \tag{19}$$

where,

$$\mu = K\left|\frac{d}{dr}\left(\frac{V_\theta}{r}\right)\right|^{n-1} \quad . \tag{20}$$

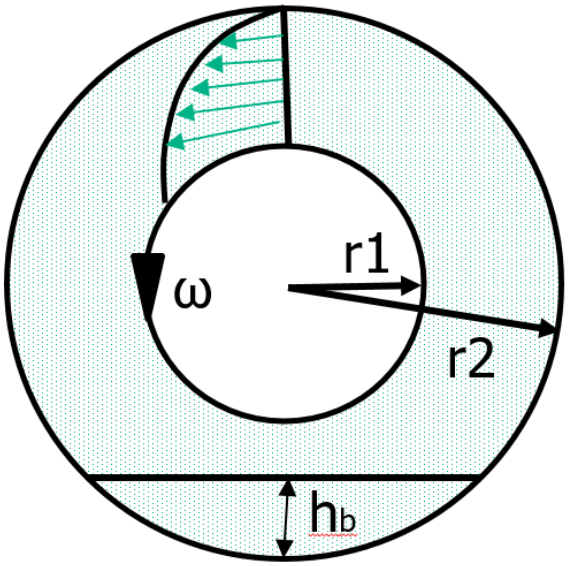

Figure 4.3 Depiction of velocity distribution in wellbore with rotating pipe

Since V_θ is decreasing with r, shear rate $r\frac{d}{dr}\left(\frac{V_\theta}{r}\right)$ will be positive. Thus,

$$\tau_{r\theta} = -K\left(r\frac{d}{dr}\left(\frac{V_\theta}{r}\right)\right)^n + \tau_y \quad . \tag{21}$$

By using the θ component of equation of motion in cylindrical coordinate system, we have

$$\frac{1}{r^2}\frac{d}{dr}(r^2\tau_{r\theta}) = 0 \quad . \tag{22}$$

Upon solving its integral we can easily get

$$\tau_{r\theta} = \frac{C_1}{r^2} \quad . \tag{23}$$

Combining Equation 18 and Equation 20 for $\tau_{r\theta}$ we get

$$\frac{d}{dr}\left(\frac{V_\theta}{r}\right) = \frac{1}{r}\left(\frac{C_1}{r^2} - \tau_y\right)^{1/n} \quad . \tag{24}$$

Boundary conditions for this equation are (see Fig. 4.3)

$$at\ r = r_1, V_\theta = \Omega r_1 \quad \text{and} \tag{25}$$

$$at\ r = r_2, V_\theta = 0 \quad , \tag{26}$$

where, r_1 is the radius of drillpipe and r_2 is the radius of wellbore.

Solution to this equation gives

$$\frac{V_\theta}{r} = -\frac{1}{2} n \left(\frac{C_1}{r^2} - \tau_y\right)^{\frac{1}{n}} \left(1 - \frac{\tau_y r^2}{C_1}\right)^{-\frac{1}{n}} F_1\left(\frac{-1}{n}, \frac{-1}{n}; \frac{n-1}{n}; \frac{\tau_y r^2}{C_1}\right) + C_2 \quad , \tag{27}$$

Here,

$$F_1\left(\frac{-1}{n}, \frac{-1}{n}; \frac{n-1}{n}; \frac{\tau_y r^2}{C_1}\right) \quad , \tag{28}$$

is a hypergeometric function that results in an infinite power series, solution to which cannot be determined mathematically. Instead, it can be assumed that the fluid is always under the shear stress greater than yield stress which reduces the equation to

$$\frac{d}{dr}\left(\frac{V_\theta}{r}\right) = \frac{1}{r}\left(\frac{C_1}{r^2}\right)^{1/n} \quad . \tag{29}$$

Integration of the equation gives

$$\int d\left(\frac{V_\theta}{r}\right) = \int \frac{1}{r}\left(\frac{C_1}{r^2}\right)^{1/n} dr \quad . \tag{30}$$

This can be solved to give

$$\frac{V_\theta}{r} = \frac{C_1^{1/n} r^{-2/n}}{-2/n} + C_2 \quad . \tag{31}$$

Putting the boundary conditions, we get

$$V_\theta = \Omega r \left[\frac{1 - \left({}^{r_2}/_{r} \right)^{2/n}}{1 - \left({}^{r_2}/_{r_1} \right)^{2/n}} \right] \quad . \tag{32}$$

For a bed height of h_b the velocity above the bed is given as

$$V_\theta = \Omega (r_2 - h_b) \left[\frac{1 - \left({}^{r_2}/_{(r_2 - h_b)} \right)^{2/n}}{1 - \left({}^{r_2}/_{r_1} \right)^{2/n}} \right] \quad . \tag{33}$$

4.3 Model formulation

As discussed in the previous section, when the velocity of drilling fluid is high, hydrodynamic forces overtakes other forces and cuttings are lifted and transported by the flowing mud. To find out the velocity at which cuttings will be lifted or rolled is the objective of this mathematical model. These velocities are called Critical velocity for Lifting (V_{CL}) and Critical Velocity for Rolling (V_{CR}). When cutting bed is formed in the wellbore it reduces the cross sectional area of flow, thus increasing velocity of the fluid. This process continues until the velocity in the wellbore reaches critical velocity when cuttings start getting removed due to high velocities. Hence an equilibrium exists between bed height and the mud flow rate. In other words, it is possible to find bed height for a fixed flow rate and vice versa. To develop the mathematical model, it is necessary to balance all the forces that were discussed in previous section. As shown in the Fig. 4.1, a particle in the wellbore experiences different forces which when balanced can give critical velocity equation. Force balance in X direction gives the following equation

$$F_L - F_P + \left(F_b - F_g\right)\sin\alpha = 0 \quad . \tag{34}$$

Substituting equations for all the forces gives

$$V_{CL} = \left[\frac{4\left\{3\tau_y\left(\phi + \left(\frac{\pi}{2} - \phi\right)sin^2\phi - cos\phi sin\phi\right) + d_p g\left(\rho_p - \rho_f\right)sin\alpha\right\}}{3\rho_f C_L}\right]^{1/2} \quad , \tag{35}$$

where, α is the wellbore inclination, and ϕ is angle of repose. This however does not include tangential velocity profile of the mud due to rotating drill pipe. Including the tangential velocity, the equation becomes

$$V_{CL} = \left[\frac{4\left\{3\tau_y\left(\phi + \left(\frac{\pi}{2} - \phi\right)sin^2\phi - cos\phi sin\phi\right) + d_p g\left(\rho_p - \rho_f\right)sin\alpha\right\}}{3\rho C_L} - V_\theta\right]^{1/2} \quad . \tag{36}$$

For rolling to occur, the momentum due to all the forces must exceed in the direction of flow. At critical conditions summation of all the momentums around a support point P will be equal to zero. This gives the equation

$$x(F_D + F_{\Delta P}) + z(F_L - F_P) + l\left(F_b - F_g\right) = 0 \quad , \tag{37}$$

where, l is the moment arm length around the support point P for the gravity and buoyancy forces, and the same is given by the equation

$$l = z\left(\sin\alpha + \frac{\cos\alpha}{\tan\phi}\right) , \tag{38}$$

$$0^\circ \leq \alpha \; and \; \phi \leq 90^\circ \quad , \text{and} \tag{39}$$

$$\phi = \tan^{-1} z/x \quad . \tag{40}$$

In this case also, the momentum increase as fluid velocity increases and there exist a balance between all the momentum forces. Substituting all the forces in the equation gives the following expression

$$V_{CR} = \left[\frac{4\left\{3\tau_y\left(\phi + \left(\frac{\pi}{2} - \phi\right) sin^2\phi - cos\phi sin\phi\right) tan\phi + d_p g(\rho_p - \rho_f)(cos\alpha + sin\alpha\, tan\phi) - d_p\left(\frac{4\tau_w}{D_{hyd}}\right)\right\}}{3\rho_f(C_D + C_L tan\phi)}\right]^{\frac{1}{2}} - V_\theta \quad (41)$$

Although equation for rolling mechanism is derived here, it is not used in the report due to the constraints that are imposed by adjacent particles on the particles that are rolling. A particle can roll only if it is not in contact with any other particle. When it gets in contact with another particle, it stops rotating due to opposite direction of motion at the point of contact. This is the process that actually creates the bed. As depicted in the Fig. 4.4, when two independently rolling particles come in contact, the point of contact experiences motion in opposing direction. The particles oppose each other's motion due to friction force and if the particle/cutting transport has to occur, the entire bed has to move after overcoming the frictional forces. In general, frictional forces are much higher than hydrodynamic forces which makes it impossible for rolling mechanism to take place.

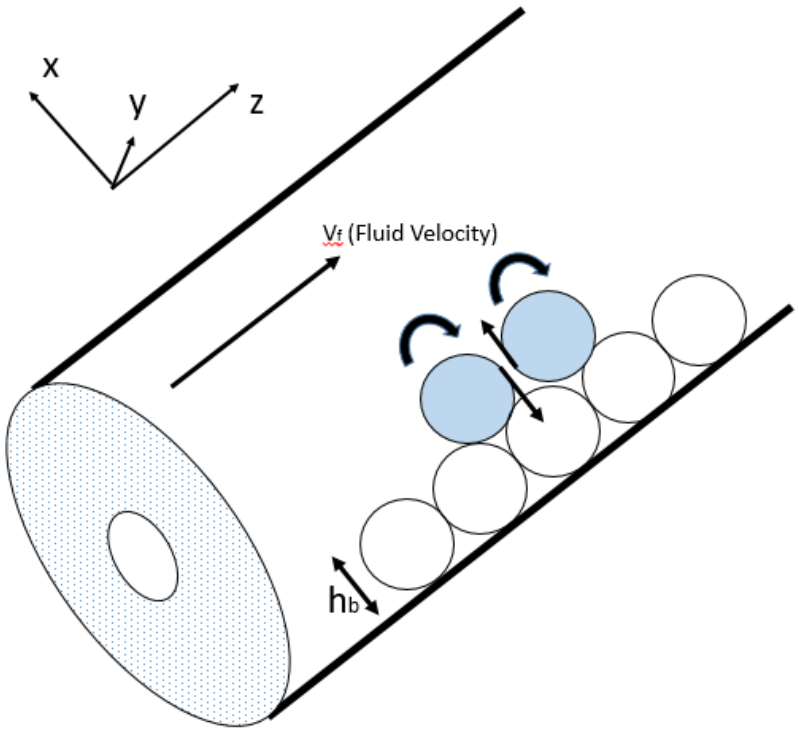

Figure 4.4 Opposite direction of motion at the point of contact in case of rolling

4.4 Cutting concentration

An important parameter that can be calculated from the steady-state weight of the cuttings inside the drill pipe is the in-situ volumetric cuttings concentration, C_c. C_c is a dimensionless parameter, expressed as a percentage, and is given by

$$C_c = \frac{V_c}{V_a}.100 \quad , \tag{42}$$

where,

V_c = Volume (in ft^3) of cuttings inside the annulus at steady state

V_a = Volume (in ft^3) of the annular section of wellbore.

Here V_C depends upon the rate of penetration which in turn can give the amount of cutting generated. For the case when there is no bed and the wellbore is completely clean, C_C is given as

$$C_c = \frac{\text{Volumetric flow rate of Cuttings}}{\text{Cross sectional area for flow} \,.\, \text{Fluid velocity in the wellbore}} \,.\, 100 \quad . \qquad (43)$$

$$\text{Volumetric flow rate of cuttings} = ROP \;.A \;\;, \qquad (44)$$

where, ROP is rate of penetration, A is cross sectional area available for flow. Considering that a fixed value of cutting concentration, C_a, is to be achieved in the wellbore, bed height can be calculated based on this value using simple trigonometry.

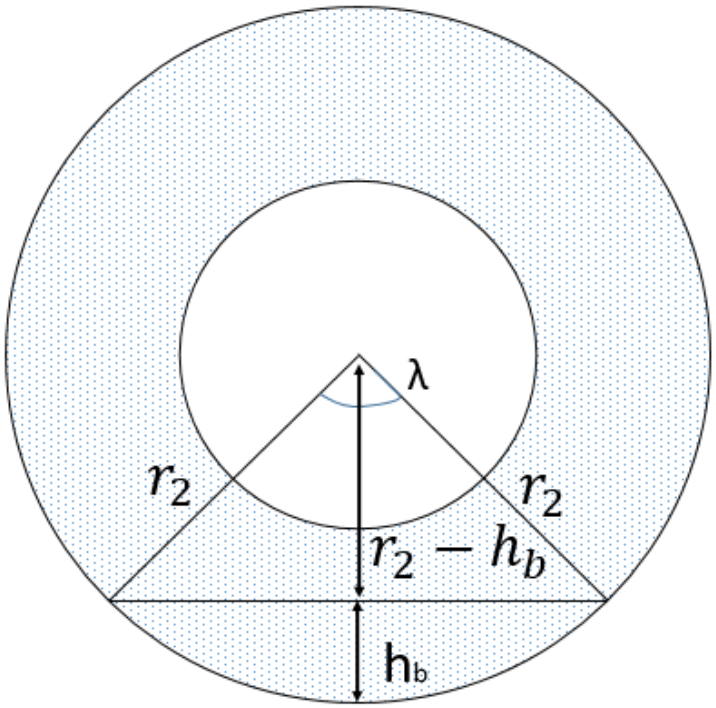

Figure 4.5 Calculation of bed height

In this Fig. 4.5, area of sector, A_b (cross sectional area of bed)

$$A_b = \frac{1}{2} r_2{}^2 (\lambda - sin\lambda) \quad . \tag{45}$$

$$\text{Area available for flow} = \text{Annular area} - A_b \quad . \tag{46}$$

Also,

$$A_b = \frac{A_a(10 - C_c)}{100} \quad , \tag{47}$$

when cuttings concentration in flowing fluid is considered constant. Here A_a is the annular area, 10 is the desired cutting concentration in the wellbore, and C_c is the cutting concentration in the fluid phase when there is no bed. In real case, this has to be solved using iterative process in which flow velocity of the fluid will change as the bed height increases, resulting in less cutting concentration suspended in the fluid phase. Thus, summation of cutting concentrations in bed and in fluid will give actual cutting concentration in the wellbore. For simplicity, fluid phase is considered to have a constant cuttings concentration (equal to C_c in fluid without cutting bed) for doing all the calculations.

Combining above two equations we get

$$\frac{A_a(10 - C_c)}{100} = \frac{1}{2} r_2{}^2 (\lambda - sin\lambda) \quad , \tag{48}$$

from which value of λ can be obtained. Using simple trigonometry, the resulting equation obtained for bed height is given as

$$h_b = r_2 - r_2 cos\frac{\lambda}{2} \quad . \tag{49}$$

Once value for λ is obtained, it can be plugged into Equation 46 for calculating bed height. Once bed height is obtained, actual flow velocity of the fluid over the bed can be calculated using mass conservation equation i.e., $A_1 V_1 = A_2 V_2$, resulting in

$$V_{f(with\ bed)} = \frac{A_a . V_{f(without\ bed)}}{A_a - A_b} \quad . \tag{50}$$

In the above equation, $V_{f(without\ bed)}$ can be obtained by the equation below

$$V_{f(without\ bed)} = \frac{6.309 \times 10^{-5} . GPM + 0.0030345 \times ROP \times 0.0006452 \times A_a}{0.0006452 \times A_a} \quad , \tag{51}$$

where, 6.309×10^{-5} is a constant to convert GPM to m^3/s, 0.0030345 is a constant to convert ROP from ft/s to m/s, and 0.0006452 is a constant to convert A_a from in^2 to m^2.

4.5 Turbulent Kinetic Energy

Turbulent flows can often be observed to arise from laminar flows as the Reynolds number, (or some other relevant parameter) is increased. This happens because small disturbances to the flow are no longer damped by the flow, but begin to grow by taking energy from the original laminar flow. Turbulent flow in fluid dynamics are often quantified using Turbulent kinetic energy, frequently referred to as TKE. It is the mean kinetic energy of a fluid per unit mass associated with eddies in turbulent flow. It is basically a measure of velocity fluctuations due to the presence of eddies in a turbulent flow and is characterized by root-mean-square velocity fluctuations. An attempt to quantify TKE results in the equation

$$k = \frac{1}{2}\left(\overline{u'^2} + \overline{v'^2} + \overline{w'^2}\right) \quad , \tag{52}$$

where u', v' and w' are Reynolds stresses in x, y and z directions. Turbulence Kinetic Energy is produced by various forces that acts on the fluid at low frequency eddie scale. These forces include friction, buoyancy, fluid shear or external force. TKE then undergoes an energy cascade which leads to its gradual dissipation. It gets totally dissipated at Kolmogorov Scale which is the smallest scale in turbulent flow. At this scale viscous forces dominates and entire TKE is dissipates as heat energy. This process can be mathematically expressed as

$$\frac{Dk}{Dt} + \nabla . T' = P - \varepsilon \quad , \tag{53}$$

where Dk/Dt is the material derivative of the mean flow, $\nabla . T'$ is the transport, P is the production, and ε is the dissipation in Turbulent Kinetic Energy. In fluid dynamics, discretization of flow field as far as the Kolmogorov Scale is necessary to numerically simulate turbulence. In computational fluid dynamics, this approach is called direct numerical simulation. To calculate TKE, CFD deploys Reynolds-averaged Navier-Stokes simulations which uses the Boussinesq eddy viscosity hypothesis to determine the stresses from averaging procedure. For simplicity most of the simulations use k-epsilon model which calculates turbulent kinetic energy and its dissipation assuming an isotropy in turbulence whereby normal stresses are equal in all the three directions i.e.,

$$\overline{u'^2} = \overline{v'^2} = \overline{w'^2} \quad . \tag{54}$$

Therefore, turbulent kinetic energy expression reduces to

$$k = \frac{3}{2}\left(\overline{u'^2}\right) \quad . \tag{55}$$

Solution for TKE is obtained using CFD simulations in this report.

CHAPTER 5

WORKFLOW AND PROCEDURE

To determine the distance between two tools for ensuring proper cleaning of the hole, a test matrix was made. In the matrix different combinations of RPM, wellbore inclination, mud flow rate, and ROP were taken to obtain critical velocity for lifting. From the mud flow rate and desired cutting concentration (10% in this report), actual flow velocity of mud over the bed is calculated. The difference between this velocity and V_{CL} is obtained and equivalent kinetic energy (KE) per unit mass of fluid is obtained using simple equation

$$KE = \frac{3}{2} {V_f}^2 \quad . \tag{56}$$

This KE is the desired amount of TKE that must be present in the mud for cleaning the hole. The first tool is placed very close to the drill bit so that it can create significant turbulence in the fluid and bring the cuttings in suspension forthwith. The turbulence thus generated by the very first tool is carried by the drilling mud in form of turbulent kinetic energy in eddies which travels along the length of the annulus towards the surface. However as discussed in the previous chapter, the TKE keeps dissipating with time or with the distance travelled by the mud along the length of the annulus. At some distance the TKE reduces and becomes just equal to the additional kinetic energy required to clean the hole. This distance is considered the ideal location for placement of another tool so that additional TKE is produced and cutting are removed before settling.

In order to quantify different force equations, various parameters including rheological properties of mud, wellbore diameter, drill pipe diameter, cutting density, and

mud density are needed. The table below gives the values assumed for all these parameters. John B. Thuren (1979) and I. Salyzhyn & M. Myslyuk (2011) investigated into rheological properties of drilling fluids based on rotational viscosimetric data. From their investigations they found effect of temperature on mud properties. Values shown in table 5.1 have been approximated from I. Salyzhyn & M. Myslyuk (2011) paper wherein consistency index and flow behavior index changed widely with temperature. Since mud weight depends on type of formation and pore pressure, a typical value of 10 ppg (which is used in Drilling lab, University of Houston) is used in the report. Also, cuttings are assumed to be sandstone which has a typical density of about 2600 kg/m^3. Clark and Bikham (1994) conducted their experiments using drillpipe diameter, bit diameter, cutting size, and angle of repose as 5in, 12.347in, 0.25in, and 40 degrees respectively. The same values are used in this report. As already discussed in chapter 4, for simplicity, pipe eccentricity is assumed to be zero and cuttings are assumed to be spherical and uniform in size.

5.1 Stepwise algorithm

- For different combinations of ROP, and mud flow rate, calculate bed height using maximum cutting concentration of 10% in the wellbore annulus.
- Calculate actual flow velocity over the bed in the annulus.
- Obtain Critical flow velocity for lifting (V_{CL}) using assumed parameters and the equations derived in the analytical solution.

- Obtain difference between critical velocity and actual velocity (V_{CL} - V). This gives additional flow velocity required to clean the hole
- Convert additional velocity required to kinetic energy.
- Run CFD Simulations to determine the distance for which TKE > Additionally-Required-KE is maintained in the annulus.
- Distance obtained is the best location for placement of another tool.

Table 5.1 Assumed parameters

Mud type	Herschel Bulkley Fluid
Consistency index, K	0.06 Pa.s^n
Flow behavior index, n	0.7
Yield Stress	10 Pa
Mud weight	10 ppg
Cutting density	2600 kg/m^3
Angle of repose of bed	40 degrees
Drill pipe diameter	5 in
Bit diameter	12.25 in
Cutting size	0.25 in
Maximum allowable cutting concentration	10%
Cutting shape	Spherical and uniform
Pipe eccentricity	0

5.2 The mechanical cleaning device

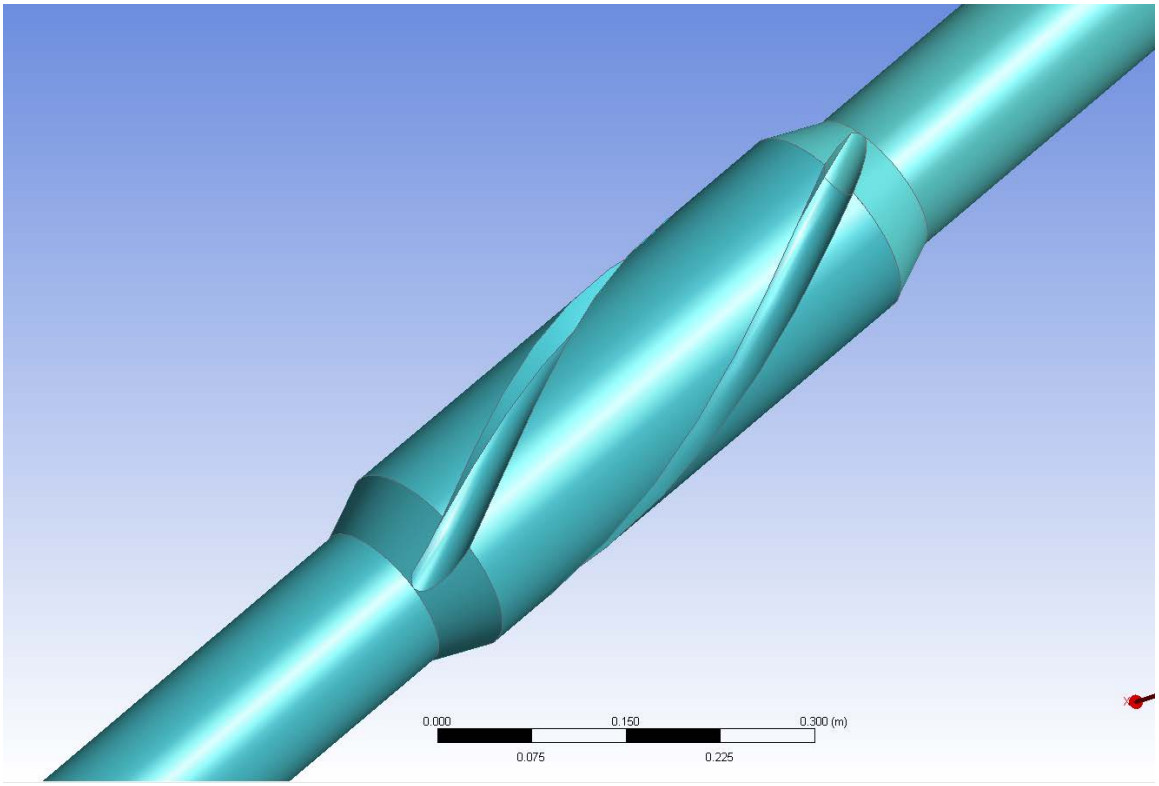

Figure 5.1 Mechanical Cleaning Device

The MCD shown in Fig. 5.1 is the down-hole cleaning tool under investigation in this project. It is a down-hole drill string tool intended for use in deviated wells where excessive buildup of cuttings causes drilling problems. The MCD is an integral drill string component consisting of a short mandrel with no moving parts, shaped in such a way so as to agitate any cuttings which have a tendency to settle out of the mud in the high angled sections of the well bore. These sections could be inside the casing or in open hole. The blades in the tool agitate the cuttings bed and help to bring the cuttings into suspension for easy removal by the flowing drilling mud. This is called scooping effect of the tool. Also, the tool generates significant amount of turbulence in the fluid that is flowing around it.

This turbulence is generated due to the grooved geometry of the tool i.e., blades of the tool. Specifications, including tool length, tool diameter, blade angle, and number of blades, are shown in Fig. 5.2 and Fig. 5.3.

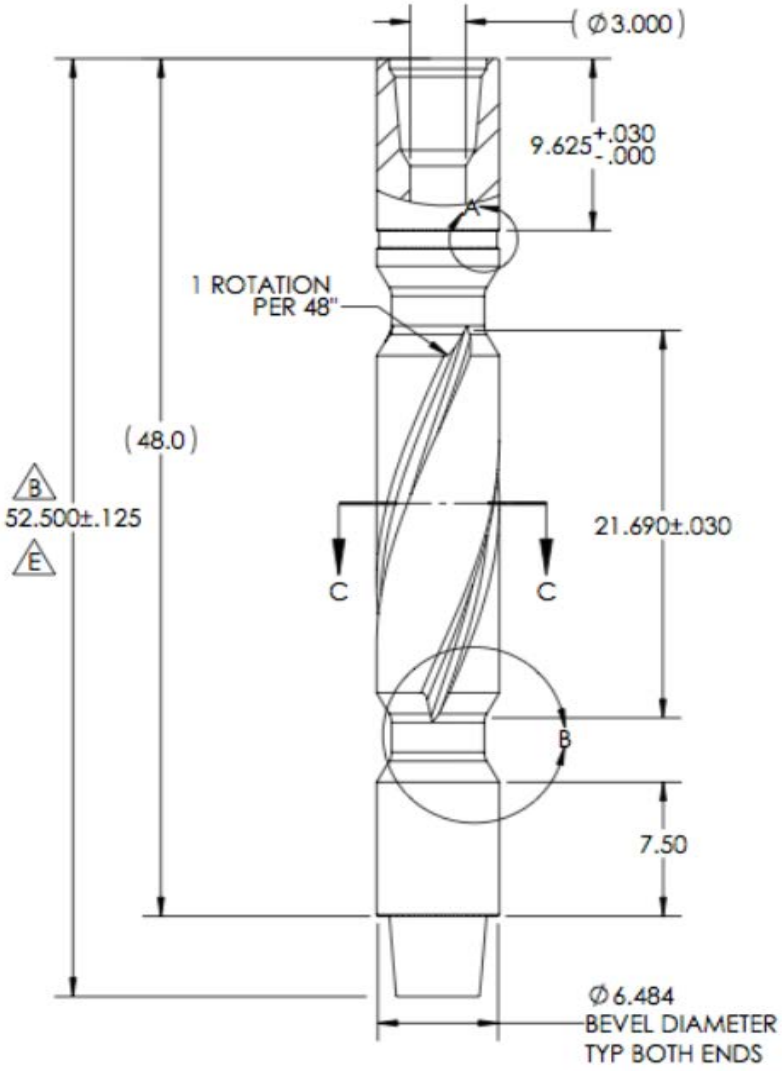

Figure 5.2 MCD tool dimensions and specifications

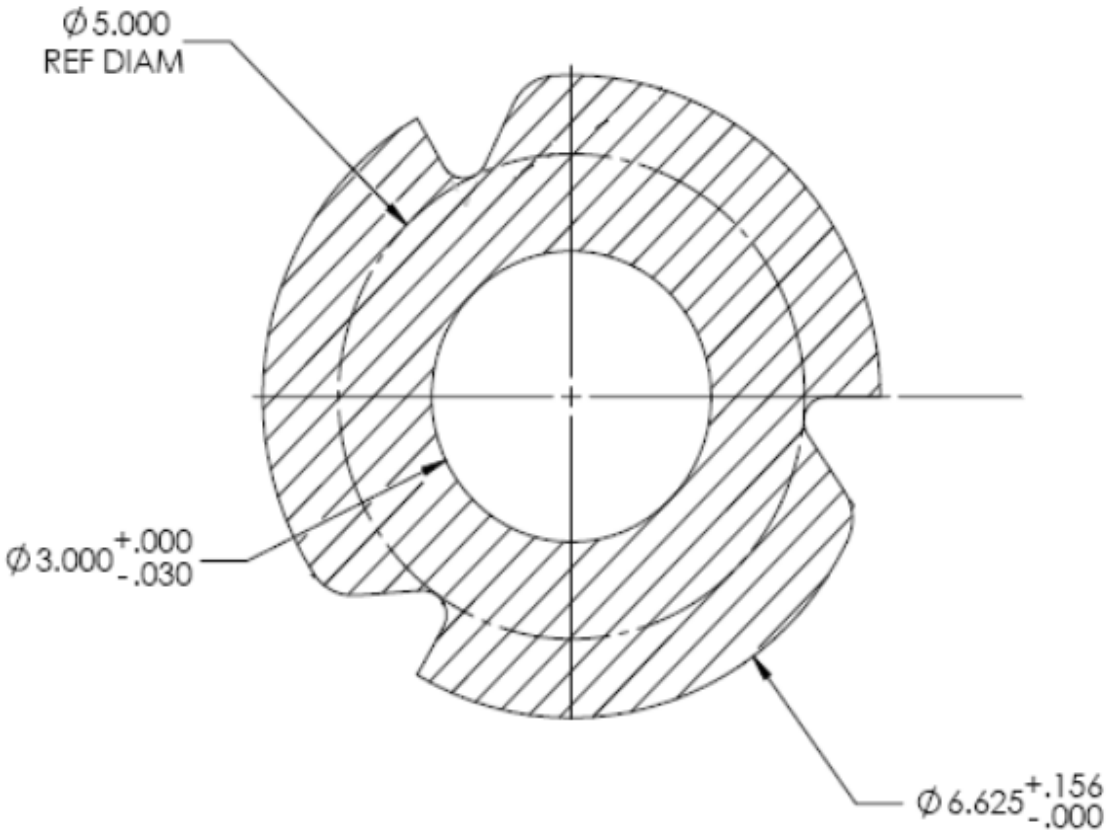

Figure 5.3 Outer and inner diameter of MCD tool

5.3 Test Matrix

The test matrix was designed to simulate real drilling scenario. Different parameters taken are shown in the Table 5.2. Different combinations of these parameters leads to 81 possible cases. For each case the algorithm was followed and values were obtained for cutting removal tool placement. Chike Nwagu et al. in their paper discussed about the applications of MCD to improve hole cleaning. They conducted trial runs for MCD in Illah fields, Nigeria and found good improvement in hole cleaning when the tool was used. In

their actual field runs they kept pipe rotation speed at 160-180 RPM. Therefore, in this report, RPM values are taken to be 200, 300 and 400 RPM.

Table 5.2 Different parameters for generating test matrix

RPM	Wellbore Inclination	Mud Flow Rate (GPM)	Cutting injection (Kg/s)
200, 300, 400	60 º, 75 º, 90 º	300, 400, 500	0.5, 0.75,1

The overall test matrix is shown in Table 5.3. All the values are obtained by using equations mentioned in earlier sections.

Table 5.3 Test Matrix

S.No	RPM	Wellbore inclination	Mud Flowrate GPM	ROP in ft/hr	Vcr Lifting m/s	Vel diff m/s	TKE required m2/s2
1	200	60	300	35.84	0.665	0.333	0.084
2	200	60	300	53.76	0.670	0.339	0.095
3	200	60	300	71.69	0.675	0.344	0.105
4	200	60	400	35.84	0.662	0.219	0.029
5	200	60	400	53.76	0.666	0.224	0.034
6	200	60	400	71.69	0.670	0.228	0.038
7	200	60	500	35.84	0.660	0.107	0.002
8	200	60	500	53.76	0.663	0.111	0.003
9	200	60	500	71.69	0.667	0.114	0.004
10	200	75	300	35.84	0.700	0.369	0.111
11	200	75	300	53.76	0.705	0.374	0.123
12	200	75	300	71.69	0.710	0.379	0.135
13	200	75	400	35.84	0.697	0.255	0.046
14	200	75	400	53.76	0.701	0.259	0.051
15	200	75	400	71.69	0.705	0.263	0.057
16	200	75	500	35.84	0.696	0.143	0.008
17	200	75	500	53.76	0.699	0.146	0.010
18	200	75	500	71.69	0.702	0.150	0.012
19	200	90	300	35.84	0.712	0.380	0.121
20	200	90	300	53.76	0.717	0.386	0.133

Table 5.3 continued.

21	200	90	300	71.69	0.722	0.390	0.145
22	200	90	400	35.84	0.709	0.267	0.052
23	200	90	400	53.76	0.713	0.271	0.058
24	200	90	400	71.69	0.717	0.275	0.064
25	200	90	500	35.84	0.707	0.155	0.011
26	200	90	500	53.76	0.711	0.158	0.013
27	200	90	500	71.69	0.714	0.161	0.015
28	300	60	300	35.84	0.592	0.260	0.007
29	300	60	300	53.76	0.606	0.274	0.014
30	300	60	300	71.69	0.618	0.287	0.024
31	300	60	400	35.84	0.584	0.142	0.001
32	300	60	400	53.76	0.595	0.153	0.000
33	300	60	400	71.69	0.606	0.164	0.001
34	300	60	500	35.84	0.580	0.027	0.020
35	300	60	500	53.76	0.589	0.036	0.015
36	300	60	500	71.69	0.597	0.045	0.010
37	300	75	300	35.84	0.631	0.300	0.017
38	300	75	300	53.76	0.644	0.313	0.028
39	300	75	300	71.69	0.656	0.325	0.040
40	300	75	400	35.84	0.624	0.182	0.000
41	300	75	400	53.76	0.635	0.193	0.002
42	300	75	400	71.69	0.644	0.203	0.005
43	300	75	500	35.84	0.620	0.067	0.009
44	300	75	500	53.76	0.629	0.076	0.005
45	300	75	500	71.69	0.637	0.084	0.003
46	300	90	300	35.84	0.644	0.313	0.022
47	300	90	300	53.76	0.657	0.326	0.033
48	300	90	300	71.69	0.669	0.337	0.047
49	300	90	400	35.84	0.637	0.195	0.001
50	300	90	400	53.76	0.648	0.206	0.004
51	300	90	400	71.69	0.657	0.215	0.008
52	300	90	500	35.84	0.633	0.080	0.006
53	300	90	500	53.76	0.642	0.089	0.003
54	300	90	500	71.69	0.650	0.097	0.001
55	400	60	300	35.84	0.471	0.140	0.040
56	400	60	300	53.76	0.502	0.170	0.018
57	400	60	300	71.69	0.528	0.197	0.005
58	400	60	400	35.84	0.454	0.012	0.098
59	400	60	400	53.76	0.479	0.037	0.069
60	400	60	400	71.69	0.502	0.060	0.046
61	400	60	500	35.84	0.444	-0.109	0
62	400	60	500	53.76	0.465	-0.088	0
63	400	60	500	71.69	0.484	-0.069	0

Table 5.3 continued

64	400	75	300	35.84	0.520	0.189	0.020
65	400	75	300	53.76	0.548	0.216	0.006
66	400	75	300	71.69	0.572	0.241	0.000
67	400	75	400	35.84	0.505	0.063	0.063
68	400	75	400	53.76	0.527	0.085	0.041
69	400	75	400	71.69	0.548	0.106	0.025
70	400	75	500	35.84	0.495	-0.058	0
71	400	75	500	53.76	0.514	-0.038	0
72	400	75	500	71.69	0.532	-0.021	0
73	400	90	300	35.84	0.536	0.204	0.015
74	400	90	300	53.76	0.563	0.231	0.003
75	400	90	300	71.69	0.587	0.255	0.000
76	400	90	400	35.84	0.521	0.079	0.053
77	400	90	400	53.76	0.543	0.101	0.034
78	400	90	400	71.69	0.563	0.121	0.020
79	400	90	500	35.84	0.512	-0.041	0
80	400	90	500	53.76	0.530	-0.023	0
81	400	90	500	71.69	0.547	-0.005	0

5.4 CFD Simulations

Geometry of the tool was prepared and properly meshed using CFD software, as shown in Fig. 5.4. Total length of the drill pipe was taken as 2432 in (48 in entry length, 22 in tool length, and 2362 in pipe length after tool) with 1 tool in it. In CFD Software, several models exist that can be used to simulate particle suspension/transport in flowing fluid. However, those models cannot be used to simulate drilling conditions because of several limitations in them. Fig. 5.5 shows the first step in simulation. In the General Tab, steady state case was chosen in all the simulations in this project. Also, gravitational pull was considered to be in -x axis if the well is completely horizontal and in -y axis is the well is completely vertical. Depending upon the inclination of the wellbore, gravity vector was split into its components along x axis and y axis. For example, if the wellbore inclination

was 60º then gravity along x axis was taken as g.sin60º = 9.8sin60º and gravity along y axis was taken as g.cos60º.

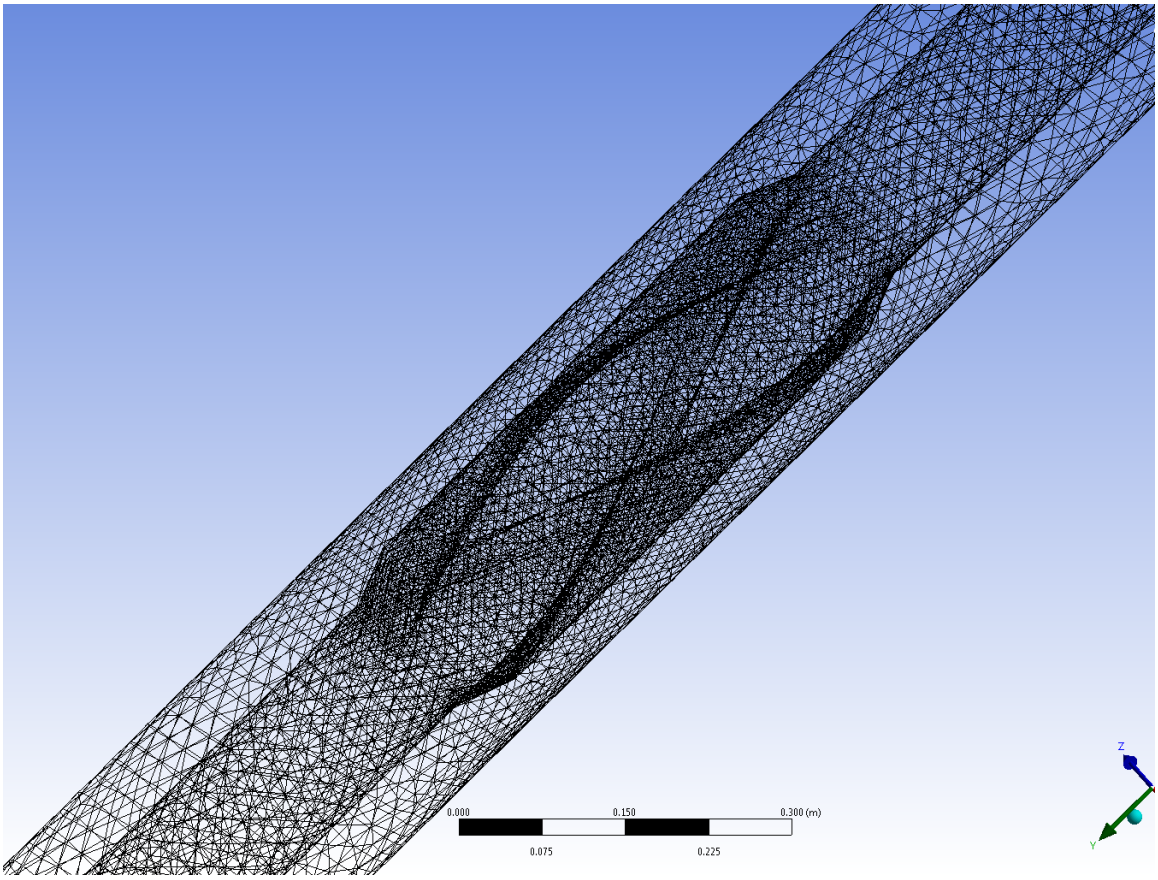

Figure 5.4 Tool geometry meshed using CFD

The next tab (Fig 5.6) is Models which displays several mathematical models that can be used to simulate various fluid flow conditions. Since it is assumed that the tool generates turbulence in the fluid, viscous k-epsilon model was chosen. Please note that in k-epsilon model, default fluid is newtonian and user command has to be given to convert fluid type from newtonian to non-newtonian. Without the command, CFD software does not show option to choose yield power law fluid model for simulation. Since the inner pipe

is rotating, realizable k-epsilon model with curvature correction was selected to yield best results. Eulerian multiphase model was not selected as it treats the particles as fluid and tries to calculate everything based on that. This means that the fluid velocity does not have to reach critical velocity to cause particle movement. The particle bed keeps moving even when the mud velocity is significantly low.

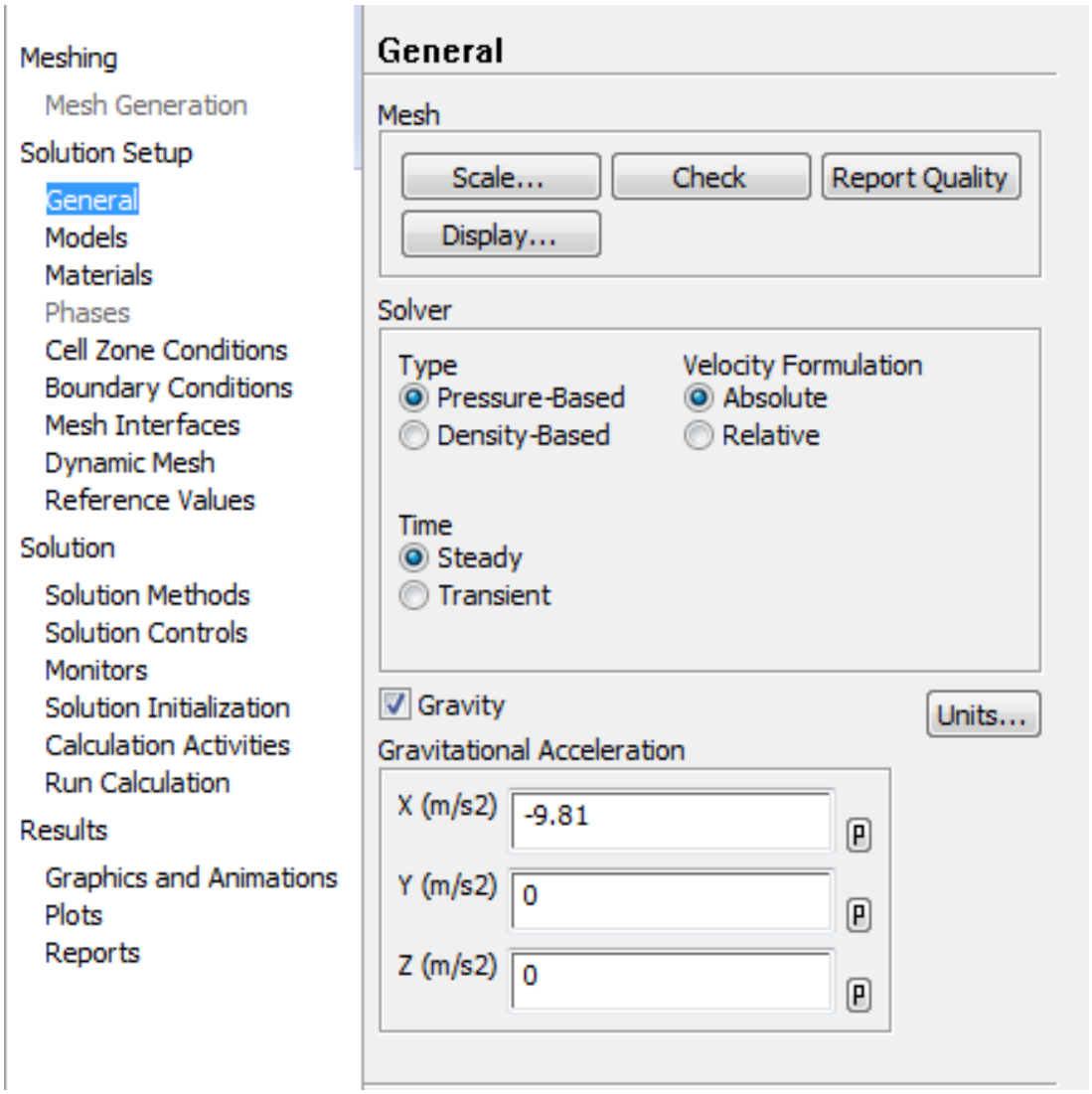

Figure 5.5 General tab in CFD

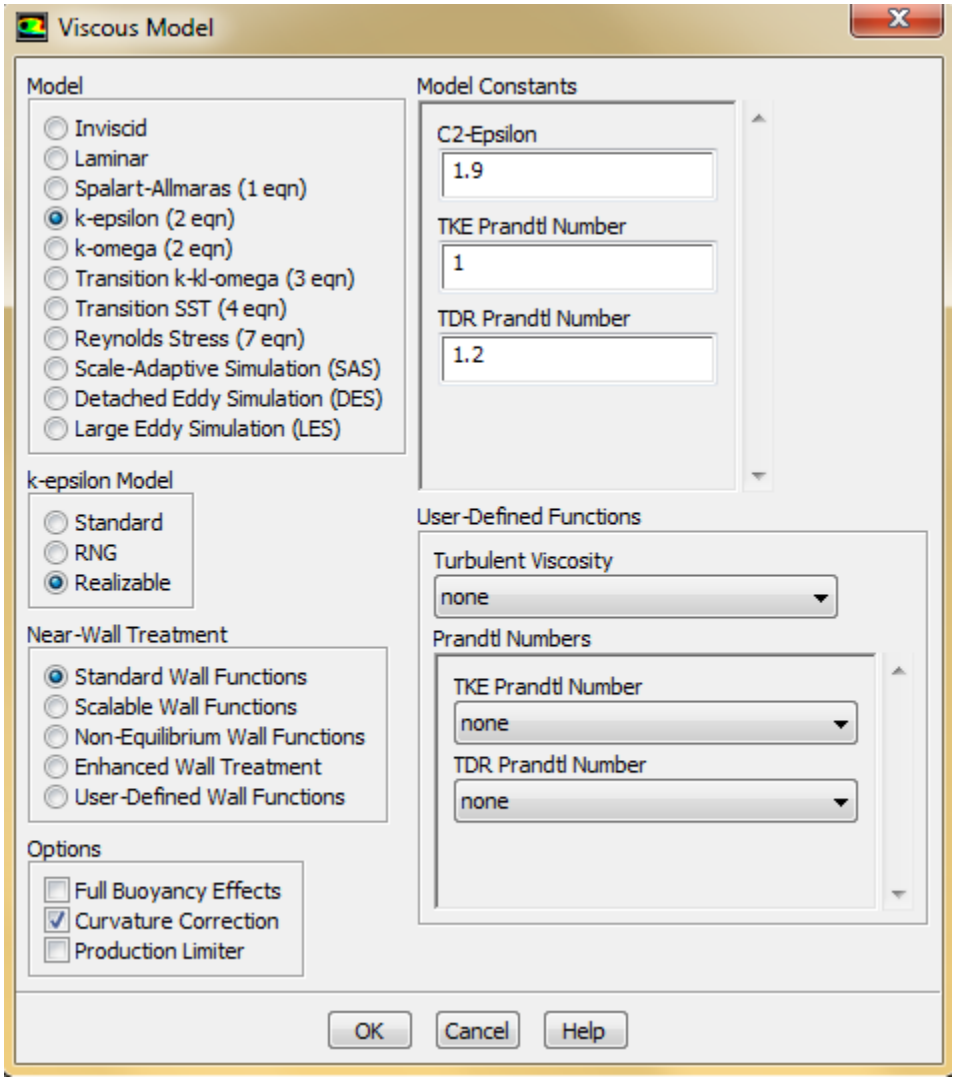

Figure 5.6 Model selection in CFD

In the next tab, i.e., Material Tab, fluid properties are defined. The fluid or mud was given a density of 1200 kg/m^3 which is equivalent to 10 ppg. Fig. 5.7 and Fig. 5.8 shows the selections made and values taken for different properties of mud.

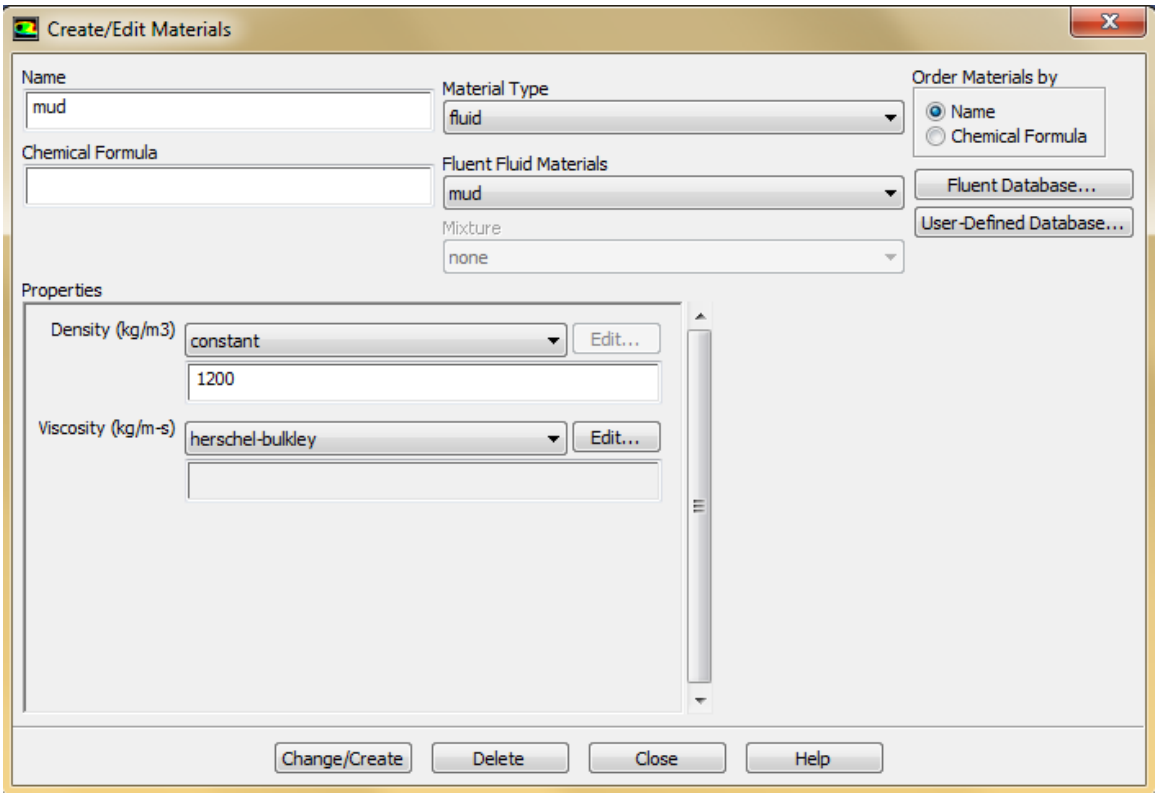

Figure 5.7 Selection of mud density and fluid model

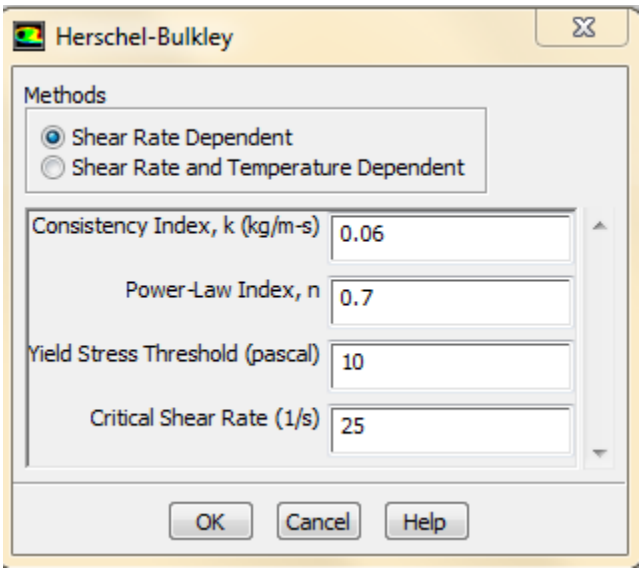

Figure 5.8 Herschel Bulkley fluid model inputs parameters

In Cell Zone Tab (Fig. 5.9), the entire zone around the tool was rotated instead of just tool rotation. This means that the entire fluid around the tool rotates along with the tool and there is no relative motion between the tool and the fluid around it. This assumption was made because of the narrow gap between wellbore wall and tool wall. It also helps the solution to converge quickly. Unit value in Y Rotation-Axis-Direction means that the fluid is rotating in clockwise direction (same as the direction of tool rotation).

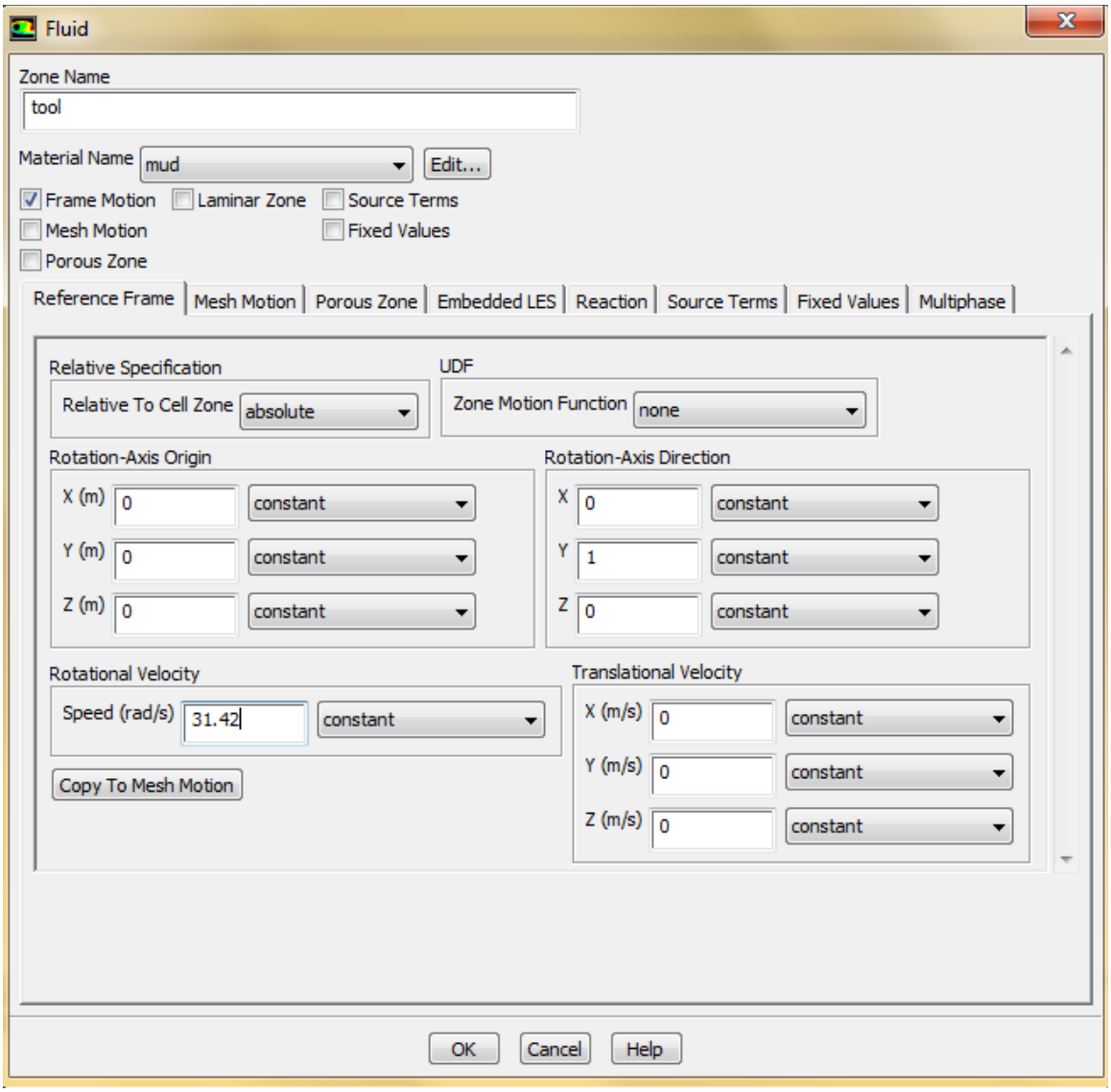

Figure 5.9 Rotation of whole cell zone around the tool

In the Boundary Conditions, the entire drill string was rotated clockwise at various speeds. In this case the entire fluid around drill pipe does not rotate as a zone but rotates because of the rotation of the drill string only. Also, based upon already calculated fluid velocity above the bed, inlet velocity value was given in CFD software as shown in Fig. 5.10.

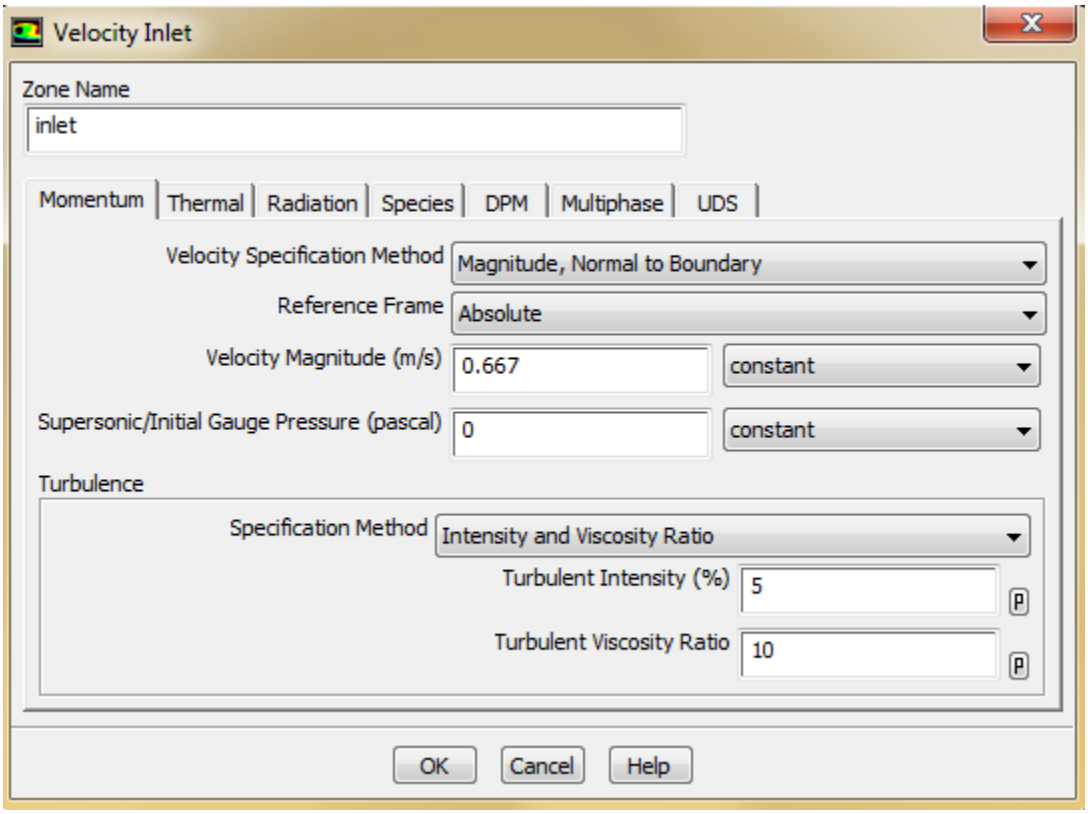

Figure 5.10 Setting of boundary conditions and inlet velocity

The next step in the simulation setup was creating an interface between annular zone and tool zone. From inlet annulus to tool annulus is the first interface and from annulus around tool to annulus around drill string in the second interface. By defining these interfaces, it was made sure that fluid flows from one zone to another in continuity (see

Fig. 5.11). This step was followed by final calculation step. Solution was initialized using default values and simulation was run till convergence.

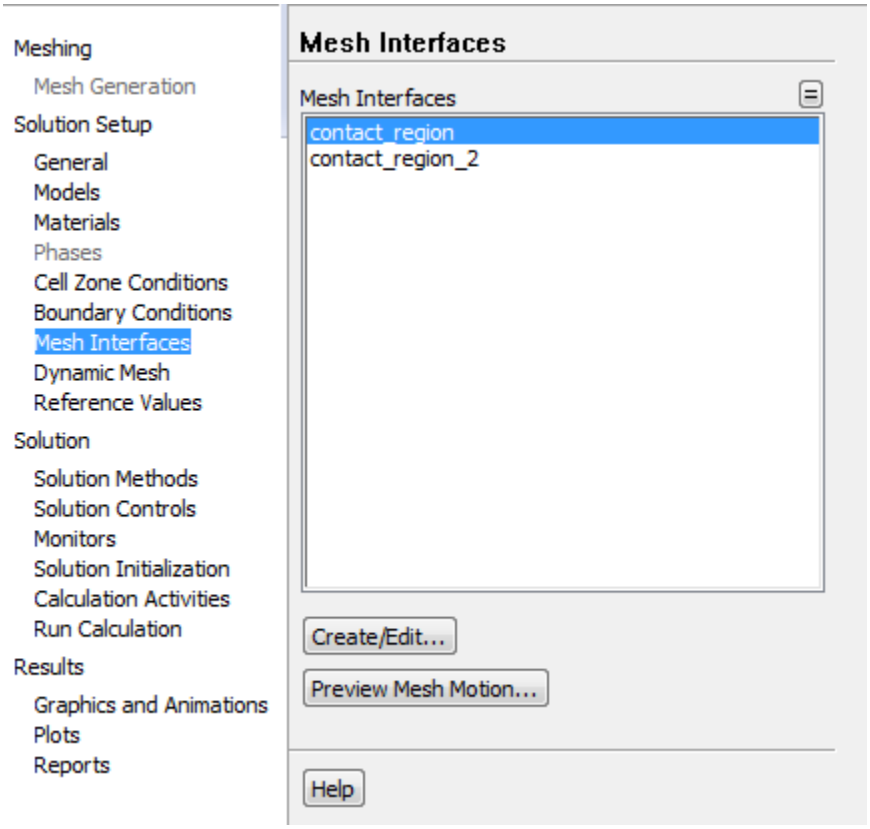

Figure 5.11 Defining mesh interface

To generate the plot of TKE vs distance, a line along the bed surface was drawn and TKE measurements were taken along that line. All the plots are given in the result and discussion section.

CHAPTER 6

RESULTS AND DISCUSSION

In the previous section, description of test matrix was given and various parameters that were chosen to proceed for calculations were mentioned. In the matrix different combinations of RPM, wellbore inclination, mud flow rate, and ROP were taken to obtain critical velocity for lifting. From the mud flow rate and desired cutting concentration (10% in this report), actual flow velocity of mud over the bed is calculated. Following the procedure discussed in previous chapter a thorough matrix was created with values of critical lift velocity and actual fluid velocity in it. From it, additional kinetic energy required to lift the cuttings was calculated. In this section, the calculated TKE is going to be used for estimating spacing between two tools.

From the calculations (Table 6.1) it can be seen that linear velocity of mud inside the annulus is almost constant for a particular GPM at different ROP/cutting injection rate. Therefore, for a particular GPM, RPM, and inclination, only 1 simulation was run. It leaves us with a total of 27 simulations to be run. However, in three cases the TKE required is 0 because the fluid velocity is already greater than critical lifting velocity. The cases are 400 RPM + 500GPM + 90º inclination, 400 RPM + 500GPM + 75º inclination, and 400 RPM + 500GPM + 60º inclination. Hence, a total of 24 simulations were run for several combinations of RPM, GPM, inclination, and ROP. Simulation results are given in the Fig. 6.1 through Fig. 6. 14.

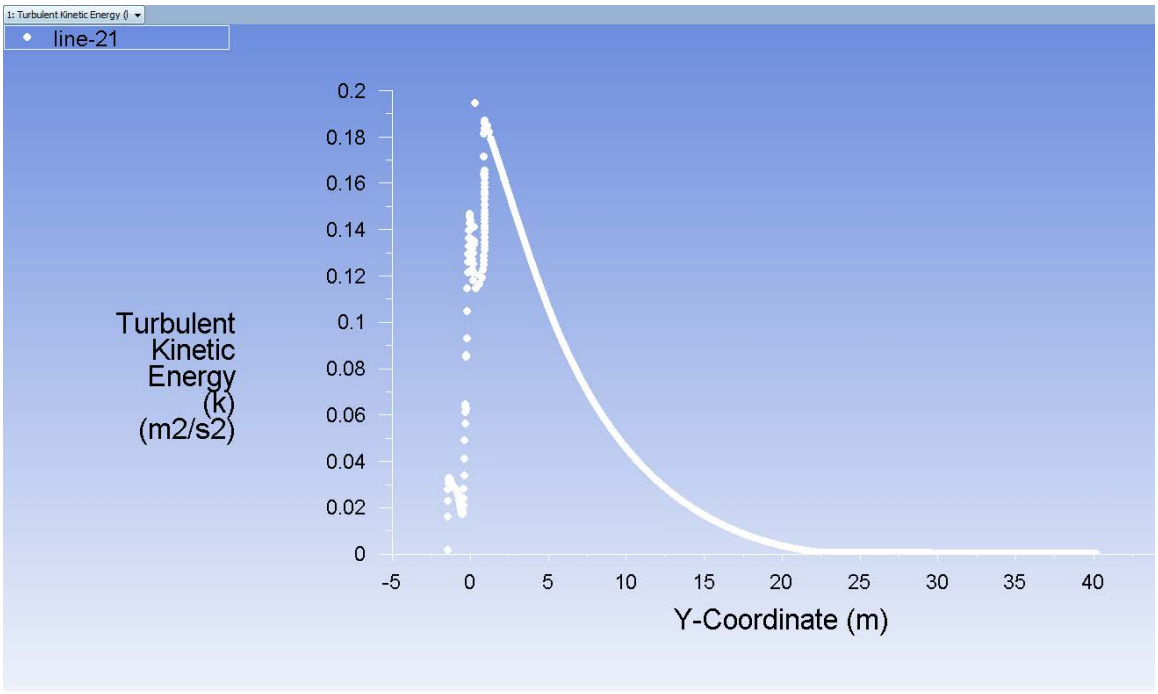

Figure 6.1 TKE dissipation for 200RPM, 300GPM, and 60 º, 75 º, 90º inclination angle

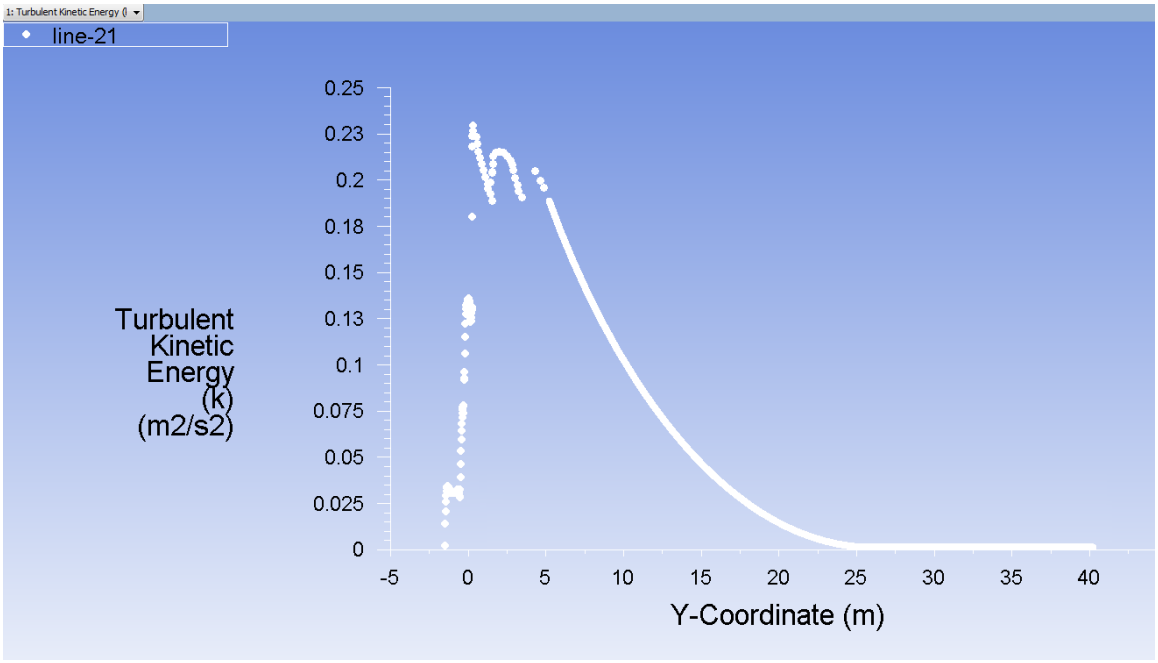

Figure 6.2 TKE dissipation for 200RPM, 400GPM, and 60 º, 75 º, 90º inclination angle

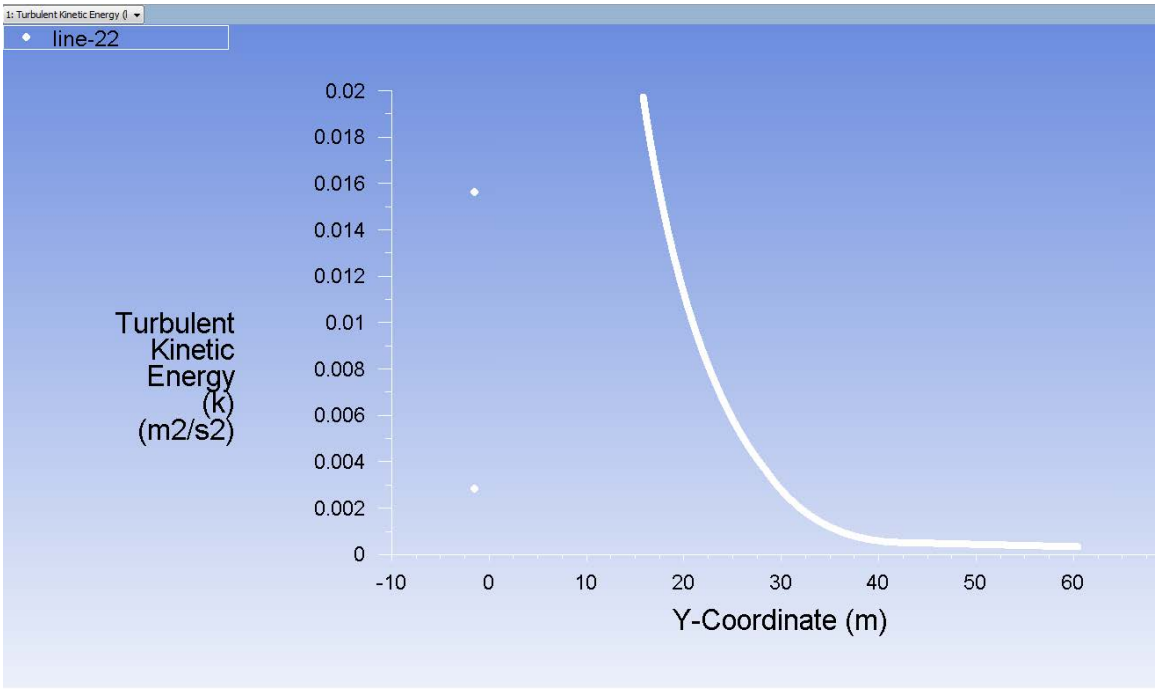

Figure 6.3 Zoomed section of TKE dissipation for 200RPM, 500GPM, and 60 º, 75 º, 90º inclination angle

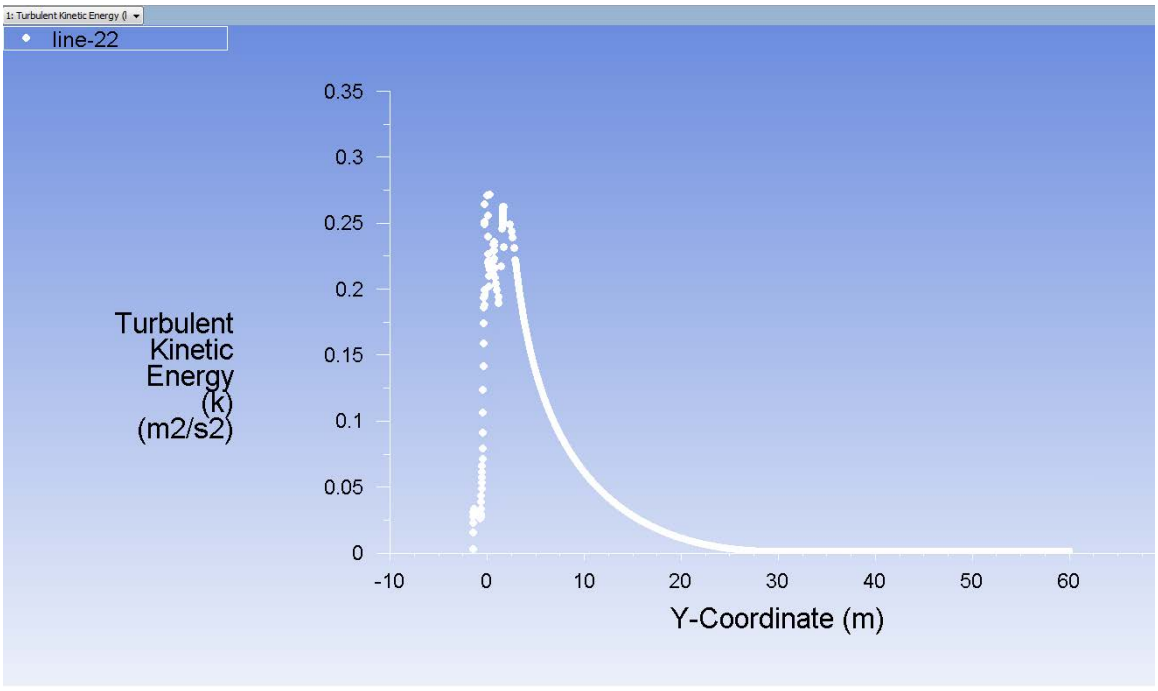

Figure 6.4 TKE dissipation for 200RPM, 500GPM, and 60 º, 75 º, 90º inclination angle

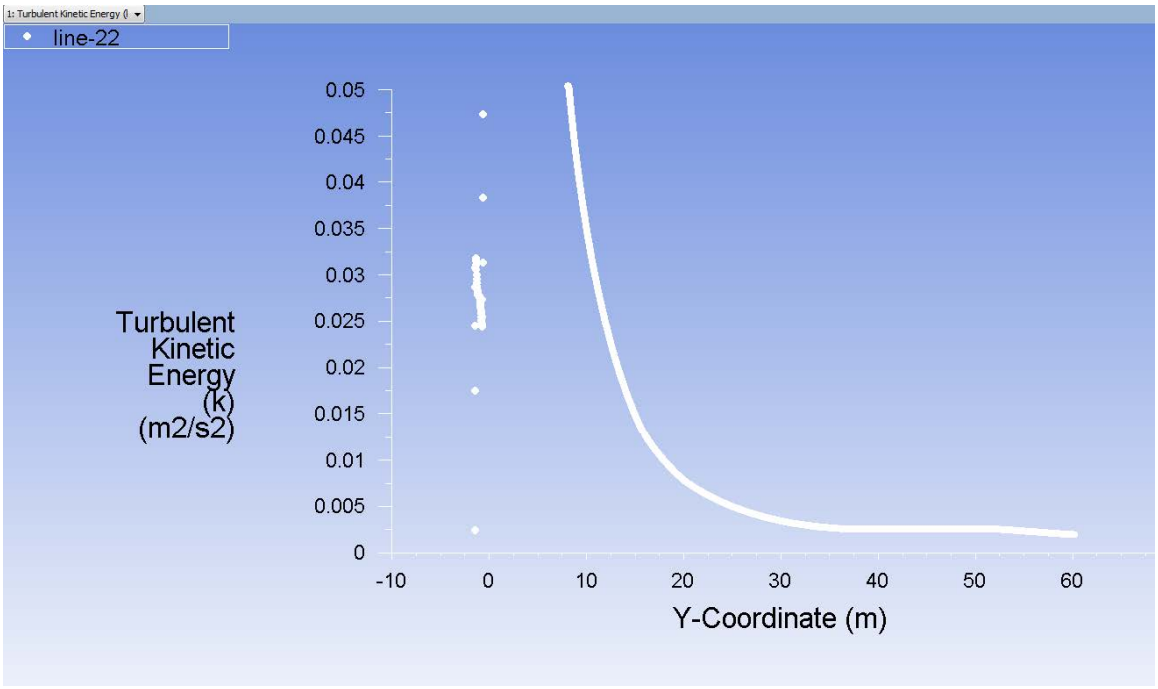

Figure 6.5 Zoomed section of TKE dissipation for 300RPM, 300GPM, and 60 º, 75 º, 90º inclination angle

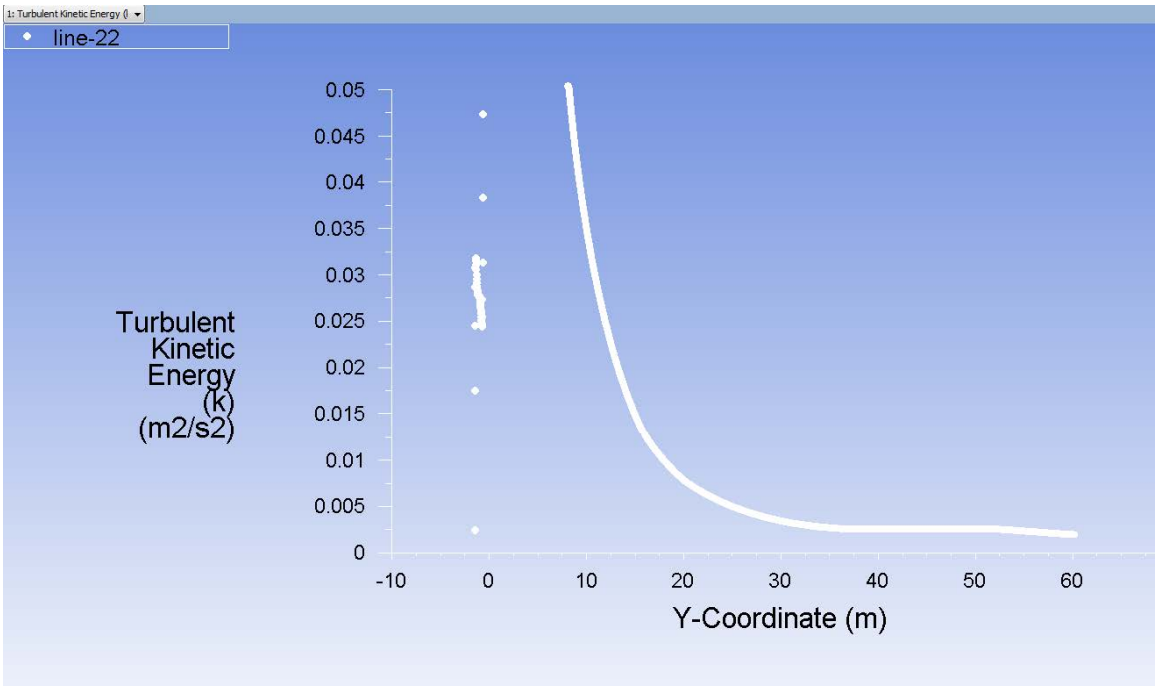

Figure 6.6 TKE dissipation for 300RPM, 300GPM, and 60 º, 75 º, 90º inclination angle

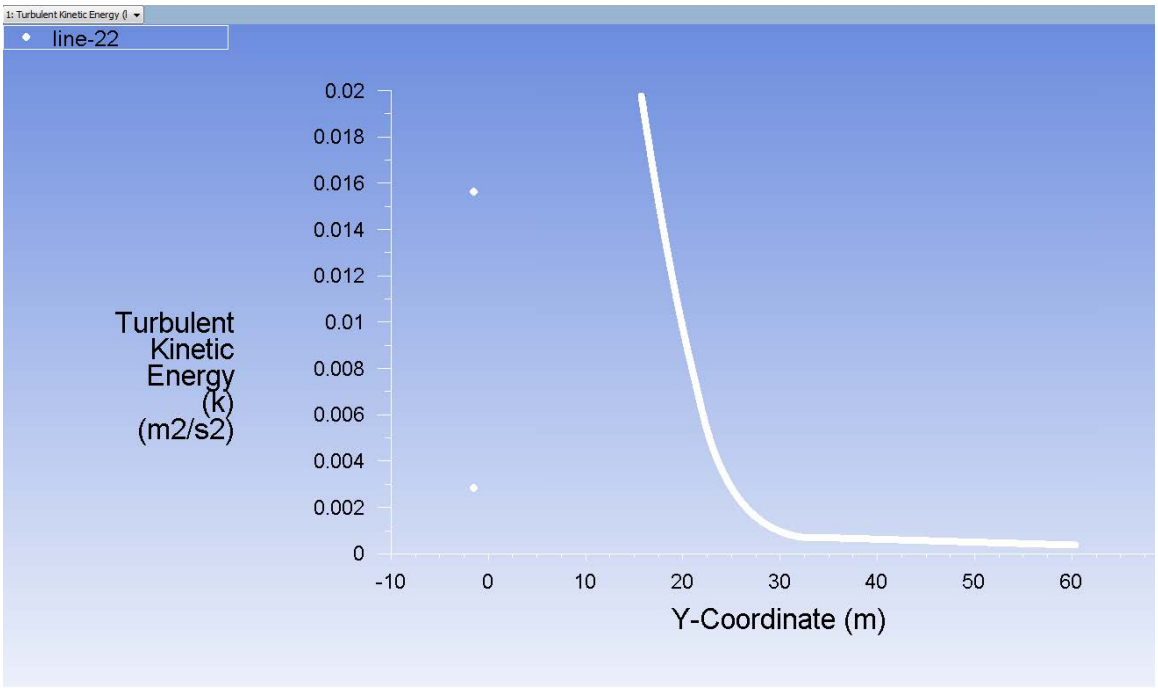

Figure 6.7 Zoomed section of TKE dissipation for 300RPM, 400GPM, and 60 º, 75 º, 90º inclination angle

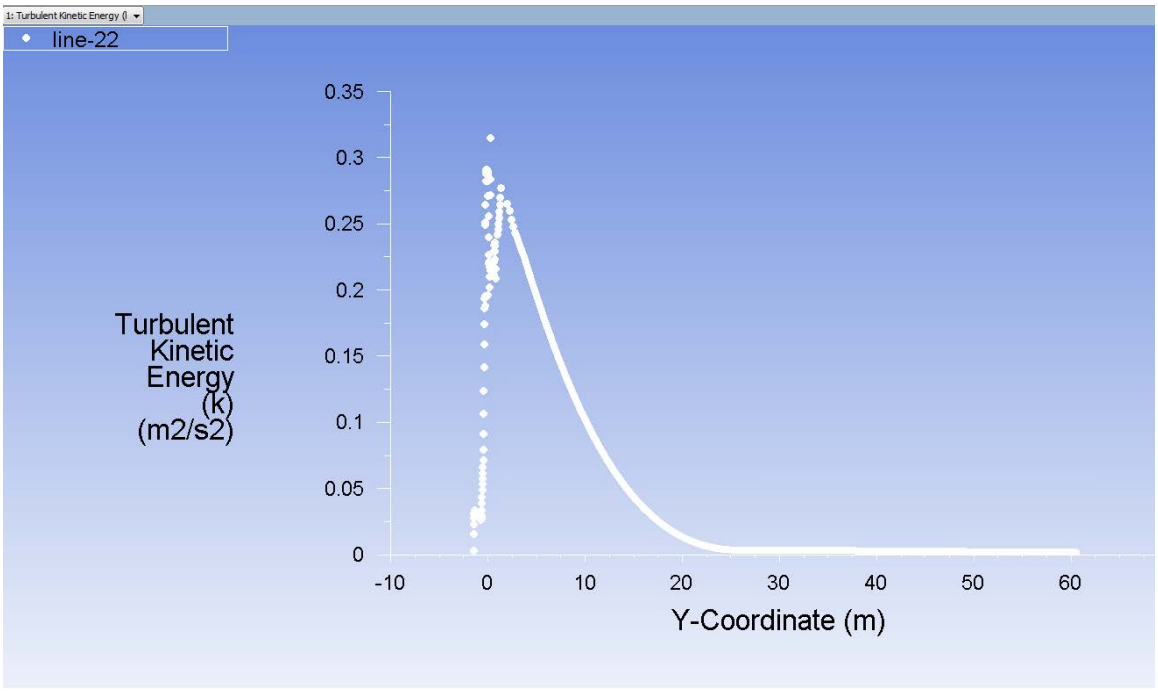

Figure 6.8 TKE dissipation for 300RPM, 400GPM, and 60 º, 75 º, 90º inclination angle

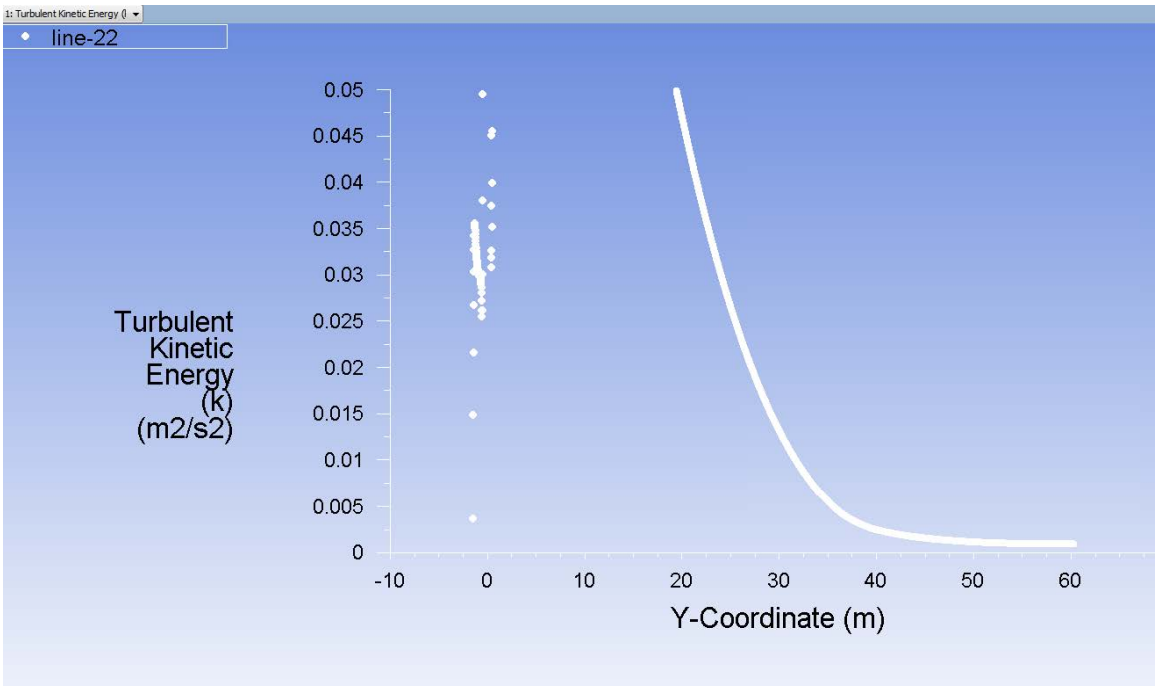

Figure 6.9 Zoomed section of TKE dissipation for 300RPM, 500GPM, and 60 º, 75 º, 90º inclination angle

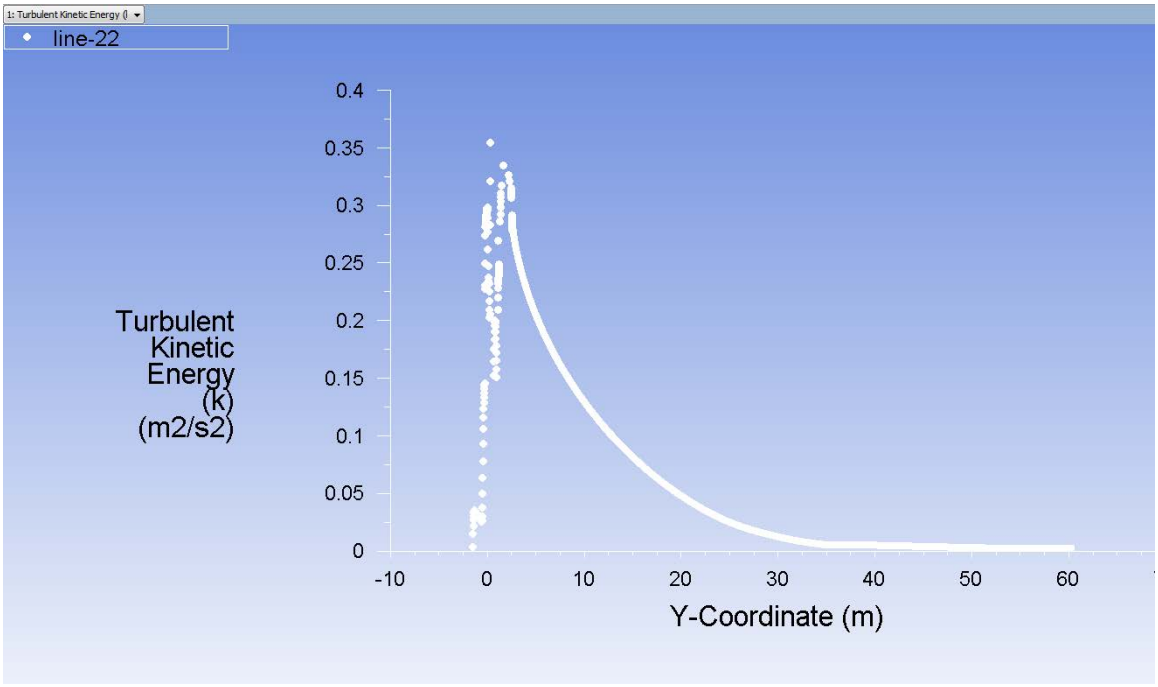

Figure 6.10 TKE dissipation for 300RPM, 500GPM, and 60 º, 75 º, 90º inclination angle

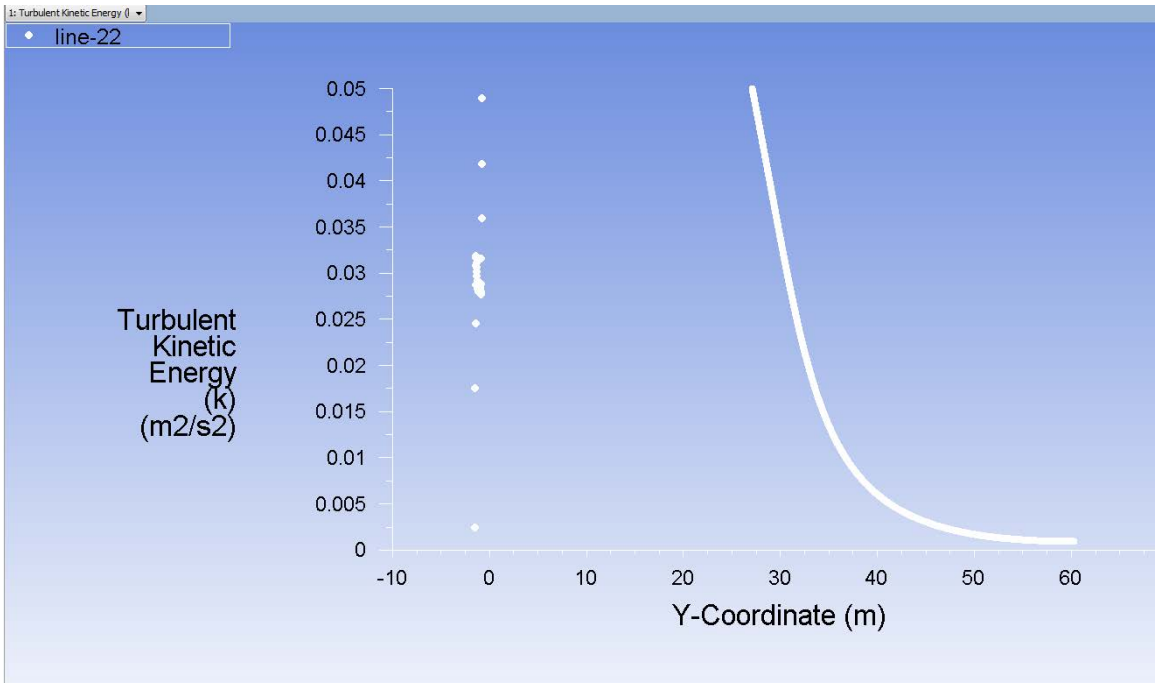

Figure 6.11 Zoomed section of TKE dissipation for 400RPM, 300GPM, and 60 º, 75 º, 90º inclination angle

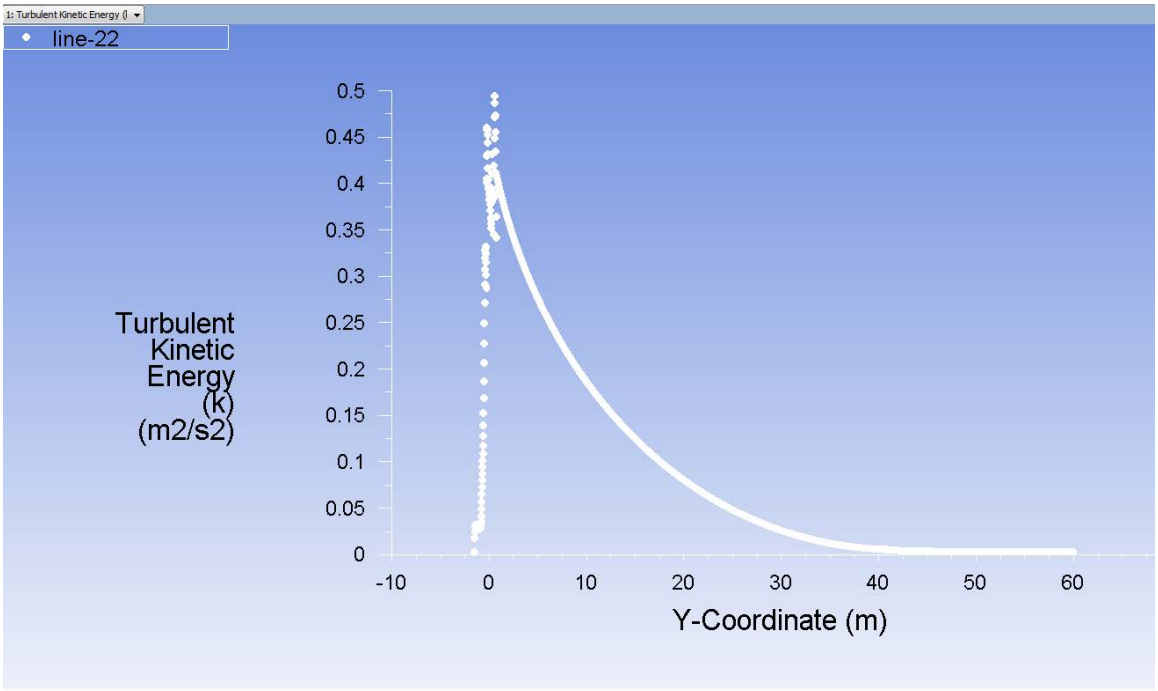

Figure 6.12 TKE dissipation for 400RPM, 300GPM, and 60 º, 75 º, 90º inclination angle

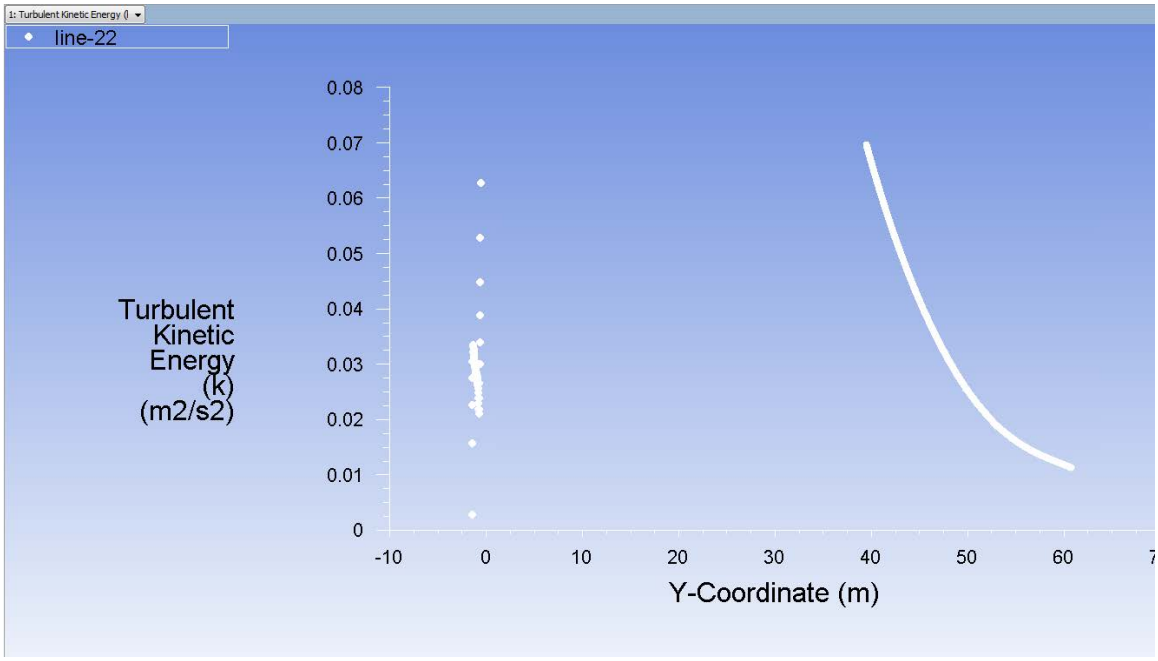

Figure 6.13 Zoomed section of TKE dissipation for 400RPM, 400GPM, and 60 º, 75 º, 90º inclination angle

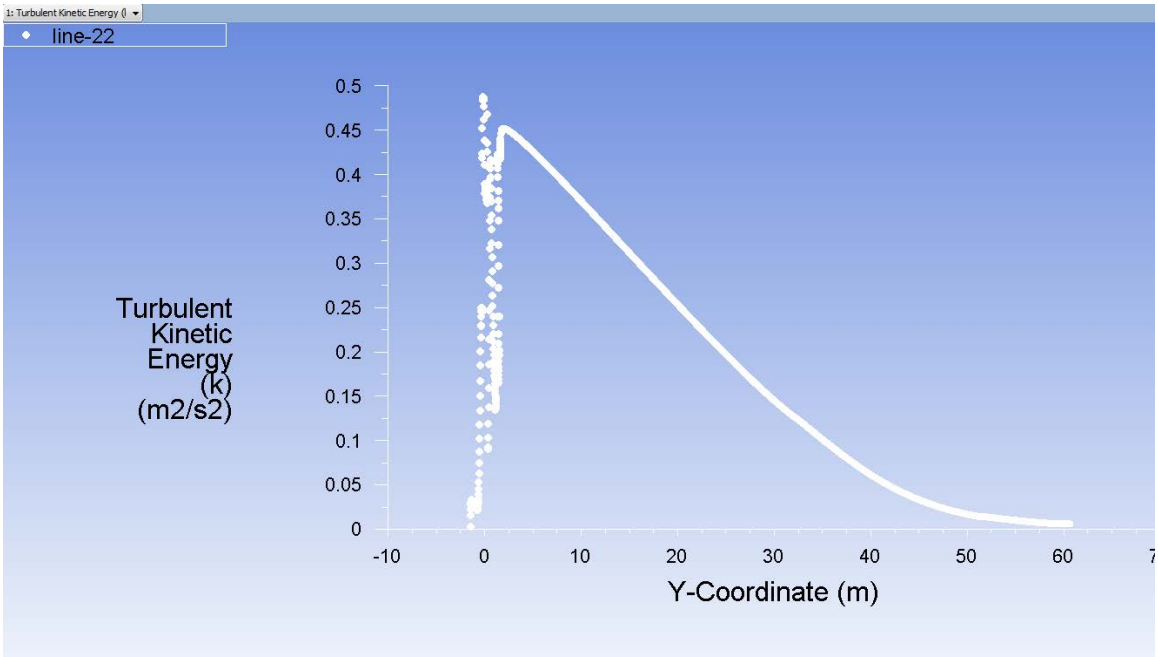

Figure 6.14 TKE dissipation for 400RPM, 400GPM, and 60 º, 75 º, 90º inclination angle

As already discussed there are four parameters namely RPM, ROP, wellbore angle, and GPM that are variables. To determine the effect of these parameters on tool placement distance a simple approach was taken. Tool placement distance was calculated by keeping all the parameters constant except for one parameter and then its effect was observed for three values. Also, to get a better picture of the tool spacing with different parameters, all the plots are shown in a single plot with overlaps in them. This is discussed in details in subsequent section.

Table 6.1 Test matrix with tool placement distance for helically grooved tool

S.No	RPM	Wellbore inclination	Mud Flowrate GPM	ROP in ft/hr	Vcr Lifting m/s	Vel diff m/s	TKE required m2/s2	Approximate Tool Placement (m)
1	200	60	300	35.84	0.665	0.333	0.084	**6**
2	200	60	300	53.76	0.670	0.339	0.095	**6**
3	200	60	300	71.69	0.675	0.344	0.105	**5**
4	200	60	400	35.84	0.662	0.219	0.029	**17**
5	200	60	400	53.76	0.666	0.224	0.034	**16**
6	200	60	400	71.69	0.670	0.228	0.038	**16**
7	200	60	500	35.84	0.660	0.107	0.002	**32**
8	200	60	500	53.76	0.663	0.111	0.003	**30**
9	200	60	500	71.69	0.667	0.114	0.004	**28**
10	200	75	300	35.84	0.700	0.369	0.111	**5**
11	200	75	300	53.76	0.705	0.374	0.123	**4**
12	200	75	300	71.69	0.710	0.379	0.135	**4**
13	200	75	400	35.84	0.697	0.255	0.046	**15**
14	200	75	400	53.76	0.701	0.259	0.051	**14**
15	200	75	400	71.69	0.705	0.263	0.057	**14**
16	200	75	500	35.84	0.696	0.143	0.008	**24**
17	200	75	500	53.76	0.699	0.146	0.010	**23**
18	200	75	500	71.69	0.702	0.150	0.012	**22**
19	200	90	300	35.84	0.712	0.380	0.121	**4**
20	200	90	300	53.76	0.717	0.386	0.133	**4**
21	200	90	300	71.69	0.722	0.390	0.145	**3**
22	200	90	400	35.84	0.709	0.267	0.052	**14**

Table 6.1 continued

23	200	90	400	53.76	0.713	0.271	0.058	**14**
24	200	90	400	71.69	0.717	0.275	0.064	**13**
25	200	90	500	35.84	0.707	0.155	0.011	**22**
26	200	90	500	53.76	0.711	0.158	0.013	**21**
27	200	90	500	71.69	0.714	0.161	0.015	**21**
28	300	60	300	35.84	0.592	0.260	0.007	**20**
29	300	60	300	53.76	0.606	0.274	0.014	**15**
30	300	60	300	71.69	0.618	0.287	0.024	**12**
31	300	60	400	35.84	0.584	0.142	0.001	**29**
32	300	60	400	53.76	0.595	0.153	0.000	**NA**
33	300	60	400	71.69	0.606	0.164	0.001	**29**
34	300	60	500	35.84	0.580	0.027	0.020	**27**
35	300	60	500	53.76	0.589	0.036	0.015	**29**
36	300	60	500	71.69	0.597	0.045	0.010	**32**
37	300	75	300	35.84	0.631	0.300	0.017	**14**
38	300	75	300	53.76	0.644	0.313	0.028	**11**
39	300	75	300	71.69	0.656	0.325	0.040	**10**
40	300	75	400	35.84	0.624	0.182	0.000	**NA**
41	300	75	400	53.76	0.635	0.193	0.002	**26**
42	300	75	400	71.69	0.644	0.203	0.005	**22**
43	300	75	500	35.84	0.620	0.067	0.009	**32**
44	300	75	500	53.76	0.629	0.076	0.005	**35**
45	300	75	500	71.69	0.637	0.084	0.003	**37**
46	300	90	300	35.84	0.644	0.313	0.022	**12**
47	300	90	300	53.76	0.657	0.326	0.033	**11**
48	300	90	300	71.69	0.669	0.337	0.047	**8**
49	300	90	400	35.84	0.637	0.195	0.001	**29**
50	300	90	400	53.76	0.648	0.206	0.004	**23**
51	300	90	400	71.69	0.657	0.215	0.008	**21**
52	300	90	500	35.84	0.633	0.080	0.006	**34**
53	300	90	500	53.76	0.642	0.089	0.003	**37**
54	300	90	500	71.69	0.650	0.097	0.001	**41**
55	400	60	300	35.84	0.471	0.140	0.040	**30**
56	400	60	300	53.76	0.502	0.170	0.018	**33**
57	400	60	300	71.69	0.528	0.197	0.005	**40**
58	400	60	400	35.84	0.454	0.012	0.098	**35**
59	400	60	400	53.76	0.479	0.037	0.069	**40**
60	400	60	400	71.69	0.502	0.060	0.046	**44**
61	400	60	500	35.84	0.444	-0.109	0.180	**NA**
62	400	60	500	53.76	0.465	-0.088	0.147	**NA**
63	400	60	500	71.69	0.484	-0.069	0.119	**NA**
64	400	75	300	35.84	0.520	0.189	0.020	**33**
65	400	75	300	53.76	0.548	0.216	0.006	**39**

Table 6.1 continued

66	400	75	300	71.69	0.572	0.241	0.000	**NA**
67	400	75	400	35.84	0.505	0.063	0.063	**41**
68	400	75	400	53.76	0.527	0.085	0.041	**45**
69	400	75	400	71.69	0.548	0.106	0.025	**50**
70	400	75	500	35.84	0.495	-0.058	0.130	**NA**
71	400	75	500	53.76	0.514	-0.038	0.104	**NA**
72	400	75	500	71.69	0.532	-0.021	0.082	**NA**
73	400	90	300	35.84	0.536	0.204	0.015	**34**
74	400	90	300	53.76	0.563	0.231	0.003	**43**
75	400	90	300	71.69	0.587	0.255	0.000	**NA**
76	400	90	400	35.84	0.521	0.079	0.053	**42**
77	400	90	400	53.76	0.543	0.101	0.034	**47**
78	400	90	400	71.69	0.563	0.121	0.020	**52**
79	400	90	500	35.84	0.512	-0.041	0.116	**NA**
80	400	90	500	53.76	0.530	-0.023	0.092	**NA**
81	400	90	500	71.69	0.547	-0.005	0.072	**NA**

6.1 Effect of RPM

From the data it can be seen that RPM does not affect bed height and linear velocity of mud flowing over the bed. It effects only the tangential velocity of the mud. With increase in RPM the tangential velocity of mud increases significantly and this leads to reduced TKE requirement for lifting of cuttings. Also, critical lifting velocity decreases as the RPM increase. This is because V_{CL} is taken as linear velocity component, and not the resultant of linear and tangential velocities. Reduced V_{CL} means that for the same hole cleaning effect, less velocity is required, i.e., less TKE is required leading to greater distance between two tools. This implies that increasing RPM is a very good way to increase hole cleaning efficiency with or without MCD tool.

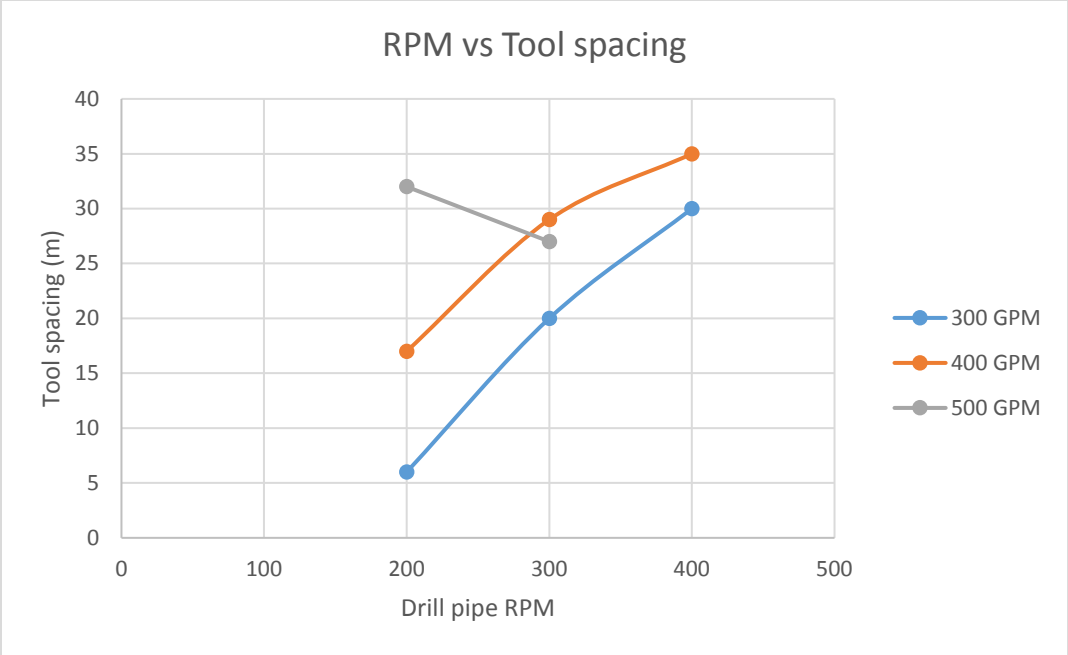

Figure 6.15 RPM vs Tool placement for helically grooved tool at different GPM and 60 degrees inclination

The plot in Fig. 6.15 shows that the trend is not linear. This means that at higher RPM values, cleaning of wellbore is more. But, at very high RPM, tool placement distance may remain same as the trend shows that it flattens out at higher RPM. A comparative plot of RPM and different GMP shows that at high GPM values, tool spacing first decrease and then increase infinitely (tool not required). This suggests that at the particular combination of 300 RPM and 500 GPM, effectiveness of MCD reduces. It also suggests that there exist an optimum combination of RPM and GPM to maintain a particular cutting concentration in the wellbore.

6.2 Effect of wellbore inclination

As evident from the equations, wellbore inclination does not affect anything other than critical lift velocity. As expected, V_{CL} increases as the inclination increases. This results in reduction in tool placement distance. As can be seen from the calculation table, for 200 RPM, 0.5kg/s cutting injection, and 300 GPM flow rate the tool placement distance reduces from 6m to 5m to 4m for 60º, 75 º and 90 º inclination angle respectively. The curve in Fig. 6.16 shows almost linear trend at lower flow rates. An analysis of sensitivity with flow rate shows that the trend remains same in all the cases. Also, at high flow rates, variation in tool spacing is much more with inclination. An important point to note here is that this data is obtained for wellbore angles that do not make angle is repose more than 40º as the bed will start to collapse in that case. For such a condition to exist wellbore inclination has to be greater than 50º.

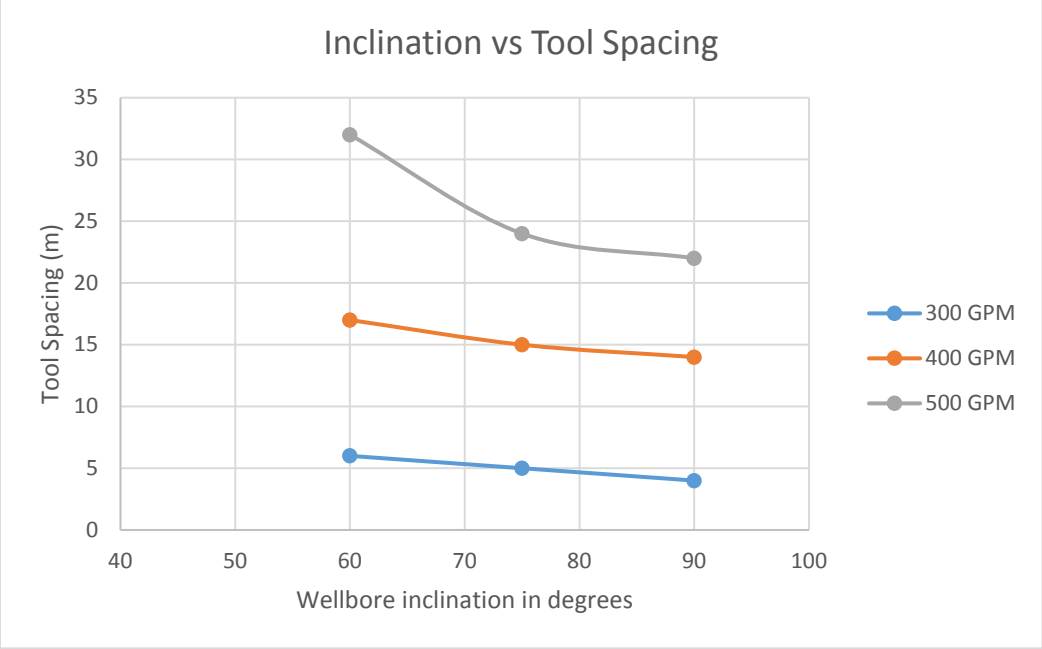

Figure 6.16 Well inclination vs Tool placement for helically grooved geometry

6.3 Effect of Flow rate

From the calculations it can be seen that with an increase in mud flow rate the linear flow velocity over the bed increases. This is in accordance with conservation of mass. Since cutting concentration in the wellbore was taken as a constant, the increase in velocity results in lower cutting concentration in the flowing fluid. Therefore, to keep the cutting concentration constant (10%), cuttings present in the bed must increase leading to more bed height. This simply means that if we want to maintain a cutting concentration of 10% in the wellbore we can afford to have more bed thickness. Because of the change in bed height, tangential velocity at the surface of the bed changes (it is a function of radius from the center of the wellbore) also changes. As the bed height increases, tangential flow velocity increases. The effect of increment in linear flow velocity and tangential flow velocity is that it drastically increases the distance between two tools. Results show that it is the most significant parameter in hole cleaning. At different rate of penetration (different amount of cutting generation), the trend remains the same. However, from the plot, it can be deduced that at low flow rates and at intermediate ROP, efficiency of MCD tool is maximum (for that particular flow rate).

The plot (Fig. 6.17) is not linear and is expected to flatten out and become parallel to y-axis. That would mean that at significantly higher flow rates there is no need of MCD tools. However, due to limitations on surface equipment sizing and flow pressure, GPM cannot always be increased to achieve such ideal conditions.

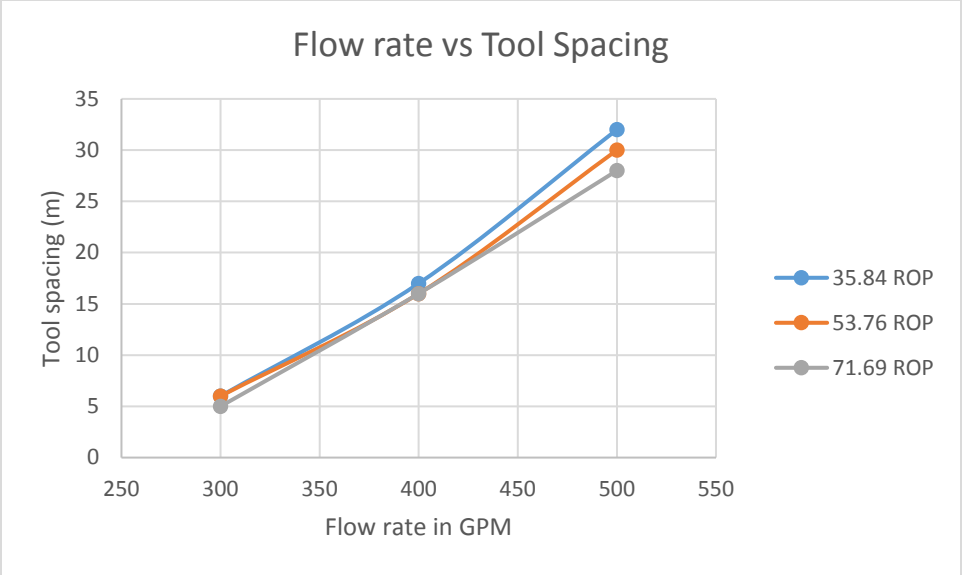

Figure 6.17 GPM vs Tool placement for helically grooved geometry

6.4 Effect of ROP

The first trend that is visible in the results is reduction in bed height with increase in ROP (cutting injection rate). This might seem contradictory at first. However, this result is for a constant cutting concentration of 10% in the wellbore. With an increment in ROP, more cuttings are generated resulting in more cutting concentration in wellbore under normal circumstances. It causes cutting concentration in fluid flowing over the bed to increases (more cleaning being done). So to maintain a constant cutting concentration of 10% in the wellbore, bed height must decrease. Because of reduced bed height, flow velocity over the bed reduces as the ROP increases. The tangential velocity also decreases at the surface of the bed (because of reduced bed height). This in turn causes critical flow velocity to increase resulting in reduced tool placement distance.

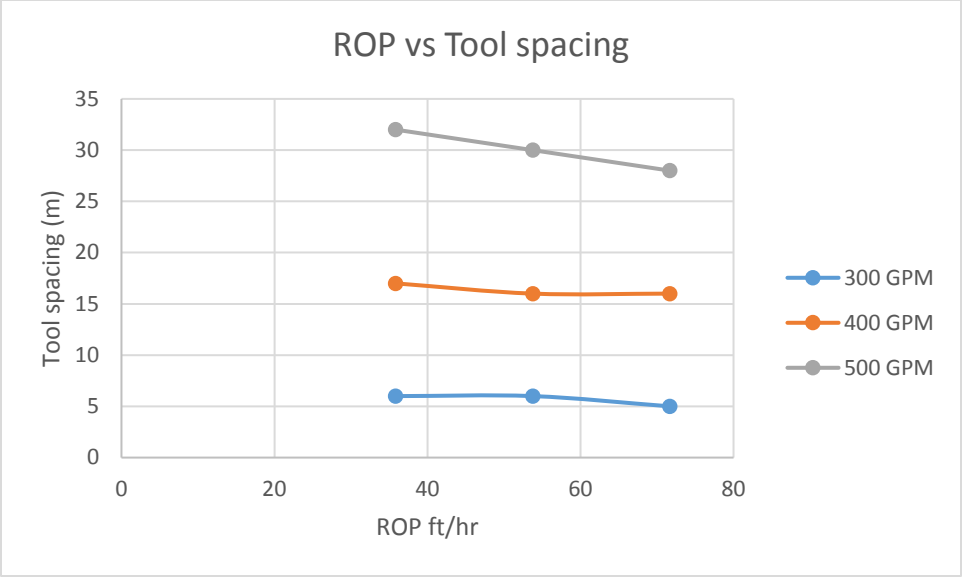

Figure 6.18 Cutting Injection rate vs Tool placement for helically grooved geometry

Fig. 6.18 shows that the plot between cutting injection rate (ROP) and tool placement distance is not linear. Also the values show that ROP does not affect tool placement a lot. It can be concluded that during drilling in the field ROP will have minimum effect on tool placement. A sensitivity analysis of the plots with flow rates indicates that at lower flow rates, tool spacing reduces insignificantly with increase in ROP. However, at higher GPM, tool spacing decreases noticeably with increasing ROP. The trend however is the same.

6.5 Tool with straightly grooved geometry

To optimize the tool performance, it is important to analyze the geometry of the tool and study the effect of blade or groove angle on the turbulence that it generates. This would also enable us to do a comparative study of tool cleaning efficiency with different

blade angles. To achieve this task, another tool was developed in CFD design modeler, with straight and parallel grooves instead of helical. All the other dimensions including drill pipe length, bit diameter, drill pipe diameter were kept same as earlier. Fluid rheology was also kept same. As the whole fluid zone around the tool is rotated along with the tool, any variation in turbulence if any would result solely from the geometry of the tool. Exactly the same steps were followed to run simulations. Figure 6.19 shows the meshed geometry that was used for simulations.

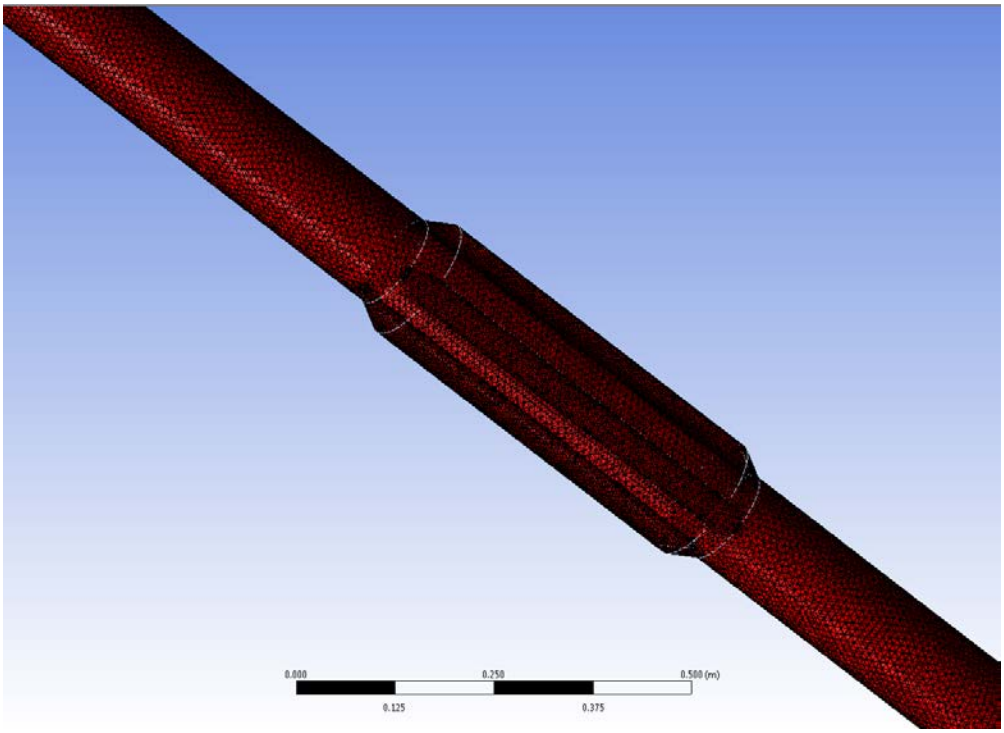

Figure 6.19 Straightly grooved tool geometry

As mentioned earlier, for running the simulations all the parameters including drill pipe length, mud rheology, cutting size, cutting density and well bore diameter were kept same as before. The results of the simulations with this new tool are shown in Fig. 6.20 through Fig 6.33.

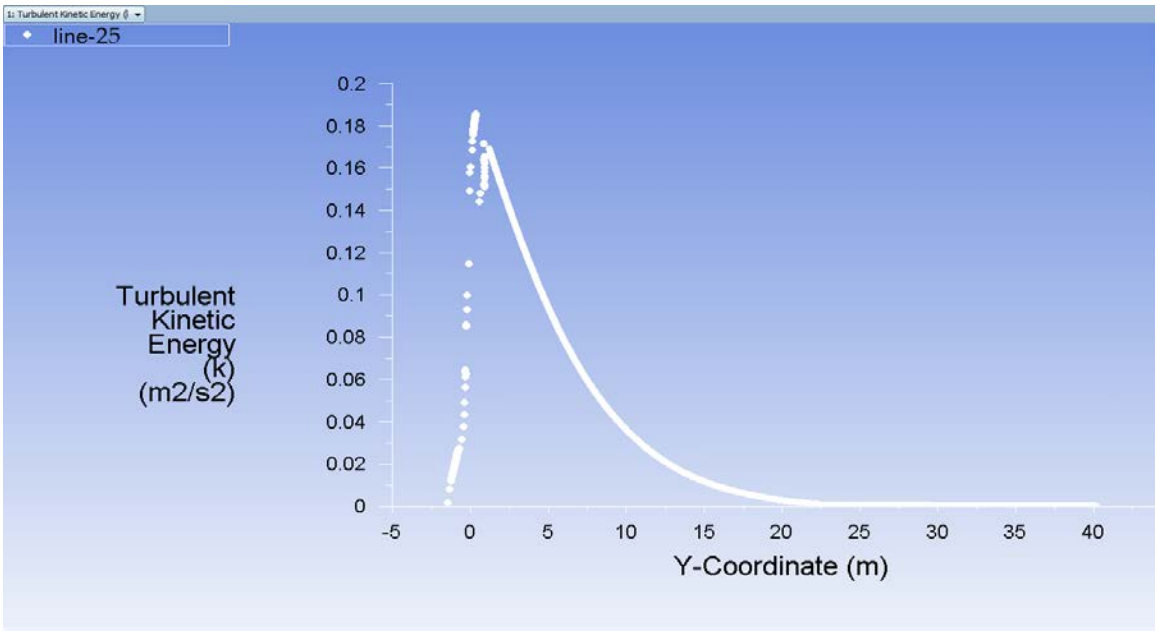

Figure 6.20 TKE dissipation for 200RPM, 300GPM, and 60 º, 75 º, 90º inclination angle with modified geometry

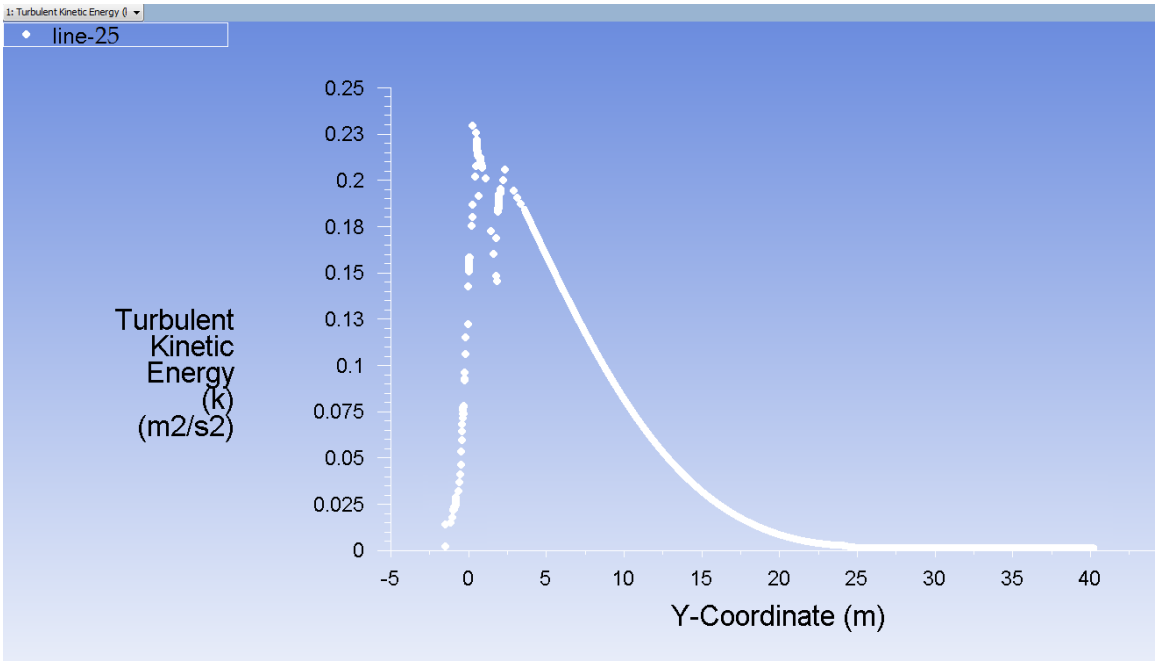

Figure 6.21 TKE dissipation for 200RPM, 400GPM, and 60 º, 75 º, 90º inclination angle with modified geometry

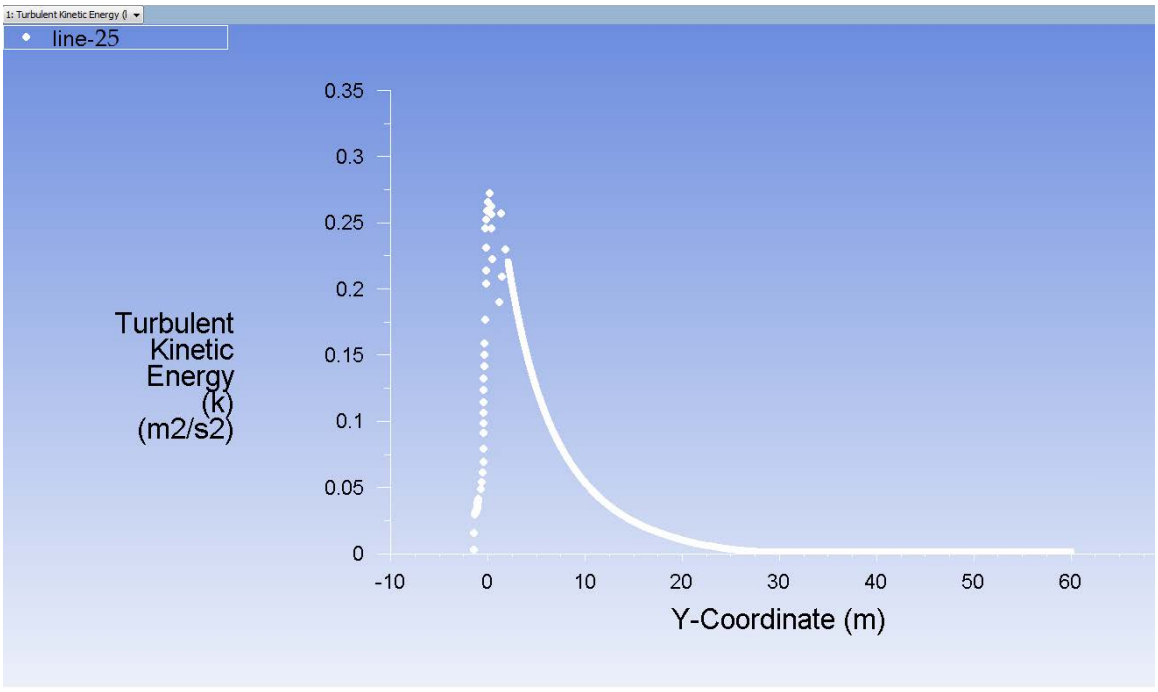

Figure 6.22 TKE dissipation for 200RPM, 500GPM, and 60 º, 75 º, 90º inclination angle with modified geometry

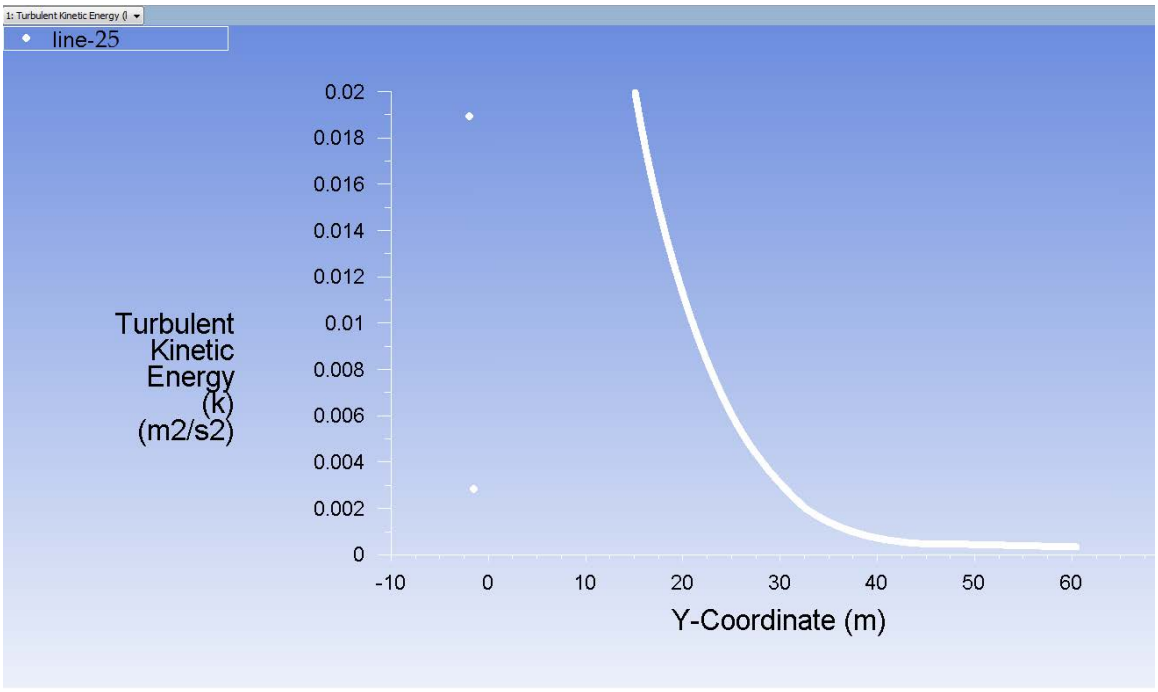

Figure 6.23 Zoomed section of TKE dissipation for 200RPM, 500GPM, and 60 º, 75 º, 90º inclination angle with modified geometry

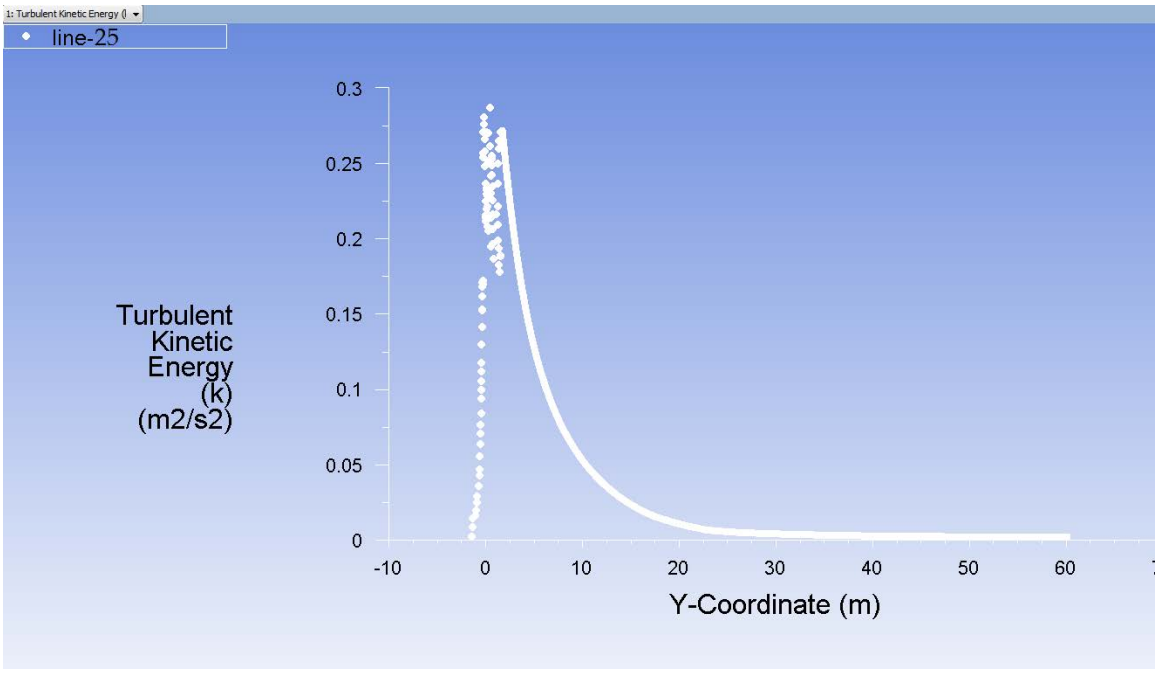

Figure 6.24 TKE dissipation for 300RPM, 300GPM, and 60 º, 75 º, 90º inclination angle with modified geometry

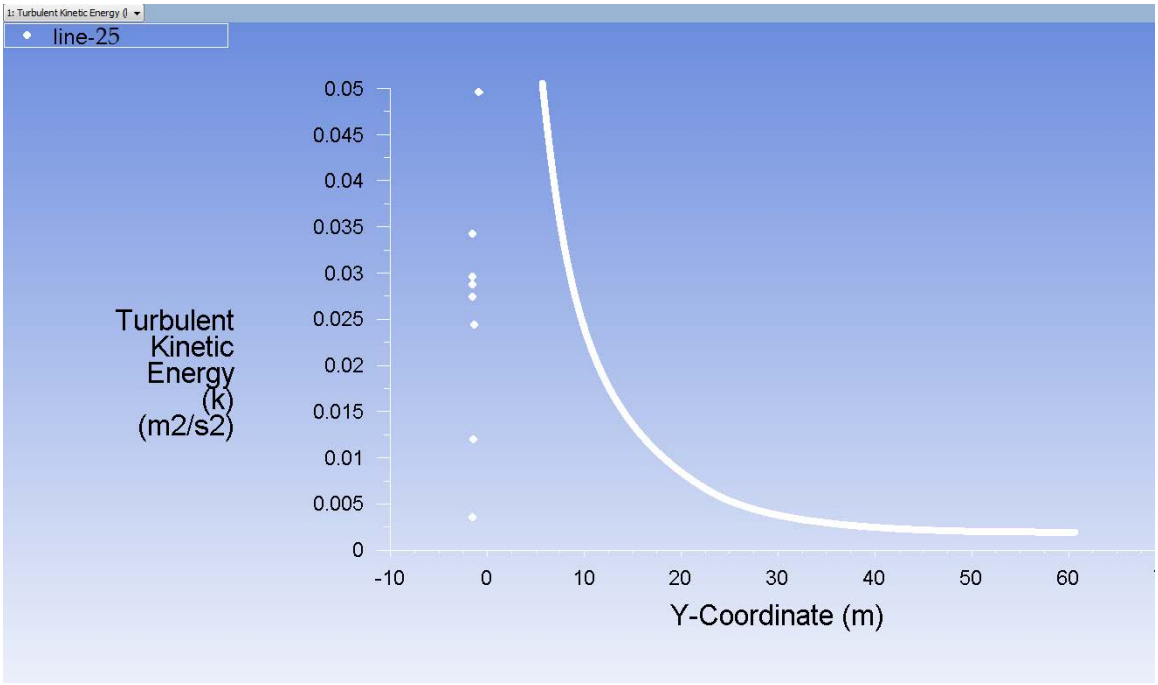

Figure 6.25 Zoomed section of TKE dissipation for 300RPM, 300GPM, and 60 º, 75 º, 90º inclination angle with modified geometry

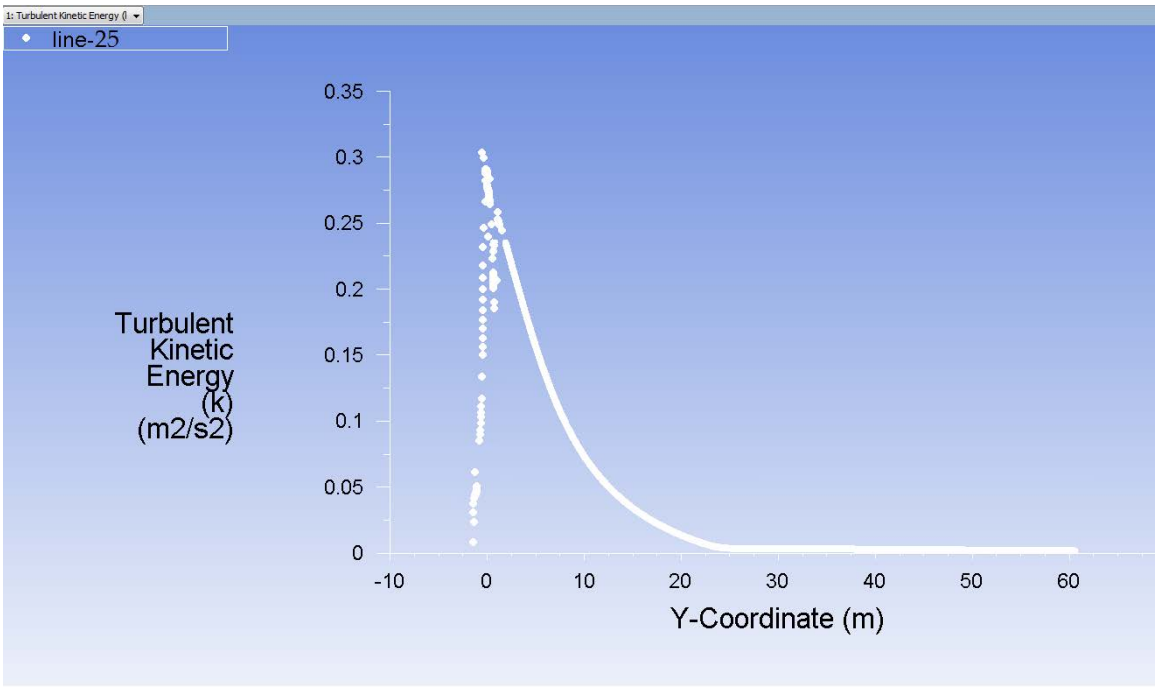

Figure 6.26 TKE dissipation for 300RPM, 400GPM, and 60 º, 75 º, 90º inclination angle with modified geometry

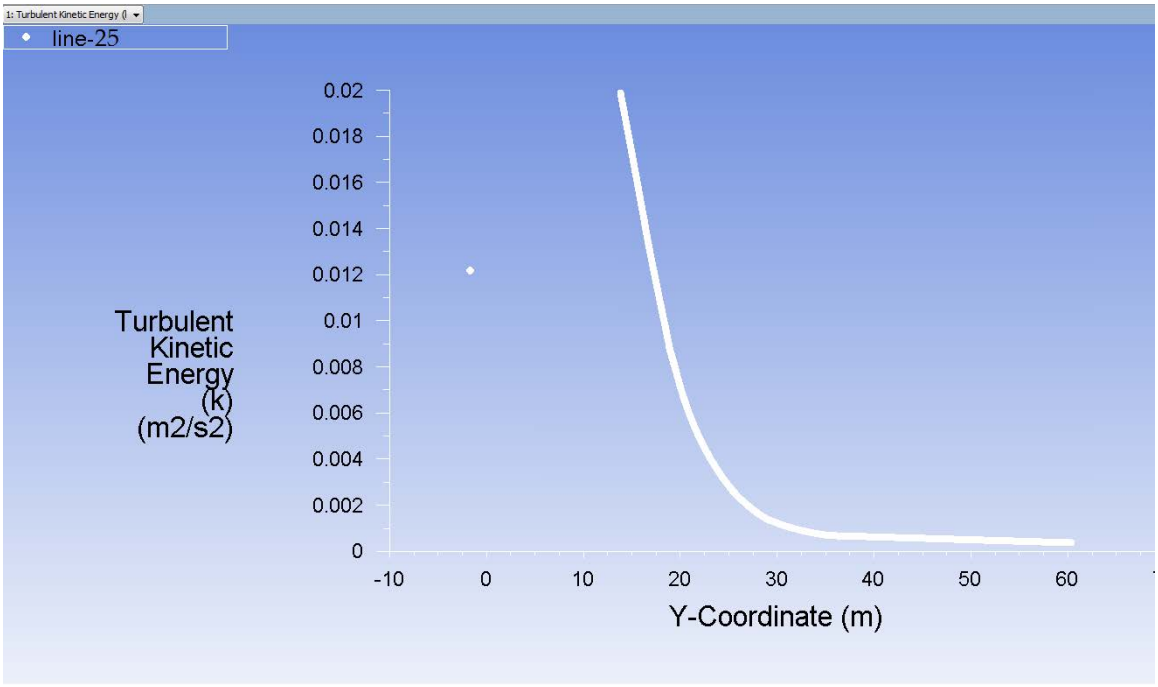

Figure 6.27 Zoomed section of TKE dissipation for 300RPM, 400GPM, and 60 º, 75 º, 90º inclination angle with modified geometry

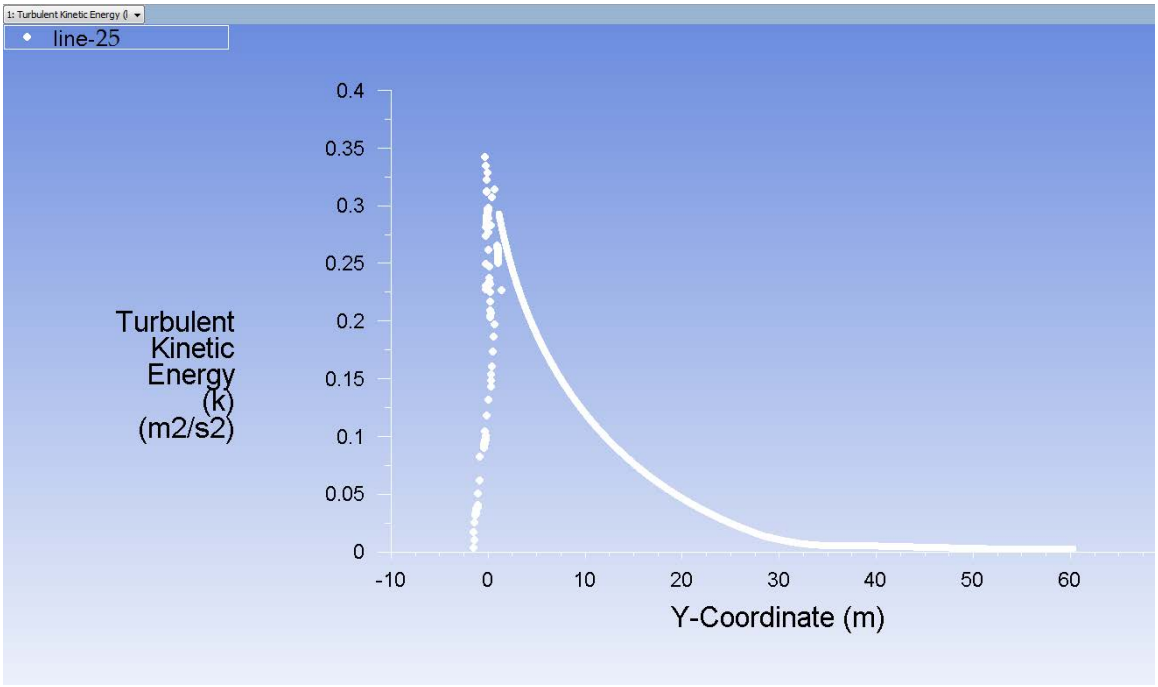

Figure 6.28 TKE dissipation for 300RPM, 500GPM, and 60 º, 75 º, 90º inclination angle with modified geometry

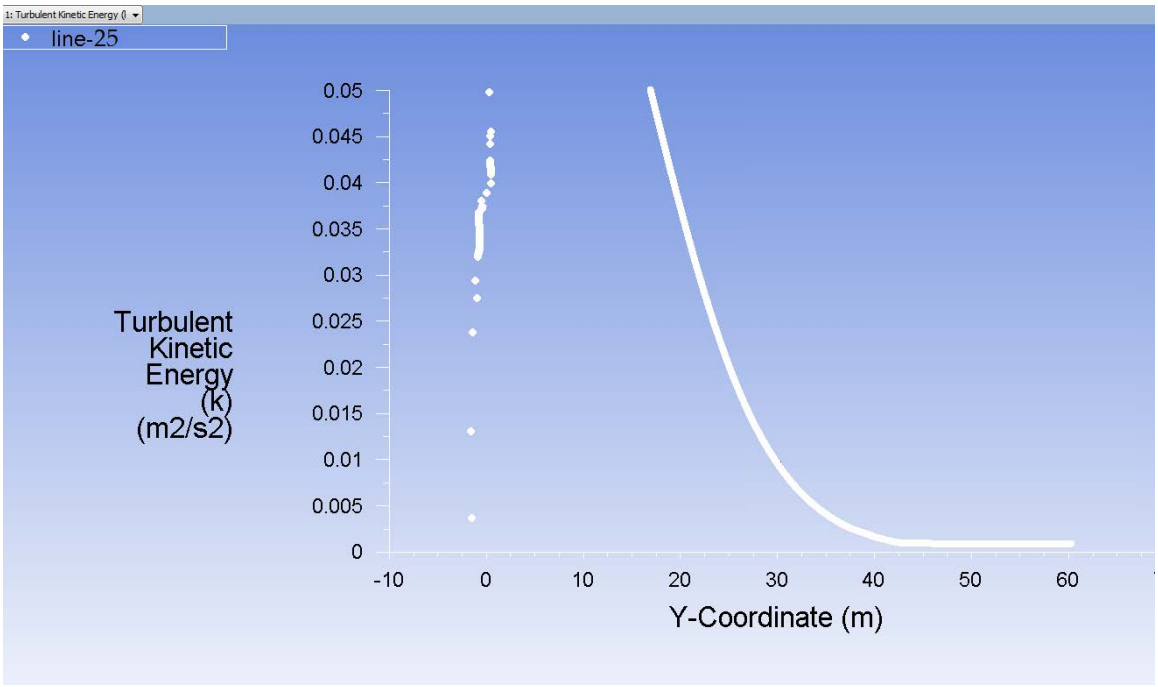

Figure 6.29 Zoomed section of TKE dissipation for 300RPM, 500GPM, and 60 º, 75 º, 90º inclination angle with modified geometry

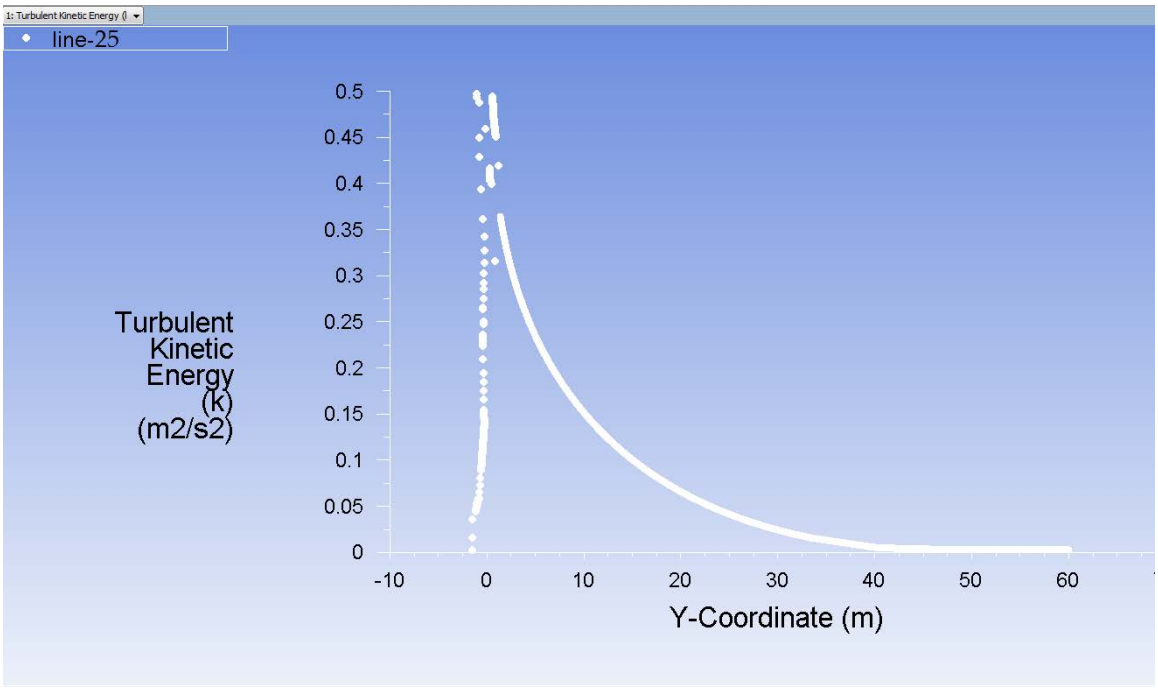

Figure 6.30 TKE dissipation for 400RPM, 300GPM, and 60 º, 75 º, 90º inclination angle with modified geometry

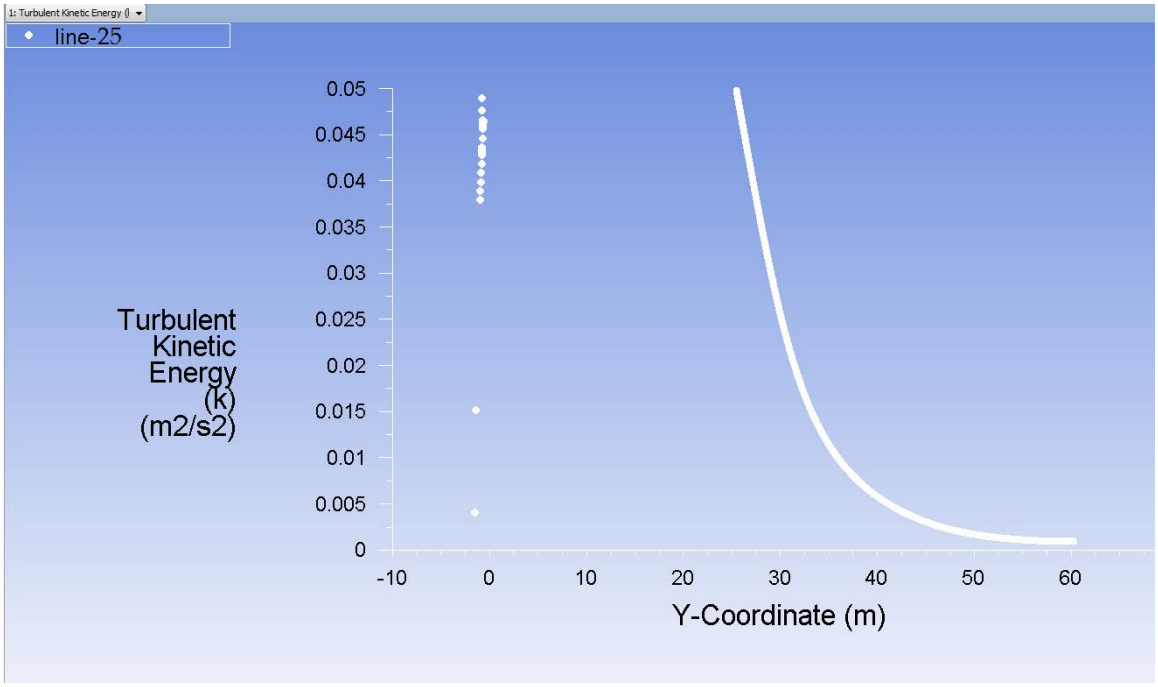

Figure 6.31 Zoomed section of TKE dissipation for 400RPM, 300GPM, and 60 º, 75 º, 90º inclination angle with modified geometry

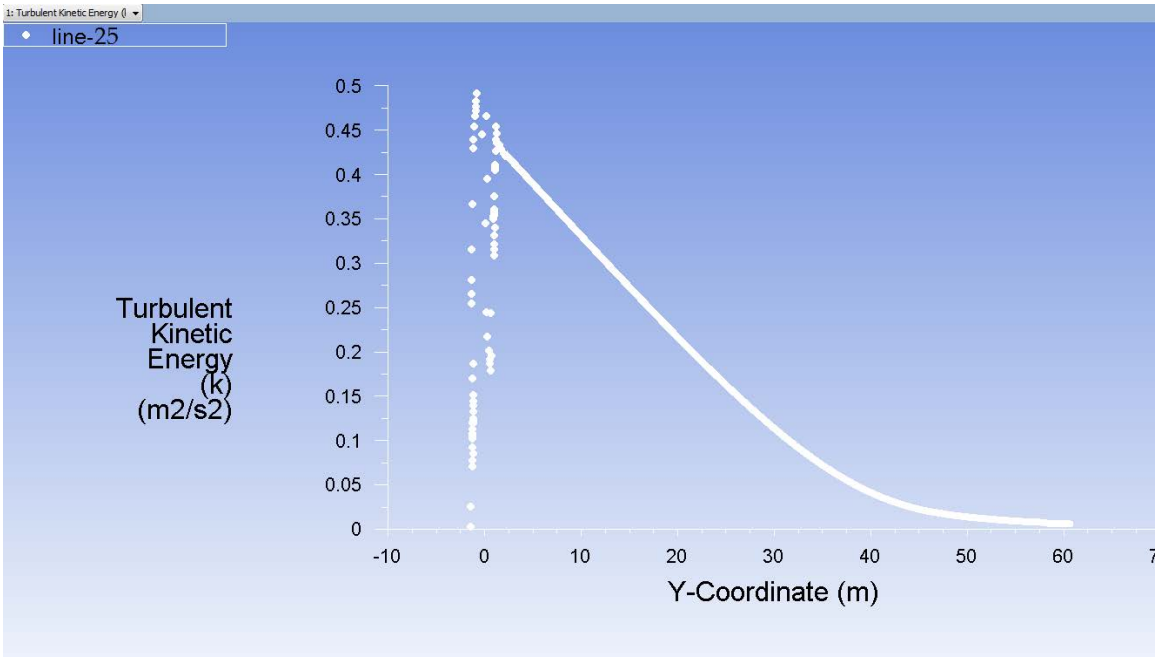

Figure 6.32 TKE dissipation for 400RPM, 400GPM, and 60 º, 75 º, 90º inclination angle with modified geometry

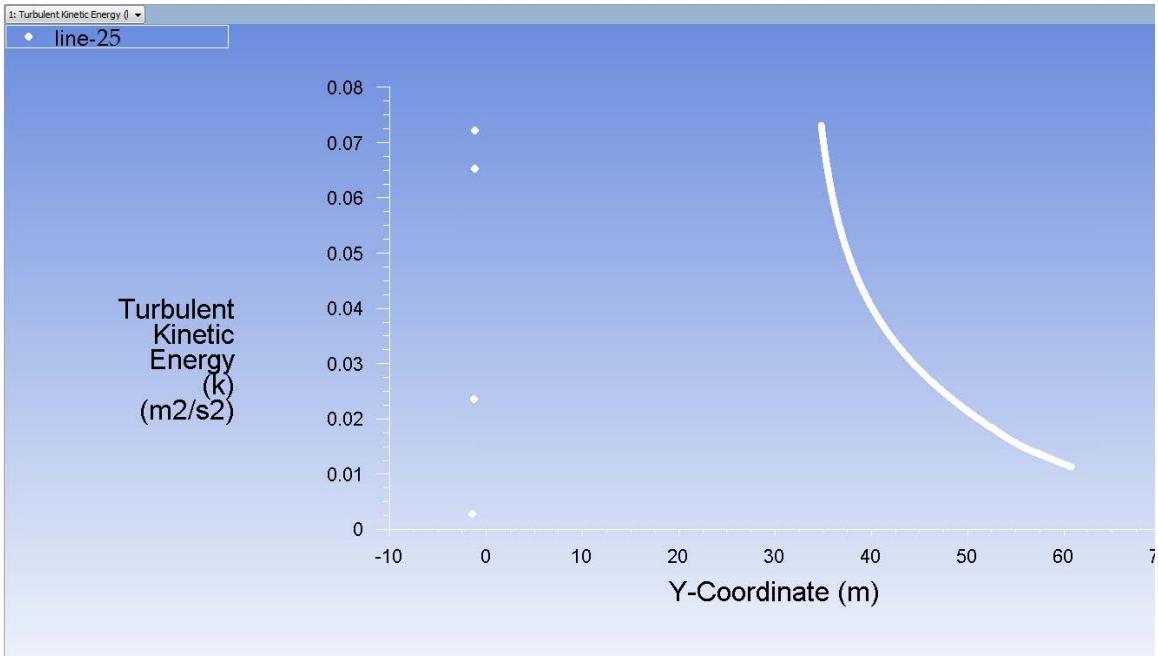

Figure 6.33 Zoomed section of TKE dissipation for 400RPM, 400GPM, and 60 º, 75 º, 90º inclination angle with modified geometry

Calculated tool placement distance is shown in Table 6.2 below.

Table 6.2 Test matrix with tool placement distance for straightly grooved tool

S.No	RPM	Wellbore inclination	Mud Flowrate GPM	ROP in ft/hr	Vcr Lifting m/s	Vel diff m/s	TKE required m2/s2	Straight Grooved Tool Placement (m)
1	200	60	300	35.84	0.665	0.333	0.084	**6**
2	200	60	300	53.76	0.670	0.339	0.095	**5**
3	200	60	300	71.69	0.675	0.344	0.105	**5**
4	200	60	400	35.84	0.662	0.219	0.029	**15**
5	200	60	400	53.76	0.666	0.224	0.034	**14**
6	200	60	400	71.69	0.670	0.228	0.038	**13.5**
7	200	60	500	35.84	0.660	0.107	0.002	**32**
8	200	60	500	53.76	0.663	0.111	0.003	**30**
9	200	60	500	71.69	0.667	0.114	0.004	**28**
10	200	75	300	35.84	0.700	0.369	0.111	**4**
11	200	75	300	53.76	0.705	0.374	0.123	**3**
12	200	75	300	71.69	0.710	0.379	0.135	**3**
13	200	75	400	35.84	0.697	0.255	0.046	**13**
14	200	75	400	53.76	0.701	0.259	0.051	**12.5**
15	200	75	400	71.69	0.705	0.263	0.057	**12.5**
16	200	75	500	35.84	0.696	0.143	0.008	**23**
17	200	75	500	53.76	0.699	0.146	0.010	**22**
18	200	75	500	71.69	0.702	0.150	0.012	**21**
19	200	90	300	35.84	0.712	0.380	0.121	**3**
20	200	90	300	53.76	0.717	0.386	0.133	**3**
21	200	90	300	71.69	0.722	0.390	0.145	**2.5**
22	200	90	400	35.84	0.709	0.267	0.052	**12.5**
23	200	90	400	53.76	0.713	0.271	0.058	**12**
24	200	90	400	71.69	0.717	0.275	0.064	**11.5**
25	200	90	500	35.84	0.707	0.155	0.011	**22**
26	200	90	500	53.76	0.711	0.158	0.013	**21**
27	200	90	500	71.69	0.714	0.161	0.015	**20**
28	300	60	300	35.84	0.592	0.260	0.007	**22**
29	300	60	300	53.76	0.606	0.274	0.014	**15**
30	300	60	300	71.69	0.618	0.287	0.024	**10**
31	300	60	400	35.84	0.584	0.142	0.001	**30**
32	300	60	400	53.76	0.595	0.153	0.000	**Not Required**
33	300	60	400	71.69	0.606	0.164	0.001	**30**
34	300	60	500	35.84	0.580	0.027	0.020	**26**
35	300	60	500	53.76	0.589	0.036	0.015	**27**
36	300	60	500	71.69	0.597	0.045	0.010	**30**
37	300	75	300	35.84	0.631	0.300	0.017	**13**

Table 6.2 continued

38	300	75	300	53.76	0.644	0.313	0.028	**9**
39	300	75	300	71.69	0.656	0.325	0.040	**7.5**
40	300	75	400	35.84	0.624	0.182	0.000	**Not Required**
41	300	75	400	53.76	0.635	0.193	0.002	**27**
42	300	75	400	71.69	0.644	0.203	0.005	**22**
43	300	75	500	35.84	0.620	0.067	0.009	**30**
44	300	75	500	53.76	0.629	0.076	0.005	**33**
45	300	75	500	71.69	0.637	0.084	0.003	**37**
46	300	90	300	35.84	0.644	0.313	0.022	**11**
47	300	90	300	53.76	0.657	0.326	0.033	**8**
48	300	90	300	71.69	0.669	0.337	0.047	**7**
49	300	90	400	35.84	0.637	0.195	0.001	**30**
50	300	90	400	53.76	0.648	0.206	0.004	**23**
51	300	90	400	71.69	0.657	0.215	0.008	**20**
52	300	90	500	35.84	0.633	0.080	0.006	**32.5**
53	300	90	500	53.76	0.642	0.089	0.003	**35**
54	300	90	500	71.69	0.650	0.097	0.001	**41**
55	400	60	300	35.84	0.471	0.140	0.040	**28**
56	400	60	300	53.76	0.502	0.170	0.018	**32.5**
57	400	60	300	71.69	0.528	0.197	0.005	**40**
58	400	60	400	35.84	0.454	0.012	0.098	**32.5**
59	400	60	400	53.76	0.479	0.037	0.069	**36**
60	400	60	400	71.69	0.502	0.060	0.046	**42**
61	400	60	500	35.84	0.444	-0.109	0.180	**Not Required**
62	400	60	500	53.76	0.465	-0.088	0.147	**Not Required**
63	400	60	500	71.69	0.484	-0.069	0.119	**Not Required**
64	400	75	300	35.84	0.520	0.189	0.020	**32**
65	400	75	300	53.76	0.548	0.216	0.006	**39**
66	400	75	300	71.69	0.572	0.241	0.000	**Not Required**
67	400	75	400	35.84	0.505	0.063	0.063	**37**
68	400	75	400	53.76	0.527	0.085	0.041	**43**
69	400	75	400	71.69	0.548	0.106	0.025	**48**
70	400	75	500	35.84	0.495	-0.058	0.130	**Not Required**
71	400	75	500	53.76	0.514	-0.038	0.104	**Not Required**
72	400	75	500	71.69	0.532	-0.021	0.082	**Not Required**
73	400	90	300	35.84	0.536	0.204	0.015	**33**
74	400	90	300	53.76	0.563	0.231	0.003	**43**
75	400	90	300	71.69	0.587	0.255	0.000	**Not Required**
76	400	90	400	35.84	0.521	0.079	0.053	**37.5**
77	400	90	400	53.76	0.543	0.101	0.034	**42**
78	400	90	400	71.69	0.563	0.121	0.020	**51**
79	400	90	500	35.84	0.512	-0.041	0.116	**Not Required**
80	400	90	500	53.76	0.530	-0.023	0.092	**Not Required**
81	400	90	500	71.69	0.547	-0.005	0.072	**Not Required**

The results show that efficiency of the tool with straight grooves is slightly less than that with helical grooves. In almost all the instances tool placement distance is found to be lower for straight grooved tool when compared to the other tool. Also, plots show that, for a fixed wellbore inclination, GPM, ROP, and RPM, the maximum peak or the maximum value that TKE achieves is slightly less in straight grooved geometry. This directly implies that the turbulence generated by tool with straight grooves is less than the tool with helical grooves. Hence it is important to have helical grooves in the geometry to maximize hole cleaning efficiency. The increment in TKE however arises due to conversion of pressure energy into TKE. Therefore, the pressure drop across helically grooved tool will be higher than what it is in straightly grooved tool. More pressure drop in the wellbore means that more pumping pressure is required at the surface to bring cutting all the way to the top. But, the surface pressure is often limited by pore pressure and formation type. Therefore, pressure drop may act as a significant deciding factor while selecting the tool geometry. Calculations for pressure drop have not been included in this project but they are certainly important to get a complete picture of tool performance.

6.6 Percentage reduction in cutting concentration.

To estimate the percentage reduction in cutting concentration, amount of cuttings deposited in the wellbore without use of any tool is required. In absence of any tool in the drill string, cuttings will continue to deposit and form a bed until critical velocity is reached by virtue of reduction in cross sectional area of flow. For the very first case which is 200 RPM rotation speed, 60º wellbore inclination, 300 GPM mud flow rate, and 35.84 ft/hr ROP, bed height is first obtained at which flow velocity will be equal to critical velocity

required for lifting. Using Equation 36 for critical lift velocity and values of different parameters given in table 5.1,

$$V_{CL} = \left[\frac{4\left\{3\tau_y\left(\phi + \left(\frac{\pi}{2} - \phi\right)sin^2\phi - cos\phi sin\phi\right) + d_p g\left(\rho_p - \rho_f\right)sin\alpha\right\}}{3\rho C_L} - V_\theta\right]^{1/2}, \quad (57)$$

V_{CL} of 0.718m/s was obtained (resultant velocity).

Cross sectional area of flow is

$$A_a = \frac{\pi}{4}(d_o^2 - d_i^2) = 98.224\ in^2\ . \quad (58)$$

Flow velocity of mud without any bed is calculated as

$$V_{f(without\ bed)} = \frac{6.309 \times 10^{-5}.GPM + 0.0030345 \times ROP \times 0.0006452 \times A_a}{0.0006452 \times A_a}, \quad (59)$$

where, 6.309×10^{-5} is a constant to convert GPM to m^3/s, 0.0030345 is a constant to convert ROP from ft/s to m/s, and 0.0006452 is a constant to convert A_a from in^2 to m^2. Substitution of 300 GPM and 200 RPM gives

$$V_{f(without\ bed)} = 0.302m/s\ . \quad (60)$$

From these three values, area available for fluid flow with bed is calculated using continuity equation as

$$A_a \times V_{f(without\ bed)} = (A_a - A_b) \times V_{f(with\ bed)}\ , \quad (61)$$

where, A_b is the bed area. From this A_b = 18.5 in^2 is obtained. From this cross sectional area of bed, angle λ in Figure 4.5 can be determined using Equation 45 as

$$A_b = \frac{1}{2}{r_2}^2(\lambda - sin\lambda) \quad (62)$$

$$or, \qquad \lambda = 1.92\, radians\,. \tag{64}$$

Once the angle is determined, bed height is obtained as

$$h_b = r_2 - r_2 cos\frac{\lambda}{2} = 2.62\ in\ . \tag{65}$$

From this height, cutting concentration comes out to be

$$C_c = \frac{V_c}{V_A}.100 = \frac{18.5}{98.224} \times 100 = 19\%\ . \tag{66}$$

To this value, cutting concentration in the fluid phase is added, which is about 1%, and an overall cutting concentration of approximately 20% is obtained. This is the maximum cutting concentration that will exist in the wellbore without any tool. With 6 m spacing in tool, the cutting concentration is reduced to 10% which is about 50% reduction in the concentration. Similarly, all the values were obtained for different parameters and the same are given in table 6.3. From the calculation results, % reduction in cutting concentration vary from 52% to 2%.

Table 6.3 Percentage reduction in cutting concentration with tool

S.No	RPM	Wellbore inclination	Mud Flowrate GPM	ROP in ft/hr	Flow Velocity without bed m/s	Cutting Conc in flow (%)	Bed height (in)	Approximate Tool Placement (m)	% Reduction in Cc
1	200	60	300	35.84	0.302	1.01	2.62	**6**	50
2	200	60	300	53.76	0.303	1.50	2.62	**6**	51
3	200	60	300	71.69	0.305	1.99	2.62	**5**	52
4	200	60	400	35.84	0.401	0.76	2.43	**17**	43
5	200	60	400	53.76	0.403	1.13	2.42	**16**	44
6	200	60	400	71.69	0.404	1.50	2.42	**16**	45
7	200	60	500	35.84	0.501	0.61	2.12	**32**	31
8	200	60	500	53.76	0.502	0.91	2.11	**30**	32
9	200	60	500	71.69	0.504	1.20	2.10	**28**	33
10	200	75	300	35.84	0.302	1.01	2.62	**5**	50
11	200	75	300	53.76	0.303	1.50	2.62	**4**	51

Table 6.3 continued

12	200	75	300	71.69	0.305	1.99	2.62	**4**	52
13	200	75	400	35.84	0.401	0.76	2.43	**15**	43
14	200	75	400	53.76	0.403	1.13	2.42	**14**	44
15	200	75	400	71.69	0.404	1.50	2.42	**14**	45
16	200	75	500	35.84	0.501	0.61	2.12	**24**	31
17	200	75	500	53.76	0.502	0.91	2.11	**23**	32
18	200	75	500	71.69	0.504	1.20	2.10	**22**	33
19	200	90	300	35.84	0.302	1.01	2.62	**4**	50
20	200	90	300	53.76	0.303	1.50	2.62	**4**	51
21	200	90	300	71.69	0.305	1.99	2.62	**3**	52
22	200	90	400	35.84	0.401	0.76	2.43	**14**	43
23	200	90	400	53.76	0.403	1.13	2.42	**14**	44
24	200	90	400	71.69	0.404	1.50	2.42	**13**	45
25	200	90	500	35.84	0.501	0.61	2.12	**22**	31
26	200	90	500	53.76	0.502	0.91	2.11	**21**	32
27	200	90	500	71.69	0.504	1.20	2.10	**21**	33
28	300	60	300	35.84	0.302	1.01	2.11	**20**	32
29	300	60	300	53.76	0.303	1.50	2.10	**15**	34
30	300	60	300	71.69	0.305	1.99	2.10	**12**	36
31	300	60	400	35.84	0.401	0.76	1.95	**29**	23
32	300	60	400	53.76	0.403	1.13	1.94	**NA**	25
33	300	60	400	71.69	0.404	1.50	1.94	**29**	27
34	300	60	500	35.84	0.501	0.61	1.70	**27**	6
35	300	60	500	53.76	0.502	0.91	1.70	**29**	9
36	300	60	500	71.69	0.504	1.20	1.69	**32**	11
37	300	75	300	35.84	0.302	1.01	2.11	**14**	32
38	300	75	300	53.76	0.303	1.50	2.10	**11**	34
39	300	75	300	71.69	0.305	1.99	2.10	**10**	36
40	300	75	400	35.84	0.401	0.76	1.95	**NA**	23
41	300	75	400	53.76	0.403	1.13	1.94	**26**	25
42	300	75	400	71.69	0.404	1.50	1.94	**22**	27
43	300	75	500	35.84	0.501	0.61	1.70	**32**	6
44	300	75	500	53.76	0.502	0.91	1.70	**35**	9
45	300	75	500	71.69	0.504	1.20	1.69	**37**	11
46	300	90	300	35.84	0.302	1.01	2.11	**12**	32
47	300	90	300	53.76	0.303	1.50	2.10	**11**	34
48	300	90	300	71.69	0.305	1.99	2.10	**8**	36
49	300	90	400	35.84	0.401	0.76	1.95	**29**	23
50	300	90	400	53.76	0.403	1.13	1.94	**23**	25
51	300	90	400	71.69	0.404	1.50	1.94	**21**	27
52	300	90	500	35.84	0.501	0.61	1.70	**34**	6
53	300	90	500	53.76	0.502	0.91	1.70	**37**	9
54	300	90	500	71.69	0.504	1.20	1.69	**41**	11

Table 6.3 continued

55	400	60	300	35.84	0.302	1.01	1.76	**30**	14
56	400	60	300	53.76	0.303	1.50	1.76	**33**	17
57	400	60	300	71.69	0.305	1.99	1.75	**40**	20
58	400	60	400	35.84	0.401	0.76	1.62	**35**	2
59	400	60	400	53.76	0.403	1.13	1.62	**40**	5
60	400	60	400	71.69	0.404	1.50	1.62	**44**	8
61	400	60	500	35.84	0.501	0.61	1.42	**NA**	
62	400	60	500	53.76	0.502	0.91	1.41	**NA**	
63	400	60	500	71.69	0.504	1.20	1.41	**NA**	
64	400	75	300	35.84	0.302	1.01	1.76	**33**	14
65	400	75	300	53.76	0.303	1.50	1.76	**39**	17
66	400	75	300	71.69	0.305	1.99	1.75	**NA**	20
67	400	75	400	35.84	0.401	0.76	1.62	**41**	2
68	400	75	400	53.76	0.403	1.13	1.62	**45**	5
69	400	75	400	71.69	0.404	1.50	1.62	**50**	8
70	400	75	500	35.84	0.501	0.61	1.42	**NA**	
71	400	75	500	53.76	0.502	0.91	1.41	**NA**	
72	400	75	500	71.69	0.504	1.20	1.41	**NA**	
73	400	90	300	35.84	0.302	1.01	1.76	**34**	14
74	400	90	300	53.76	0.303	1.50	1.76	**43**	17
75	400	90	300	71.69	0.305	1.99	1.75	**NA**	20
76	400	90	400	35.84	0.401	0.76	1.62	**42**	2
77	400	90	400	53.76	0.403	1.13	1.62	**47**	5
78	400	90	400	71.69	0.404	1.50	1.62	**52**	8
79	400	90	500	35.84	0.501	0.61	1.42	**NA**	
80	400	90	500	53.76	0.502	0.91	1.41	**NA**	
81	400	90	500	71.69	0.504	1.20	1.41	**NA**	

CHAPTER 7

WORKFLOW TO USE THE STUDY

The aim of this study is to determine tool placement distance using a combination of CFD simulations and analytical modeling for cutting transport. Now that we have simulation results for various combinations of parameters, the tool placement distance can be calculated for other desired cutting concentrations in the wellbore. However, if tool placement distance is pre-decided, other parameters such as cutting concentration and ROP can be estimated by back calculation. Therefore, this study can be used to estimate cutting concentration, ROP, and tool placement distance if any two out of these three parameters are given along with RPM, GPM, wellbore size, drill pipe size, particle size, and wellbore inclination for Herschel Bulkley fluid with fixed n, K, and τ_y values. Workflow and procedure for calculations are given below. Please note that simulation results are obtained by solving Navier-Stokes equation and depend upon fluid type, tool geometry, RPM, and flow rate. Therefore, no flexibility can be exercised with these parameters and they must be kept constant.

7.1 Case 1: Determination of tool placement distance for fixed C_c and ROP.

Given data: C_c = 7%, ROP = 54 ft/hr, flowrate = 500 GPM, RPM = 200, and wellbore inclination of 75º. Herschel Bulkley fluid parameters are n = 0.7, K = 60cp, and τ_y = 10 Pa with drill pipe dia = 12.25 in and wellbore dia = 5in.

Solution:

First flow velocity is calculated assuming there is no bed using Equation 48 in chapter 4 as

$$V_{f(without\ bed)} = \frac{6.309 \times 10^{-5}.GPM + 0.0030345 \times ROP \times 0.0006452 \times A_a}{0.0006452 \times A_a} \ , \qquad (67)$$

where, 6.309×10^{-5} is a constant to convert GPM to m^3/s, 0.0030345 is a constant to convert ROP from ft/s to m/s, and 0.0006452 is a constant to convert A_a from in^2 to m^2.

Substituting the value of ROP and GPM we get

$$V_{f(without\ bed)} = 0.502 \frac{m}{s} \ . \qquad (68)$$

Next, cutting concentration in the flow is obtained using Equation 42 in chapter 4 as

$$C_c = \frac{V_c}{V_a}.100 \ , \qquad (69)$$

where,

V_c is Volume (in ft^3) of cuttings inside the annulus at steady state and V_a is Volume (in ft^3) of the annular section. This gives

$$C_c = \frac{\frac{\pi\ (OD)^2}{4} \times \frac{ROP \times 12}{3600}}{V_{f(without\ bed)} \times 39.37 \times A_a} \times 100 = 1.09\ \% \ , \qquad (70)$$

where, OD is bit diameter and is equal to 12.25in, ROP is in ft/hr, V_f is in m/s and A_a is in in^2. This is the minimum cutting concentration that can exist in the wellbore for the given conditions. Since 7% is the desired cutting concentration, remaining concentration of 5.9% must be contributed by the bed with a specific height.

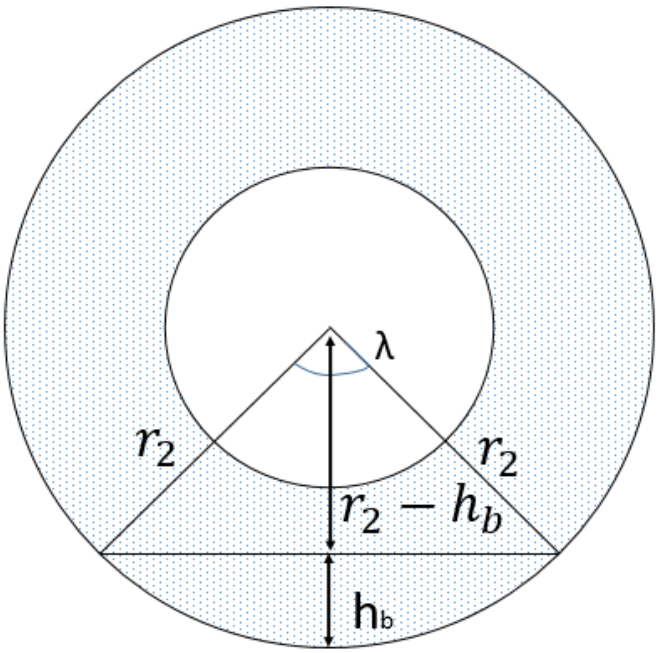

Figure 7.1 Calculation of angle and bed height

From the cutting concentration cross sectional area of bed is obtained using Equation 47 in chapter 4 as

$$A_b = \frac{A_a \times 5.64}{100} = 5.8\ in^2\ . \tag{71}$$

From this cross sectional area, angle given in Fig. 7.1 is obtained as

$$A_b = \frac{1}{2} r_2{}^2(\lambda - sin\lambda) \tag{72}$$

$$or\ \lambda = 1.262\ radians\ \ . \tag{73}$$

From this angle, bed height is obtained using Equation 49 in chapter 4 as

$$h_b = r_2 - r_2 cos\frac{\lambda}{2} = 1.18\ in\ \ . \tag{74}$$

Because of this bed height, flow velocity will increase in the wellbore which can be calculated using Equation 50 in chapter 4 (mass conservation equation) as

$$V_{f(with\ bed)} = \frac{A_a . V_{f(without\ bed)}}{A_a - A_b} = \frac{98.224 \times 0.502}{98.224 - 5.8} = 0.534\ m/s \quad . \tag{75}$$

Also, from the bed height, tangential velocity that will exist due to pipe rotation in the wellbore is obtained using Equation 33 in chapter 4 which gives

$$V_\theta = \Omega(r_2 - h_b)\left[\frac{1 - \left({}^{r_2}/_{(r_2 - h_b)}\right)^{2/n}}{1 - \left({}^{r_2}/_{r_1}\right)^{2/n}}\right] = 0.186\frac{m}{s}\ , \tag{76}$$

where, $\Omega = 200\ RPM$.

This is followed by calculation of critical lift velocity for the particle by using Equation 36 in chapter 4 which gives the value

$$V_{CL} = \left[\frac{4\left\{3\tau_y\left(\phi + \left(\frac{\pi}{2} - \phi\right)sin^2\phi - cos\phi sin\phi\right) + d_p g(\rho_p - \rho_f)sin\alpha\right\}}{3\rho_f C_L} - V_\theta\right]^{1/2} \tag{77}$$

$$= 0.727\ m/s \quad .$$

This is the velocity that must exist in the wellbore for the particle to get lifted. However, as calculated earlier, the actual velocity that exist in the wellbore is 0.427 m/s with a tangential velocity of 0.179 m/s. Difference between the velocities comes out to be

$$0.727 - \sqrt{0.534^2 + 0.186^2} = 0.161\frac{m}{s} \quad . \tag{78}$$

This translates to kinetic energy per unit mass (using Equation 52 in chapter 4) of

$$k = \frac{3}{2}\left(\overline{u'^2}\right) = 0.04 m^2 s^2 \quad . \tag{79}$$

Once this value is obtained, simulations were run for the given set of parameters and the following plot was obtained for turbulent kinetic energy. From Fig. 7.2, the distance at which TKE becomes $0.04 m^2 s^2$ is 12 m. Hence, spacing between two tools should be about 12 m to maintain 7% cutting concentration in the wellbore.

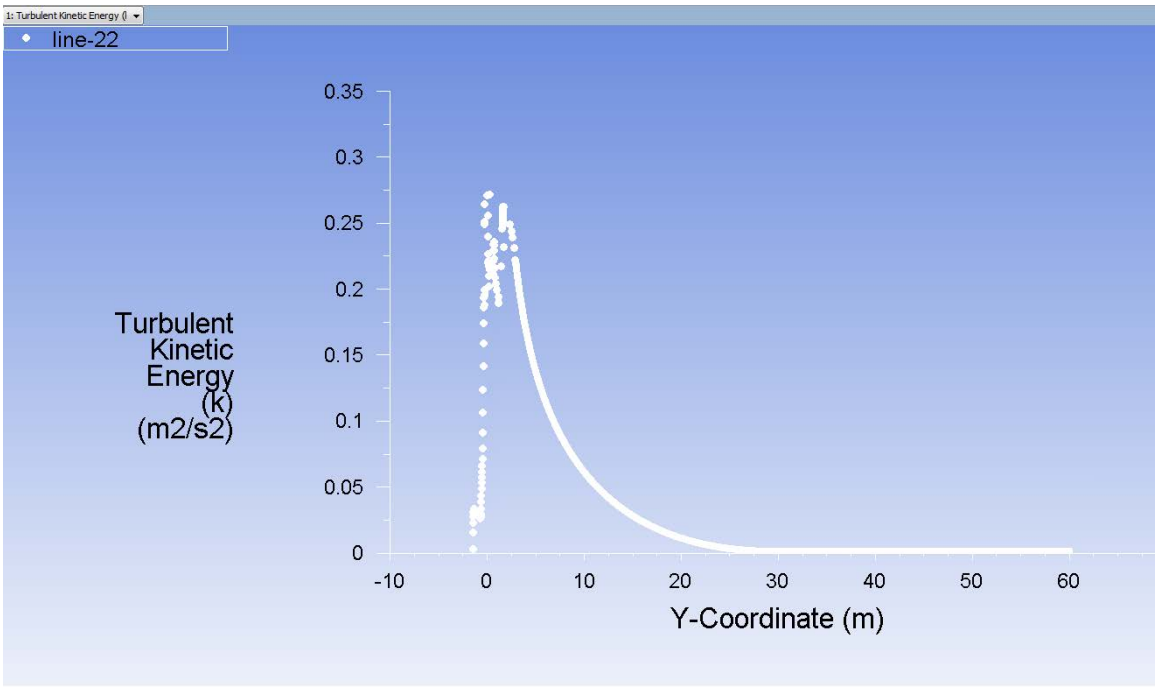

Figure 7.2 TKE plot for 200 RPM, 500 GPM and 75º wellbore inclination.

7.2 Case 2: Determination of C_c for fixed tool placement distance and ROP.

For a fixed ROP, GPM, RPM, and a given number of tools deployed, cutting concentration inside a wellbore can be determined using the results obtained in the previous sections. All the previous calculations were done based on 10% cutting concentration. However, if it was assumed that the hole has to be totally cleaned, the tool placement would have been different. To determine cutting concentration for a given set of parameters, let us first determine the tool placement distance for the case of helically grooved tool with

200 RPM rotation speed, 300 GPM flow rate, and ROP of 35.84 ft/hr. From ROP and GPM, flow velocity in the wellbore is first calculated as

$$V_{f(without\ bed)} = \frac{6.309 \times 10^{-5}.GPM + 0.0030345 \times ROP \times 0.0006452 \times A_a}{0.0006452 \times A_a} \ , \qquad (80)$$

where, 6.309×10^{-5} is a constant to convert GPM to m^3/s, 0.0030345 is a constant to convert ROP from ft/s to m/s, and 0.0006452 is a constant to convert A_a from in^2 to m^2.

Substituting the value of ROP and GPM we get

$$V_{f(without\ bed)} = \frac{0.302m}{s} \ . \qquad (81)$$

Next, cutting concentration is calculated, assuming there is no bed in the wellbore using the expression

$$C_c = \frac{V_c}{V_a}.100 \ , \qquad (82)$$

where,

V_c is Volume (in ft^3) of cuttings inside the annulus at steady state and V_a is Volume (in ft^3) of the annular section. Substitution gives

$$C_c \ = \frac{\frac{\pi\ (OD)^2}{4} \times \frac{ROP \times 12}{3600}}{V_{f(without\ bed)} \times 39.37 \times A_a} \times 100 = 1.205\% \ , \qquad (83)$$

where, OD is bit diameter and is equal to 12.25in, ROP is in ft/hr, V_f is in m/s and A_a is in in^2. This is the minimum cutting concentration that can exist in the wellbore for the given conditions.

There will be no tangential velocity in this case because velocity at the walls is zero (bed height is 0). This means that any particle that is dropping down at the bottom of the

wellbore is being lifted up only because of the turbulence and linear component of the fluid velocity. This is followed by calculation of modified Reynolds number given as

$$R_{em} = \frac{(10^{-3}d_p)^n V_f^{(2-n)}(10^3\rho_f)}{K} \quad , \tag{84}$$

where, n is power law index and K is consistency index for a yield power law fluid. Substitution of particle diameter, $d_p = 6.35\ mm$, $V_f = 0.302 m/s$, $\rho_f = 10 ppg$, n = 0.7, and K = 0.06 Pa.s^n gives $R_{em} = 122$.

Critical lift velocity is then calculated which results in

$$V_{CL} = \left[\frac{4\left\{3\tau_y\left(\phi + \left(\frac{\pi}{2} - \phi\right)sin^2\phi - cos\phi sin\phi\right) + d_p g(\rho_p - \rho_f)sin\alpha\right\}}{3\rho_f C_L} - V_\theta\right]^{\frac{1}{2}} \tag{85}$$

$$= \frac{0.718m}{s} \ .$$

Difference between the velocities is $V_{CL} - V_f = 0.718 - 0.302 = 0.416 m/s$. This velocity difference translates to additional TKE requirement of 0.259m^2/s^2 (using equation 52). Now, by referring to plot 6.1 we can obtain the tool placement distance. From the plot, it is clear that the tool does not produce that much turbulence to cater the need, therefore, tool has to be placed next to each other to keep the wellbore clean. Repeating the same steps for a different GPM however gives different results. For the case of 200RPM, 400GPM and 35.84ft/hr ROP, required TKE is 0.149 m^2/s^2. This give a value of about 7.5m for tool spacing from simulation plots (Figure 6.2). Till 7.5 m distance the wellbore will be clean and cutting will start making a bed beyond this distance. From the table 6.1, to maintaining 10% cutting concentration the tool placement has to be 17m. Assuming that beyond 7.5m of distance from the tool, bed starts to form with linear increment in bed

height with distance, equation for bed height increment can be derived which then can be used to estimate bed height just before the placement of another tool. Important point to note here is that this bed height can reach up to the maximum value of bed height at which flow velocity becomes equal to critical lift velocity (can be obtained using simple mass balance equation $A_1V_1=A_2V_2$). Bed height is calculated using Equation 49 in chapter 4 and it comes out to be 1.602in. Now, let us assume that the length of the inclined section of wellbore is L and N_T number of tools are placed in the drill string. Distance between two tools is then 1000/ N_T. Using this distance, bed height just before the second tool is given as h_b x L/9.5/ (N_T – 7.5) if it is less than maximum bed height, or the maximum bed height. Volume of this bed can then be calculated and new cutting concentration can be obtained.

Sample calculation for the case of 200 RPM, 400GPM and 35.84 ft/hr ROP.

For N_T = 25, and L = 1000m, tool spacing is given as

$$\Delta L = \frac{1000}{25} = 40m \quad . \tag{86}$$

Following the previous steps, bed height for maintaining 10% concentrations is

$$h_b = 1.602in \quad . \tag{87}$$

From Table 6.1, tool placement distance for maintaining 10% concentration is 17 m and fluid velocity without bed, V_f is 0.401m/s. Additional velocity required is calculated as

$$V_{CL} - V_f = 0.718 - 0.401 = 0.317 \text{ m/s.} \tag{88}$$

From this, equivalent TKE is obtained as

$$\text{TKE} = 3/2 \text{ x } (0.317)^2 = 0.151 \text{ m}^2/\text{ s}^2. \tag{89}$$

From plot 6.2, tool placement distance for keeping wellbore totally clean is 7.5 m. Therefore, increment in bed height with distance is given as

$$1.6 \text{ x } (\Delta L\text{-}7.5)/9.5 \quad , \tag{90}$$

in which, negative values are ignored and not considered for further calculations.

Total bed height that will result with 25 tools and 40 m spacing is

$$1.6 \text{ x } (40\text{-}7.5)/9.5 = 5.47 \text{ in.} \tag{91}$$

Using iterative method, 2.43in bed height is obtained for which resultant velocity is equal to the critical lifting velocity. This is the maximum bed height that can be reached therefore theoretical bed height of 5.47 in. is ignored and a maximum value of 2.43 in. for bed height is taken.

Distance till which maximum allowable bed height will be reached is calculated as

$$2.43 \text{ x } 9.5/1.6 + 7.5 = 22 \text{ m.} \tag{92}$$

Therefore, beyond 22 m, bed height is considered to be constant, which is maximum possible bed height, 2.43in. This is depicted in Fig. 7.3 wherein all the dimensions are mentioned as per calculations. Once all the dimensions for bed are obtained, volume of bed is calculated as

$$V_b = A_b \times (40 - 22) \times 39.37 + \frac{(22 - 7.5) \times 39.37 \times 2.43 \times 12.25 \times sin\frac{1.845}{2}}{3}. \tag{93}$$

where, A_b is maximum bed cross sectional area, $12.25 \times sin\frac{1.845}{2}$ is chord length.

From the calculation, volume comes out to be 16243.477in^3 which is used to determine cutting concentration as

$$C_c = \frac{V_b}{V_a} \times 100 + C_{c\,min} = 12.1\% \quad . \tag{94}$$

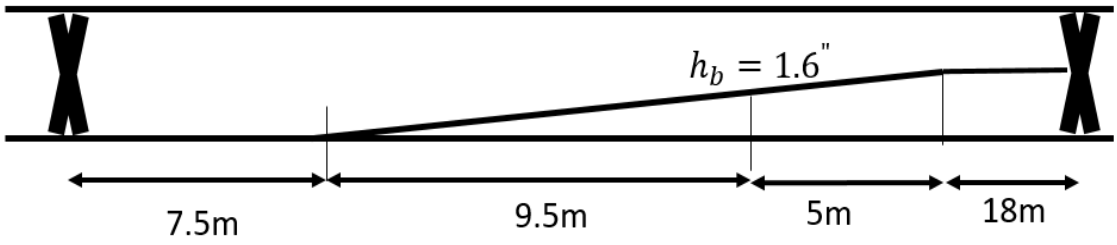

Figure 7.3 Growth of bed height with 200 RPM, 400 GPM and 35ft/hr ROP

7.3 Case 3: Determination of ROP for fixed tool placement distance and C_c.

Similar to cutting concentration calculation, ROP can also be estimated if number of tools deployed, RPM, GPM, Cutting Concentration, and inclination are given. Cutting concentration and ROP are closely related to each other because ROP determines the amount of cuttings generated which in turn determines the cutting concentration. Taking the same case of 200RPM, 400 GPM, 60º inclination, and 25 number of tools (N_T) over a wellbore length of 1000m (L), cutting concentration was obtained as 12.1%. If this cutting concentration is changed it would mean that whatever increment is there in the cutting concentration, it is because of the amount of cuttings in fluid phase only (since the tool placement distance is still same as in the previous case). Let us assume that a cutting concentration of 20% is to be maintained in the wellbore while keeping all other parameters

constant. This gives an excess of 20% – 12.1% = 7.9% cutting concentration in the fluid phase. Therefore, expression for cutting concentration becomes

$$\frac{\frac{ROP \times 12}{3600} \times (A_a - A_b)}{(A_a - A_b) \times V_f \times 39.37} \times 100 = 7.9\% \quad . \tag{95}$$

From previous calculations, h_b = 2.43 in. was obtained which translates to 16.57 in^2. cross sectional area of bed. From this, actual flow area is obtained and fluid velocity is calculated using material balance, which comes out to be V_f = 0.483m/s. After plugging in these values in Equation 95, value of ROP is obtained as

$$\frac{\frac{ROP \times 12}{3600} \times (98.224 - 16.57)}{(98.224 - 16.57) \times 0.483 \times 39.37} \times 100 = 7.9\% \ \ or \tag{96}$$

$$ROP = 450 \frac{ft}{hr} \quad . \tag{97}$$

7.4 Guidelines to use the MCD

Based on the study conducted in this report, the MCD under consideration shall be used as an add-on to the drill string to create turbulence in the wellbore fluid. Since the length of one drill string is fixed (about 30 ft), the MCD can be placed only at a minimum distance of 30ft. However, to optimize overall economics of the project, the tool is advised to be used after every 2 to 3 strings. Accordingly, drill string RPM and flowrate must be adjusted. Also, it is important to determine pressure drop across the tool when it rotates so that accurate measurements of pressures can be made. As already discussed in the literature review section, D. Yao and R. Samuel (2008) developed mathematical model to calculate pressure drop across various stand-off devices and the same can be applied here. Apart

from this, direction of rotation of the drill string is important because of the helical geometry on of the tool surface. Tool shall be oriented in such a way that the helical pitch moves towards the flow of fluid when the tool rotates. In other words, the tool shall act as impeller of a pump in favor of fluid flow and not against it. Since the tool helps in removing the deposited bed, it does not have to be present in the vertical section of the wellbore. Only deviated section has to have the tool. Moreover, overall drilling plan including tool spacing must be available prior to usage of the tool because once the tool is inside the hole, it cannot be pulled out to change its spacing or orientation. Apart from this, difference between tool diameter and drill string diameter should be sufficiently large to optimize the results. Tool diameter, however, must not be equal to bit diameter. Also, it is advised to place the first MCD close to the drill bit so that cuttings do not get deposited right behind the drill bit. Keeping all these guidelines in mind, the MCD can be utilized efficiently for cleaning deviated wellbores.

CHAPTER 8

CONCLUSIONS

The analysis of the data gathered from simulations on TKE and the spacing of mechanical cleaning device yields valuable insights into the usability of MCD under investigation. The test matrix for the simulation was broad in nature and covered most of the important parameters on which transport efficiency depends. Variables that were selected are flow rate, inclination angle, pipe rotation speed, and rate of penetration. Since different combination of all these variables give too many cases, only three data points were taken for each setting of these variables giving rise to a total of 81 cases. Shortcoming of such a selection is that the trends depicted by three data points are limited in their description of the system. To conclude this research work, below are some remarks given that highlights some important features and trends of MCD.

1) Increasing RPM has the most significant impact on hole cleaning. It was observed that higher the RPM, higher the hole cleaning efficiency of the tool is. Higher RPM of the drill pipe induces more tangential velocity in the mud and eventually leads to higher turbulence in wellbore. When the resultant velocity reaches critical velocity, wellbore cleaning takes place and cuttings are removed.
2) ROP can have both positive and negative effect on hole cleaning. At higher RPM and flowrate (GPM), increasing ROP leads to an increase in tool placement distance. However, at low RPM and GPM, increasing ROP leads to reduction in tool placement distance.
3) Increasing GPM increases the tool efficiency significantly. This is simply because of the increment in fluid velocity in the wellbore due to increase in GPM. As the

fluid velocity approaches critical velocity for lifting, cuttings start getting lifted and removed from the wellbore.

4) All the simulations were done using constant mud properties including viscosity, fluid type, density, and yield strength. Cutting removal results from the combination of all these properties, particle properties, and type of MCD tool. The MCD alone cannot significantly improve hole-cleaning all by itself; selection of appropriate drilling mud is essential. The cleaning device helps to stimulate the cuttings out of the bed and bring them into suspension. However, it is the task of the drilling mud to carry them away. If the mud does not have a good carrying capacity, then the agitation of the cuttings will be of little use.
5) Wellbore inclination does not affect TKE generated by the tool. It only effects critical velocities. In the derivation of equation for critical velocity for lifting, wellbore inclination plays an important part while in determining both the forces and moment acting on a particle in the wellbore. However, wellbore inclination does not appear anywhere in the equations for turbulent kinetic energy.
6) Geometry of the tool plays an important role in determining the hole cleaning efficiency. From the simulations for helically grooved and straightly grooved geometry, it was observed that helically grooved tool performs well as it was able to generate slightly more turbulence for a given set of parameters.

CHAPTER 9

RECOMMENDATIONS

The current study on the mechanical cleaning device is generalized and simplistic in its approach. However, despite of several simplistic assumptions, the study can act as a basis for future research work on characterizing the behavior of the MCD using CFD simulations. To make the research more accurate and effective, several suggestions are made in this section in an attempt to guide future research on this topic. Below mentioned are some important aspects that should be kept in mind while attempting to improve this research work.

Drill Pipe Orbital Motion

In the present research, it was assumed that there is no orbital motion in the drillpipe. However, when an eccentric pipe is rotated about its axis in an annulus, orbital motion of the drill pipe may take place. It may cause redistribution of velocity fields, Reynolds stress, TKE, and pressure fluctuations leading to higher turbulence. Higher turbulence or TKE indirectly means that there will be more chances of a particle getting removed.

Drill Pipe Eccentricity

In real life, due to so many forces acting on the drillpipe, it is seldom concentric. By keeping the drillpipe concentric in this research, tangential velocity profile was smooth, uniform and symmetric. In real case, however, drill pipe can sag and rests on the lower side of the annulus while being concentric at the ends. If the drillpipe is settled at the bottom

section of inclined wellbore, or if it is embedded inside the cutting bed, dynamics will totally change. Tangential velocity profile may not even exist in such conditions. It is anticipated that cleaning will be more is the drillpipe is closer to or embedded in the bed, however, torque and drag will also be higher. Therefore, the effect eccentricity on cuttings transport with the tools must be ascertained to simulate real case scenarios.

Drill String Vibrations/Dynamics

In real drilling scenarios, large vibrations are induced when the pipe is rotated, which can enhance cuttings transport because of the redistribution and fluctuations of the velocity field. Therefore, fluid structure interaction (FSI) simulation approach should be taken to get most accurate results.

Fluid type

Simulations for MCDs were run with Herschel Bulkley mud having a fixed viscosity of 60cp. A lower viscosity fluid has lower cuttings carrying capacity. Due to this it exerts less interfacial shear stress on the cuttings bed as compared to high viscosity fluid. Therefore, the cuttings that are picked up by low viscosity fluids fall back onto the bed after traveling a certain distance. On the other hand, a high viscosity mud removes more cuttings and is able to suspend them for a longer length. The mechanical cleaning device functions in such a way that it agitates the cuttings bed and helps to bring the cuttings into suspension for removal by the flowing fluid. If the fluid does not have the capability to suspend and transport the agitated cuttings, then these will fall back and the effect of the tool will be mitigated. Also, TKE generated is expected to be more in high viscosity fluid as compared to TKE in low viscosity fluid. However, it is also expected that dissipation of

TKE will be more quick in high viscosity fluid. This means that there has to be a tradeoff between viscosity and TKE for efficient hole cleaning. Therefore, it is a combination of the MCD agitation (TKE) as well as the fluid carrying capacity which will dictate how efficiently the hole is cleaned. Hence simulations must be run to quantify effect of mud viscosity on TKE.

Bed Height

Calculation of bed height in this report was simplistic and did not include iterative method. It was calculated by first determining the cutting concentration without any bed followed by bed height estimation using a fixed value of desired cutting concentration in the wellbore. However, even with iterative process the results vary very minutely and insignificantly. But to simulate real drilling case, iterations can be done.

Tool Geometry

Geometry of the tool plays an important role in determining the hole cleaning efficiency. From the simulations for helically grooved and straightly grooved geometry, it was observed that helically grooved tool performs well as it was able to generate more turbulence for a given set of parameters. However, to get a better picture of how the fluid interacts with the tool, it is important to run same simulations with tools having different blade angles.

Particle size distribution

Particles and cuttings that are generated during drilling are never uniform and vary significantly in shape and size. To determine a more realistic estimate, relatively complex approach can be taken and particle size distribution can be included in the calculations. For

different particles critical velocities will be different, and therefore, the wellbore may never be 100% clean. It is very likely that heavy particles will remain in the wellbore and form a bed while lighter particles will get carried away by the mud.

CFD simulation model

There are several models that exist in literature and that can be used by CFD software to simulate cutting transport. Some models are discrete phase model, dense discrete phase model, multiphase model, detached eddy simulation model, and large eddy simulation model. Out of these, discrete phase model and dense discrete phase model is advised to be used because of its capability to track and locate position of every particle. Injection rates can also be varied. However, it is complicated model which is difficult to converge.

Above all of these major recommendations, there are several parameters that play an important role in cutting transport efficiency. Some of these parameters are temperature, cuttings and fluid interaction, momentum transfer between fluid and particles, interaction of cuttings with other cuttings, size of wellbore, size of drill pipe, and sphericity of particles. Including all these factor in the simulations all at once may not be possible but these factors certainly are important and must be studied.

REFERENCES

1) R. J. S. Pigott, “Mud Flow in Drilling”, Drill & Prod. Prac., API (1941)

2) H. N. Hall, H. Thompson, and F. Nuss, “Ability of Drilling Mud to Lift Bit Cuttings” presented at the Petroleum Branch meeting at Columbus, September 25-28 and at the San Antonio meeting of the Petroleum branch, October 5-7, 1949.

3) Saffman. P.G., “The Lift on a Small Sphere in a Slow Shear Flow”, Journal fluid mechanic, 1964, Vol.22, part 2, pp. 385-400.

4) E. A. Hopkin, Shell Development Co. “Factors Affecting Cuttings Removal During Rotary Drilling” Paper SPE 1697 presented at the SPE Third Conference on Drilling and Rock Mechanics held in Austin, Texas, Jan 25-26, 1967.

5) Ansley, R. W., and T. N. Smith, “Motion of Spherical Particles in a Bingham Plastic,” AIChE J. 13, 1193–1196, 1967.

6) B.E. Launder and D.B. Spalding, “The Numerical Computation of Turbulent Flows”, North-Holland Publishing, 1974.

7) John B. Thuren, Martin E. Chenevert, Woon-Tsing Wally Huang, Edwin Szymanski, and Philip Arkeketa, “Determining Temperature Limits of Drilling Fluids,” US Energy Research and Devlopment Administration Contract No; EC40-1)-5218, 1979.

8) R. P. Thomas, J. J. Azar, T. E. Becker “Drill Pipe Eccentricity Effect on Drilled Cuttings Behavior” Paper SPE 9701 presented at the Deep Drilling and Production Symposium of the Society of Petroleum Engineers of AIME, held in Amarillo, Texas, April 5-7, 1981.

9) Gu, D., and R. I. Tanner, “The Drag on a Sphere in a Power-Law Fluid,” J. Non-Newtonian Fluid Mech. 17, 1–12, 1985.

10) A. A. Gavignet and I.J. Sobey, “Model Aids Cutting Transport Prediction”, JPT, 1989.

11) J. M Peden, J. T. Ford, M. B. Oyeneyin “Comprehensive Experimental Investigation of Drilled Cuttings Transport in Inclined Wells Including the Effects of Rotation and Eccentricity” Paper SPE 20925 presented at Europec 90, The Hague, Netherlands, 22-24 October, 1990.

12) Ford, J.T., Peden, J.M., Oyeneyin, M.B. et al. 1990. Experimental Investigation of Drilled Cuttings Transport in Inclined Boreholes. Presented at the SPE Annual Technical Conference and Exhibition, New Orleans, 23–26 September. SPE-20421-MS.

13) Adam T. Bourgoyne Jr. Marten E. Chenevert, Keith K. Millheim, F. S. Young Jr., “Applied Drilling Engineering Vol. 2” Society of Petroleum Engineers, Richardosn, TX, 1991.

14) White, F. M. (1991). Viscous Fluid Flow (2nd ed.) (pp. 181–200). New York: McGraw-Hill.

15) A. L. Martins, C. Costapinto Santana “Evaluation of Cuttings Transport in Horizontal and Near Horizontal Wells –A Dimensionless Approach” Paper SPE 23643 Presented at the second Latin American Petroleum Engineering Conference of the Society of Petroleum Engineers held in Caracas, Venezuela, march 8-11, 1992.

16) Sifferman, T. R., & Becker, T. E., “Hole Cleaning in Full-Scale Inclined Wellbores,” Society of Petroleum Engineers, 20422-PA, 1992.

17) S.H. Javadpour and S.N. Bhattacharya, “Axial Flow in a Rotational Coaxial Rheometer System II: Herschel Bulkley Model”, J. Sci. I. R. Iran, 1992.

18) T. D. Reed, A. A. Pilhevari “A New Model for Laminar, Transitional and Turbulent Flow of Drilling Muds” Paper SPE 25456 presented at the Production Operations Symposium held in Oklahoma City, Ok, March 21—23, 1993.

19) R. A. Clark and K. L. Bickham “A Mechanistic Model for Cuttings Transport” Paper SPE 28306 presented at the SPE 69th Annual Technical Conference and Exhibition held in New Orleans, LA, USA, 25-28 September 1994.

20) Yuejin Luo, P. A. Bern, B. D. Chambers and D. S. Kellingray “Simple Charts to Determine Hole Cleaning Requirements” Paper SPE 27486 presented at IADC/SPE Drilling Conference held in Dallas, Texas, 15-18 February, 1994

21) Marco Rasi “Hole Cleaning in Large, High-Angle Wellbores” Paper SPE 27464 presented at the IADC/SPE Drilling Conference held in Dallas, Texas, 15—18 February 1994.

22) Bruce R. Munson, Donald F. Young, Theodore H. Okiishi, “Fundamentals of Fluid Mechanics”, Second Edition, John Wiley & Sons, Inc., New York, 1994

23) A. L. Martins, A. M. F. Lourenco, L. G. M. Freire, and W. Campos, “Experimental Determination of Interfacial Friction Factor in Horizontal Drilling with a Bed of Cuttings” Paper SPE 36075 presented at the fourth SPE Latin American and Caribbean Petroleum Engineering Conference held in Port of Spain, Trinidad and Tobago, 23—26 April 1996

24) T. I. Larsen, A. A. Pilehvari, J. J. Azar "Development of a New Cuttings Transport Model for High-Angle Wellbores Including Horizontal Wells" Paper SPE 25872 presented at the SPE Rocky Mountain Regional/Low Permeability Reservoirs Symposium held in Denver, CO, USA, April 12 – 14, 1997.

25) S. F. Chien, "Effect of Hydraulics and Fluid Rheology on the Transportation of Drill Cuttings in Horizontal drilling" paper presented at the 8th Annual International Energy Week Conference and Exhibition, Houston (Jan. 28-30, 1997)

26) S. Walker, J. Li "The Effects of Particle Size, Fluid Rheology, and Pipe Eccentricity on Cuttings Transport" Paper SPE 60755 presented at the SPE/ICoTA Coiled Tubing Roundtable held in Houston, Texas, April 5-6, 2000.

27) J. G. Boulet, J. A. Shepherd, J. Batham and L. R. Elliott "Improved Hole Cleaning and Reduced Rotary Torque by New External Profile on Drilling Equipment" Paper SPE 59143 presented at IADC/SPE conference held in New Orleans (23-25 February 2000).

28) Bilgesu, H. I., Ali, M. W., Aminian, K., & Ameri, S. (2002, January 1). Computational Fluid Dynamics (CFD) as a Tool to Study Cutting Transport in Wellbores. Society of Petroleum Engineers. doi:10.2118/78716-MS

29) Ali, M.Q., "Study on the Mechanical Cleaning Device," M.S. Thesis, University of Tulsa, OK, 2004.

30) Thomas J. Danielson, "Sand Transport Modeling in Multiphase Pipelines," Offshore Technical Conference-18691, 2007.

31) M. Duan, S. Miska, M. Yu, N. Takach, and R. Ahmed, “Critical Conditions for Effective Sand-Sized Solids Transport in Horizontal and High-Angle Wells,” Society of Petroleum Engineers, SPE-106707, 2007.

32) Samuel, Robello, “Downhole Drilling Tools,” 2007, 215-231.

33) Harve Tabuteau, P. Coussot, J.R. Bruyn, “Drag Force on a Sphere in Steady Motion Through a Yield Stress Fluid,” J. Rheology, 51(1), 125-137, 2007.

34) Yao, D., & Samuel, R., “Annular-Pressure-Loss Predictions for Various Standoff Devices,” Society of Petroleum Engineers, 112544-MS, 2008.

35) Costa, S. S., Stuckenbruck, S., Fontoura, S. A. B., & Martins, A. L. (2008, January 1). Simulation of Transient Cuttings Transportation and ECD in Wellbore Drilling. Society of Petroleum Engineers. doi:10.2118/113893-MS

36) Pratap Singh, A., & Samuel, R., “Effect of Eccentricity and Rotation on Annular Frictional Pressure Losses with Standoff Devices,” in Society of Petroleum Engineers, ATCE, paper 124190-MS, January 2009.

37) Ahmed, R.M. and Miska, S.Z., “Drilling Hydraulics: Advanced Drilling and Well Technology,” Society of Petroleum Engineering, 2009, Chap 4.1, 191-220.

38) Ahmed, R. M., Sagheer, M., Takach, N., Majidi, R., Yu, M., Miska, S. Z., … Boulet, J. G. (2010, January 1). Experimental Studies on the Effect of Mechanical Cleaning Devices on Annular Cuttings Concentration and Applications for Optimizing ERD Systems. Society of Petroleum Engineers. doi:10.2118/134269-MS

39) S.-M. Han, Y.-K. Hwang, N.-S. Woo, and Y.-J. Kim, “Solid-Liquid Hydrodynamics in a Slim Hole Drilling Annulus,” Journal of Petroleum Science and Engineering, vol. 70, no. 3-4, pp. 308–319, 2010.

40) Z. Wang, Y. Zhai, X. Hao, X. Guo, and L. Sun, “Numerical Simulation on Three Layer Dynamic Cutting Transport Model and its Application on Extended Well Drilling,” Asia Pacific Drilling Technology Conference and Exhibition, IADC/SPE-134306, 2010.

41) Abbas H. Sulaymon, Sawsan A. M. Mohammed, Abeer I. Alwared, “Hydrodynamic Interaction Between Two Spheres in Newtonian and non-Newtonian Fluid”, Journal of Applied Sciences Research, 7(7): 1222-1232, 2011.

42) I. Salyzhyn and M. Myslyuk, “Studies of the Rheological Properties of Drilling Fluids,” Annual Transactions of the Nordic Rheology Society, 2011.

43) Aniket, A., Pratap Singh, A., & Samuel, R., “Analytical Model to Predict the Effect of Pipe Friction on Downhole Temperatures for Extended Reach Drilling (ERD),” in Society of Petroleum Engineers, ATCE, paper 151254-MS, January 2012.

44) Uduak Mme and Pal Skalle, “CFD Calculations of Cuttings Transport Through Drilling Annuli at Various Angles,” International Journal of Petroleum Science and Technology, ISSN 0973-6328, Vol 6, 2012, pp. 129-141.

45) Van Puymbroeck, L., & Williams, H. (2013, August 12). Increasing Drilling Performance in ERD Wells with New Generation Drill Pipe. Society of Petroleum Engineers, SPE-168690 / URTEC2013-108.

46) Vijay Ashok Mulchandani, “Experimental Analysis on Bidispersed Cuttings Transport in Laminar Pipe Flow,” SPE-167639-STU, 2013.

47) E. Cayeux, T. Mesagan, S. Tanripada, M. Zidan, and K.K. Fjelde, “Real-Time Evaluation of Hole Cleaning Conditions with a Transient Cuttings-Transport Model,” SPE Drilling & Completion, SPE/IADC, SPE-163492, 2014.

48) Nwagu, C., Awobadejo, T., & Gaskin, K. (2014, August 5). Application of Mechanical Cleaning Device: Hole Cleaning Tubulars, To Improve Hole Cleaning. Society of Petroleum Engineers-172403-MS, 2014.

49) S. Akhshik, M. Behzad, and M. Rajabi, “CFD-DEM Approach to Investigate the Effect of Dtill Pipe Rotation on Cuttings Transport Behavior,” J. Petroleum Science and Engineering, 127, 2015, pp. 229-244.

50) Okot, M., Campos, M., Muñoz, G., Alalsayednassir, A. G., Weber, M., & Muneer, Z. (2015, October 11). Utilization of an Innovative Tool to Improve Hole Cleaning Efficiency in Extended Reach Wells in Saudi Arabia. Society of Petroleum Engineers-175165-MS, 2015.

51) Behnam Amanna, M. R. K. Movaghar, “Cuttings Transport Behavior in Directional Drilling Using Computational Fluid Dynamics (CFD),” Journal of Natural Gas Science and Engineering 34, 2016, pp. 670-679.